Mesenchymal Liver Tumors - Pathologic Basis and Imaging Features

Poster No.: C-2133

Congress: ECR 2012

Type: Educational Exhibit

Authors: M. L. O. O. Coelho[1], L. Curvo Semedo[2], B. Gonçalves[2], M. Pontes[2], A. G. Saraiva[2], F. Caseiro Alves[2]; [1]Porto/PT, [2]Coimbra/PT

Keywords: Abdomen, Liver, Ultrasound, CT, MR, Diagnostic procedure, Neoplasia

DOI: 10.1594/ecr2012/C-2133

Learning objectives

The purpose of this educational exhibit is to review the pathologic background and imaging findings - ultrasound, computed tomography and magnetic ressonance - of benign and malignant mesenchymal tumors occurring in the liver.

Background

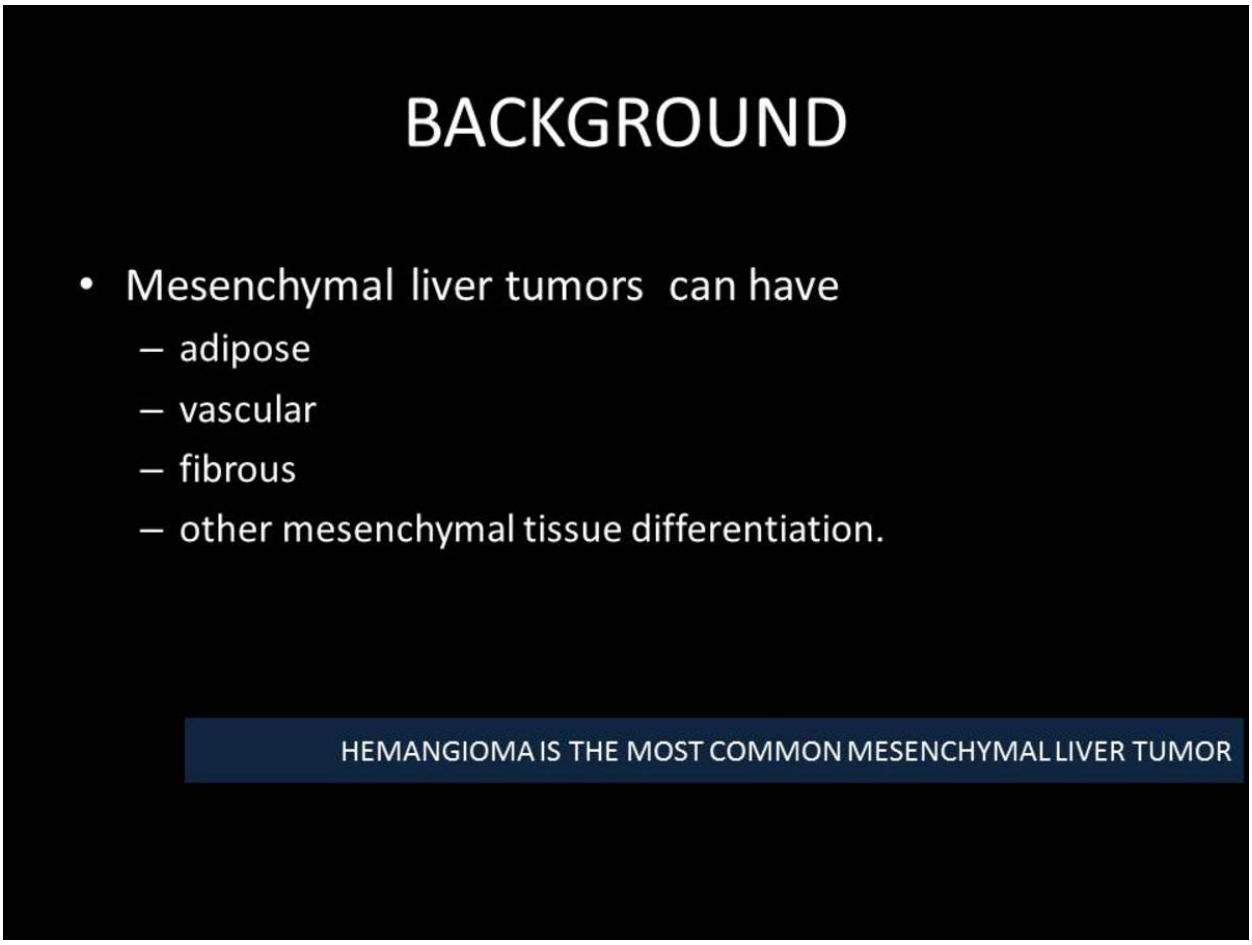

Fig. 1: 1
References: M. L. O. O. Coelho; radioogia, Porto, PORTUGAL

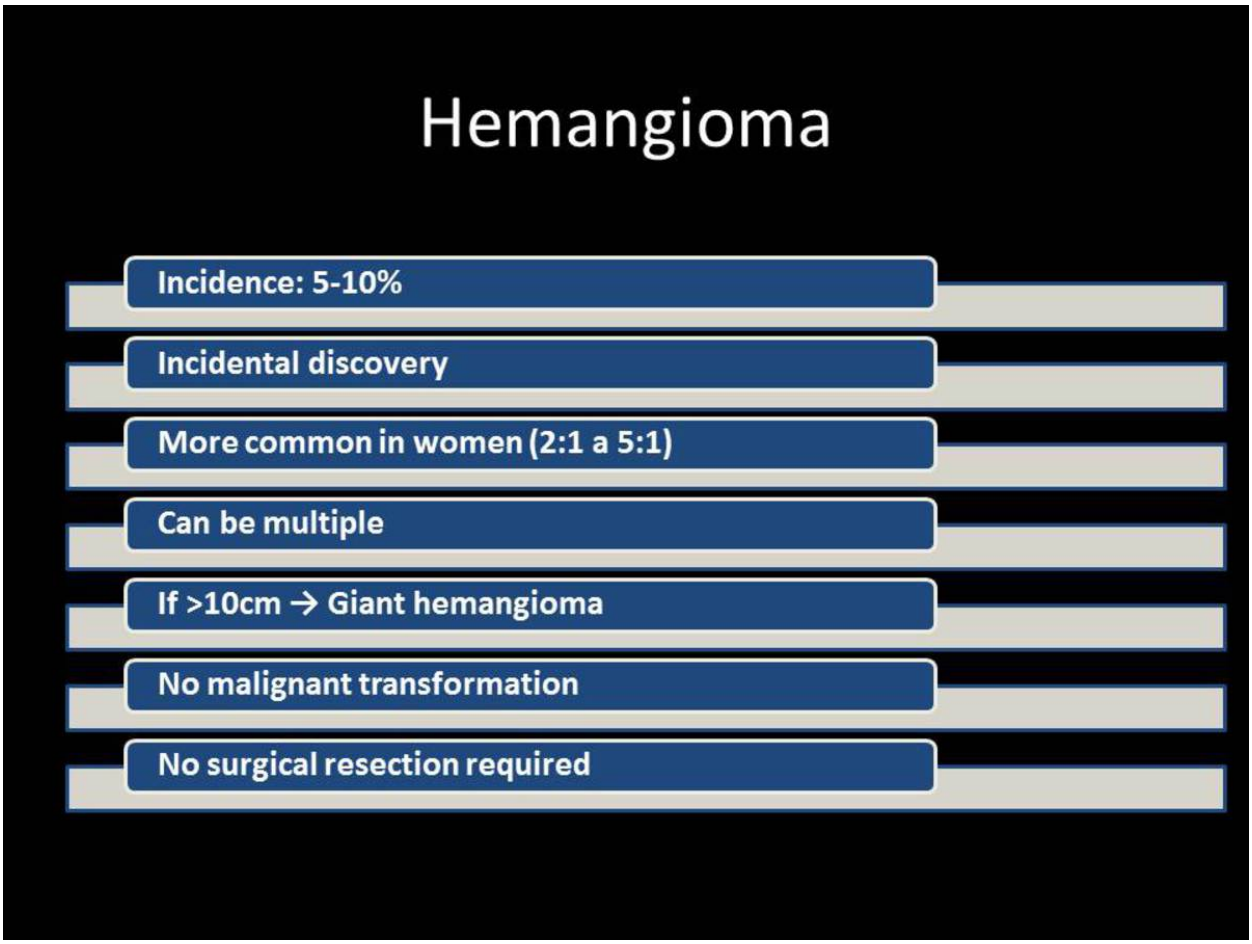

Fig. 2: 2
References: M. L. O. O. Coelho; radioogia, Porto, PORTUGAL

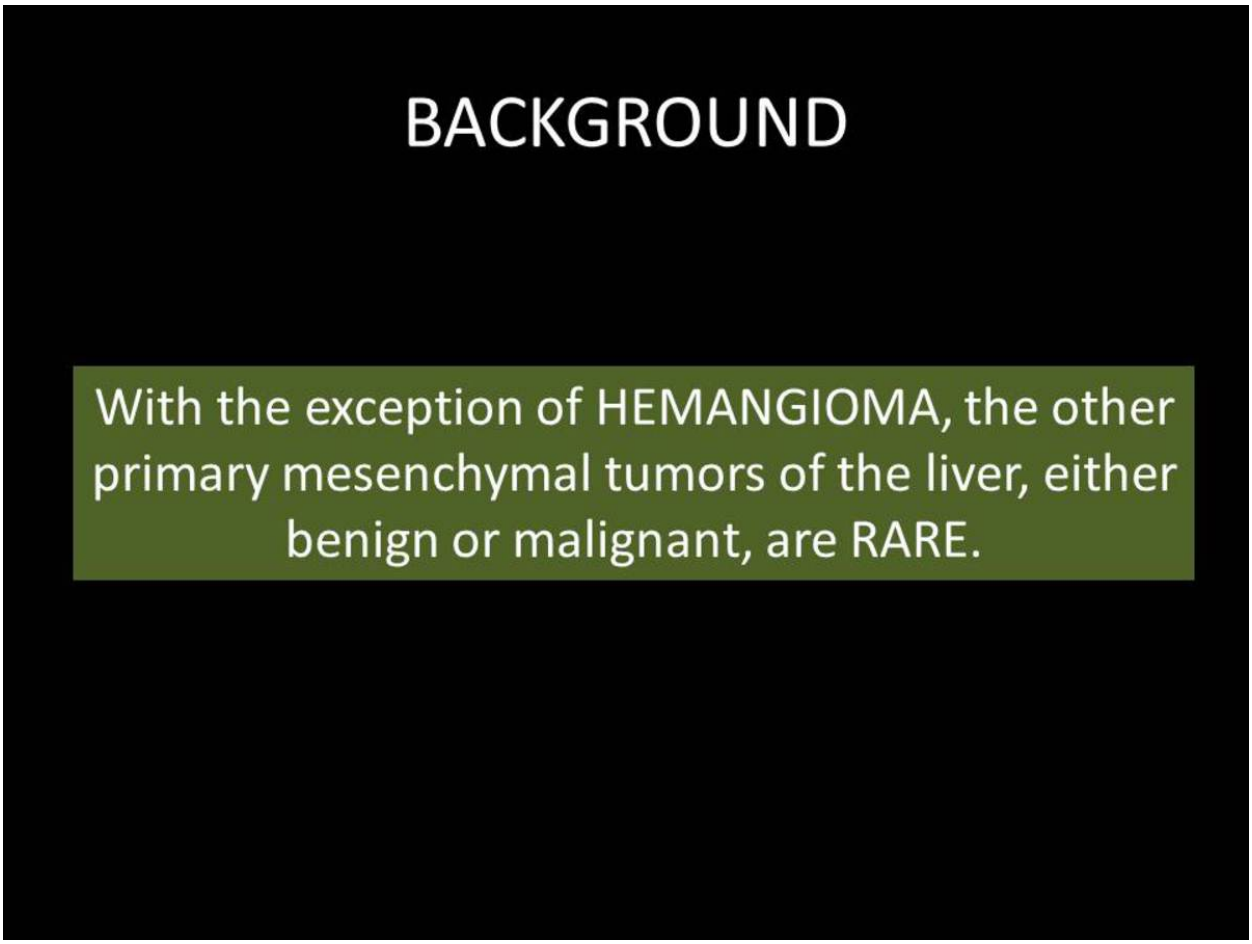

Fig. 4: 4
References: M. L. O. O. Coelho; radioogia, Porto, PORTUGAL

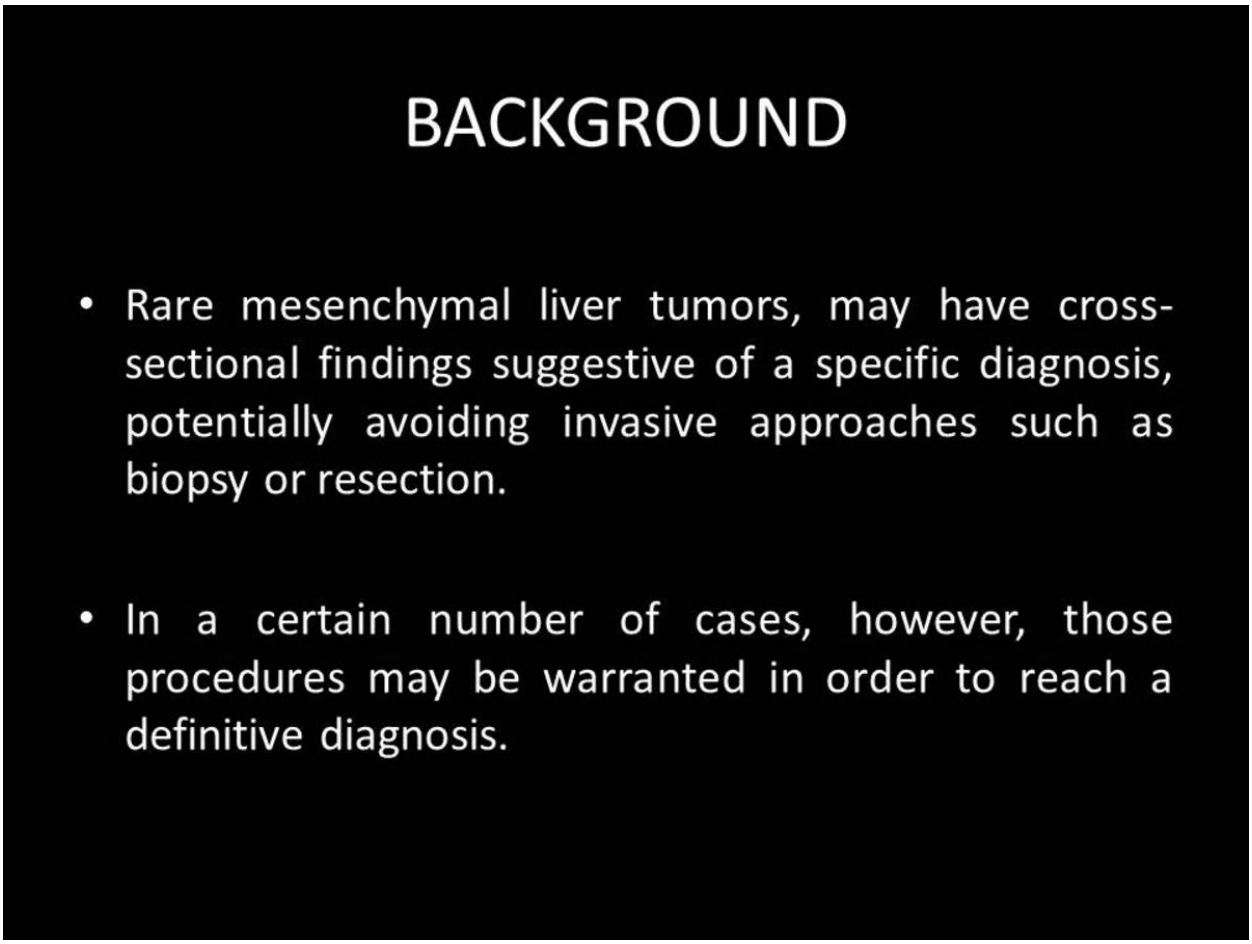

Fig. 5: 5
References: M. L. O. O. Coelho; radioogia, Porto, PORTUGAL

Imaging findings OR Procedure details

• Primary mesenchymal liver tumors have a wide range of imaging appearances:

• some are similar to those appearing in epithelial tumors, metastasis or even inflammatory lesions, like abscesses

• other are characteristic and can guide us to the diagnosis.

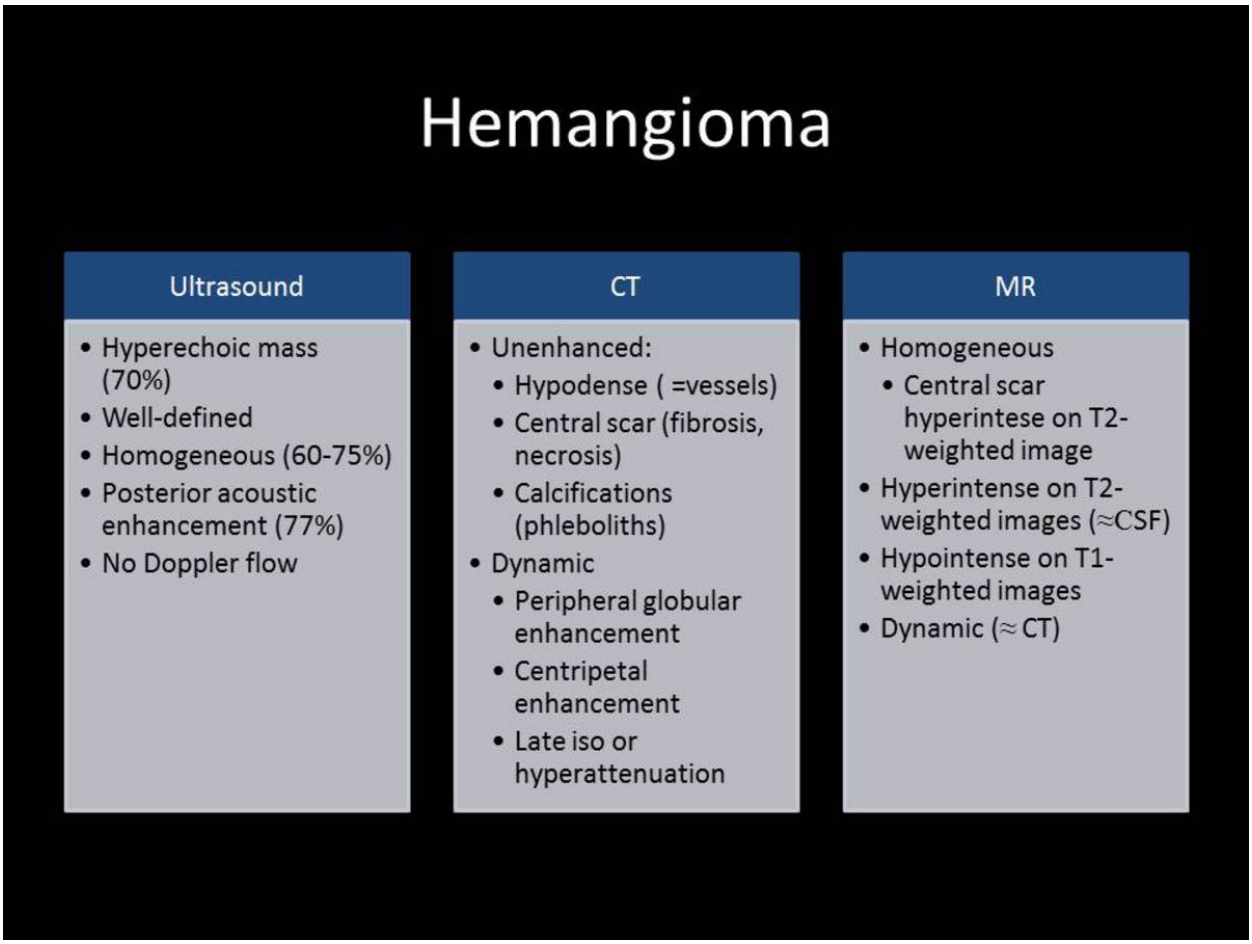

Fig. 7: 7
References: M. L. O. O. Coelho; radioogia, Porto, PORTUGAL

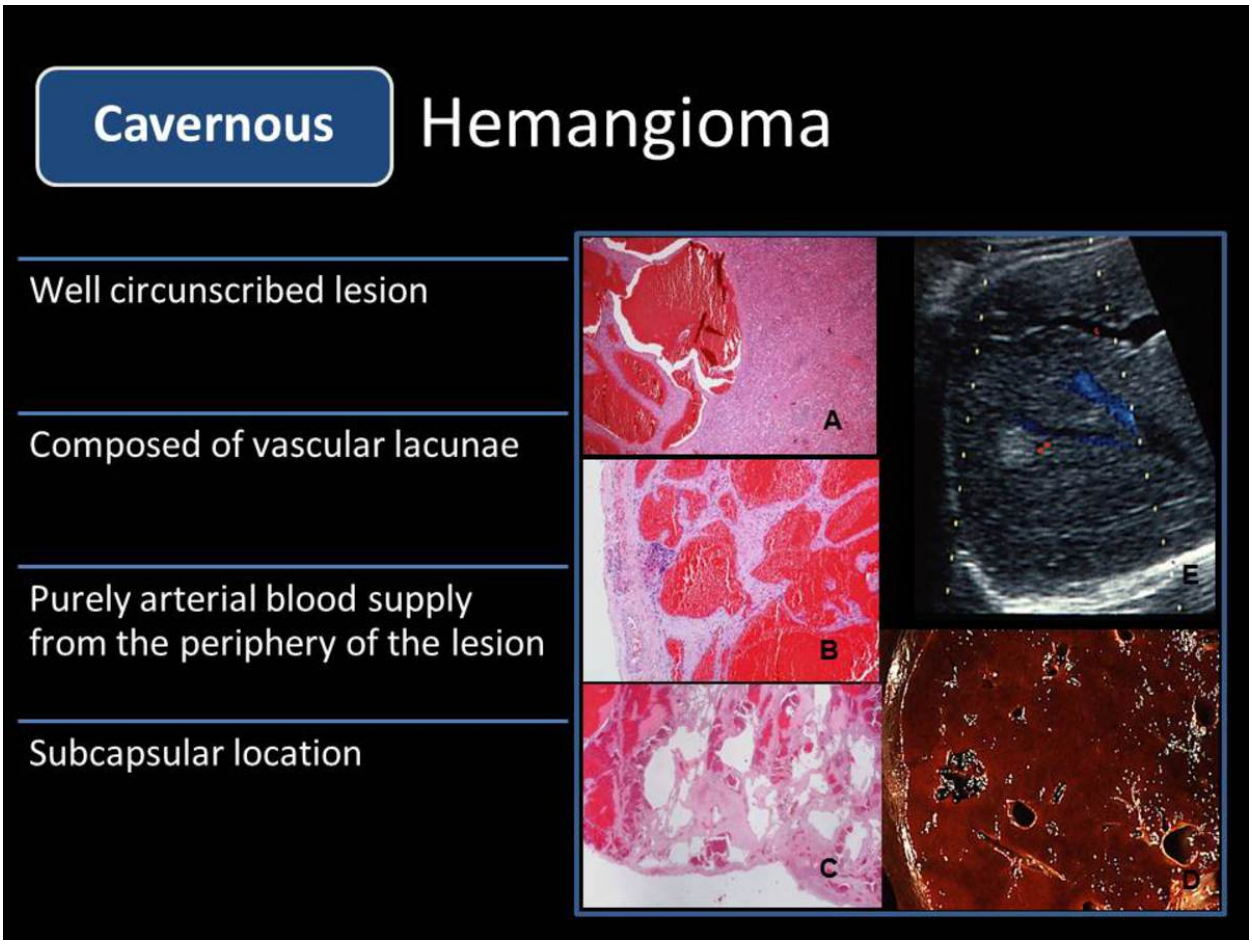

Fig. 8: A, B - Microscopic appearance: blood cells within vascular channels; C - Thin fibrous septations; D - Gross appearance: cut-section of a hemangioma demonstrates its well-defined borders. E - Ultrasound: homogeneous, hyperechoic, well defined nodule.
References: M. L. O. O. Coelho; radioogia, Porto, PORTUGAL

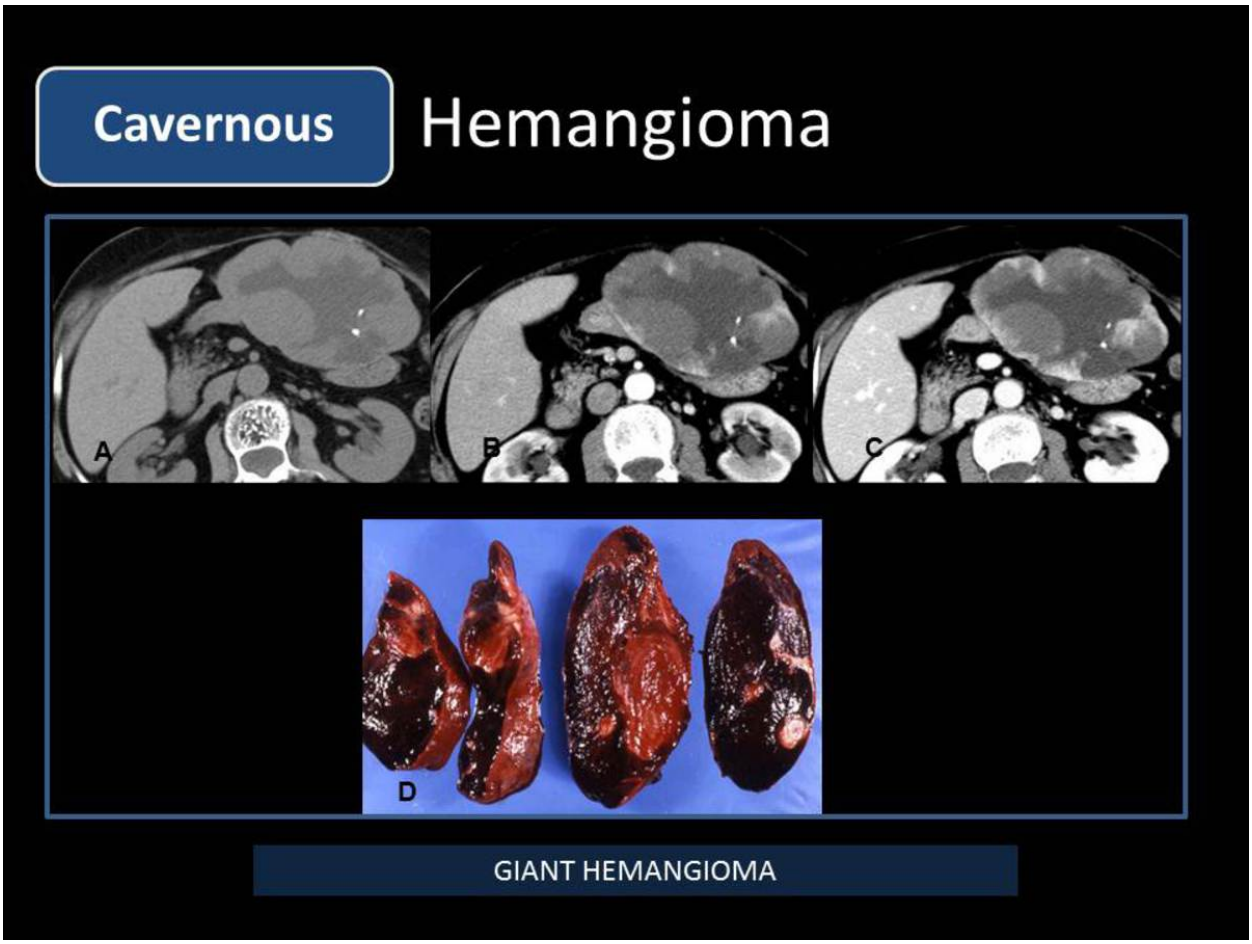

Fig. 9: A. Unenhanced CT shows a heterogeneous well-defined mass, with lobulated borders and some punctate calcifications (phleboliths) B-C. Dynamic study demonstrates progressive peripheral, globular and centripetal enhancement (arterial and venous phases) and a conspicuous central hypodense area (regressive changes) D. Pathologic specimen shows areas of internal necrosis and myxomatous degeneration

References: M. L. O. O. Coelho; radioogia, Porto, PORTUGAL

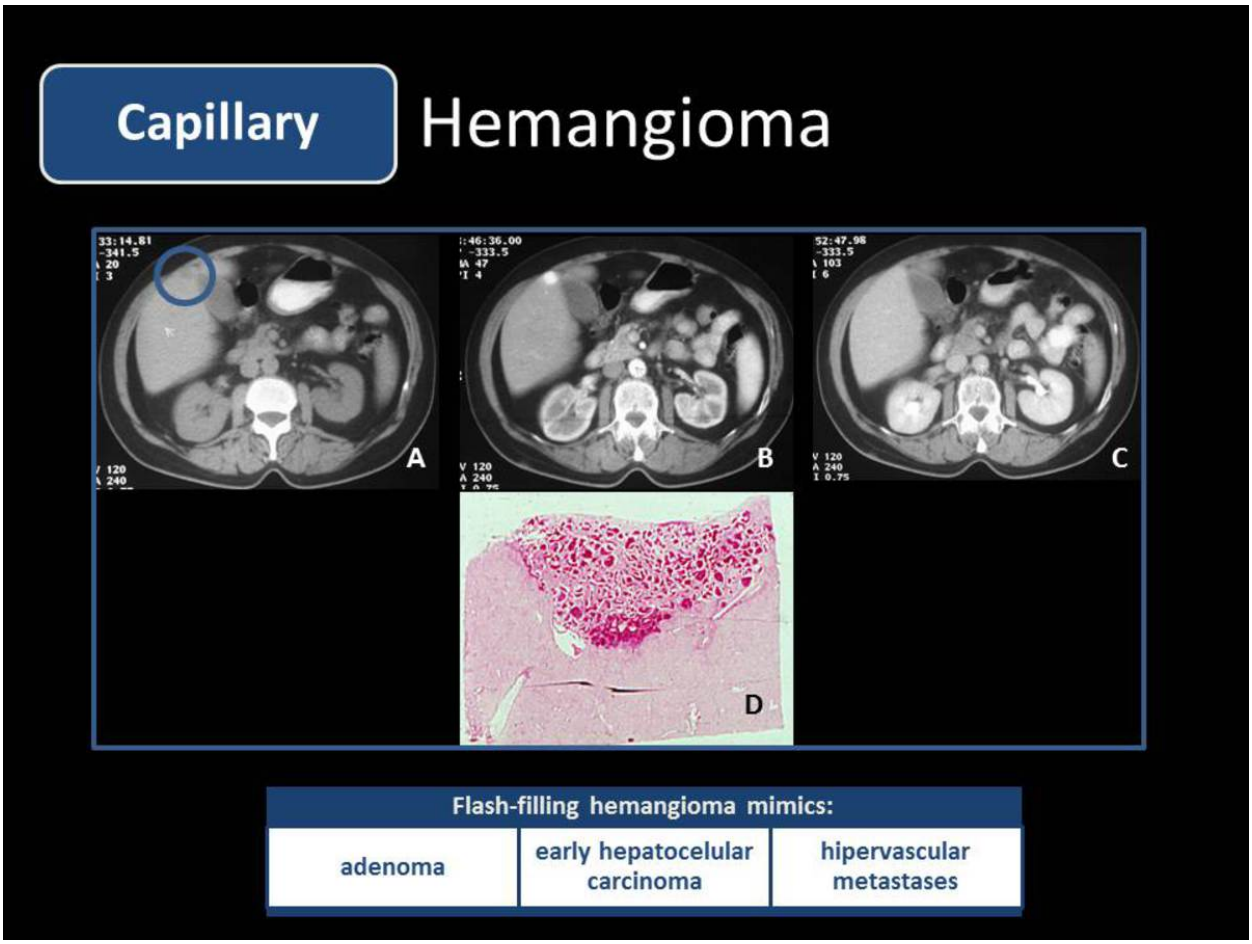

Fig. 10: A. Unenhanced CT shows slightly hypoattenuating subcapsular nodule in left lobe (1,5cm). B. Flash-filling pattern in arterial scan phase. C. Indistinct and iso-attenuating compared with the surrounding parenchyma during late phase scan. D. Microscopic appearance of capillary hemangioma.
References: M. L. O. O. Coelho; radioogia, Porto, PORTUGAL

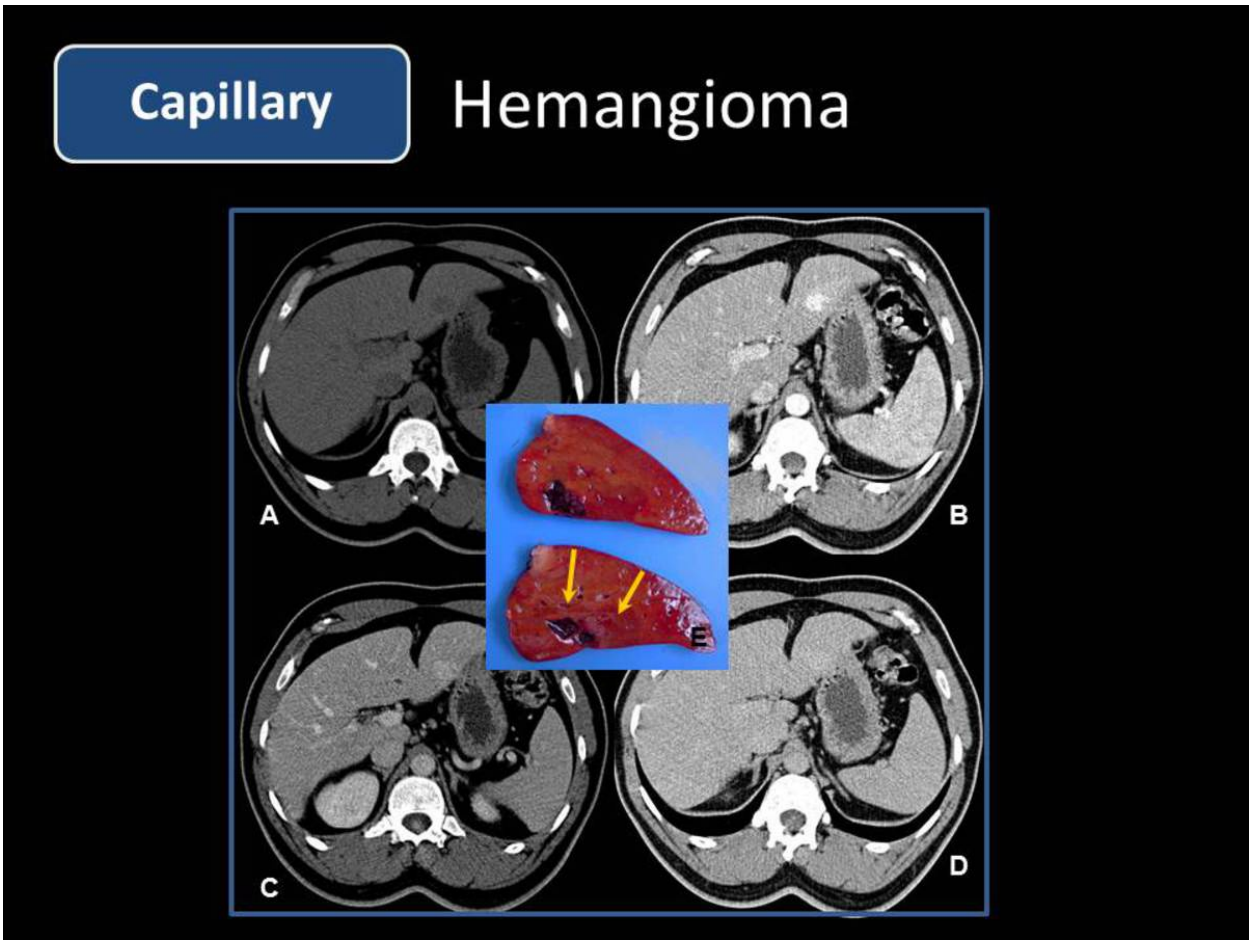

Fig. 11: A. Unenhanced CT shows slightly hypoattenuating nodule in left lobe (2cm). B. Flash-filling pattern in arterial scan phase. C. Slight hyperattenuation compared with the surrounding parenchyma during venous and late phase scan. E. Pathologic specimen shows a vascular lesion (arrows) with an eccentric thrombus within vascular spaces.

References: M. L. O. O. Coelho; radioogia, Porto, PORTUGAL

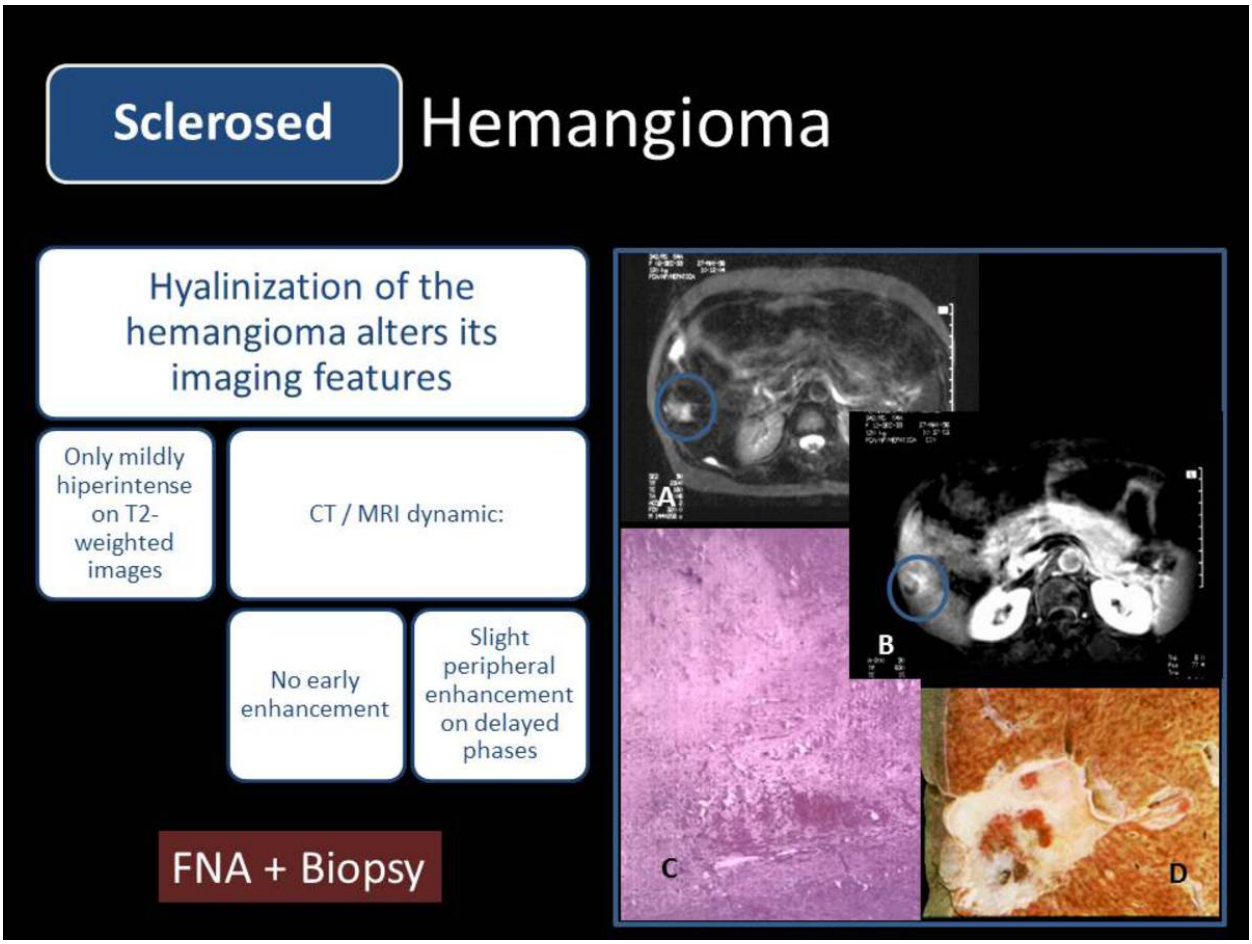

Fig. 12: A. T2-weighted MR image shows a heterogeneous lesion, less hyperintense than cerebrospinal fluid (as usual in typical hemangiomas). B. Dynamic gadolinium-enhanced T1-weighted MR image obtained at delayed phase shows peripheral enhancement. C. Photomicrograph shows dilated vessels with fibrosis. D. Hyalinised fibrotic tissue (considered the end-stage of involution of a haemangioma).
References: M. L. O. O. Coelho; radioogia, Porto, PORTUGAL

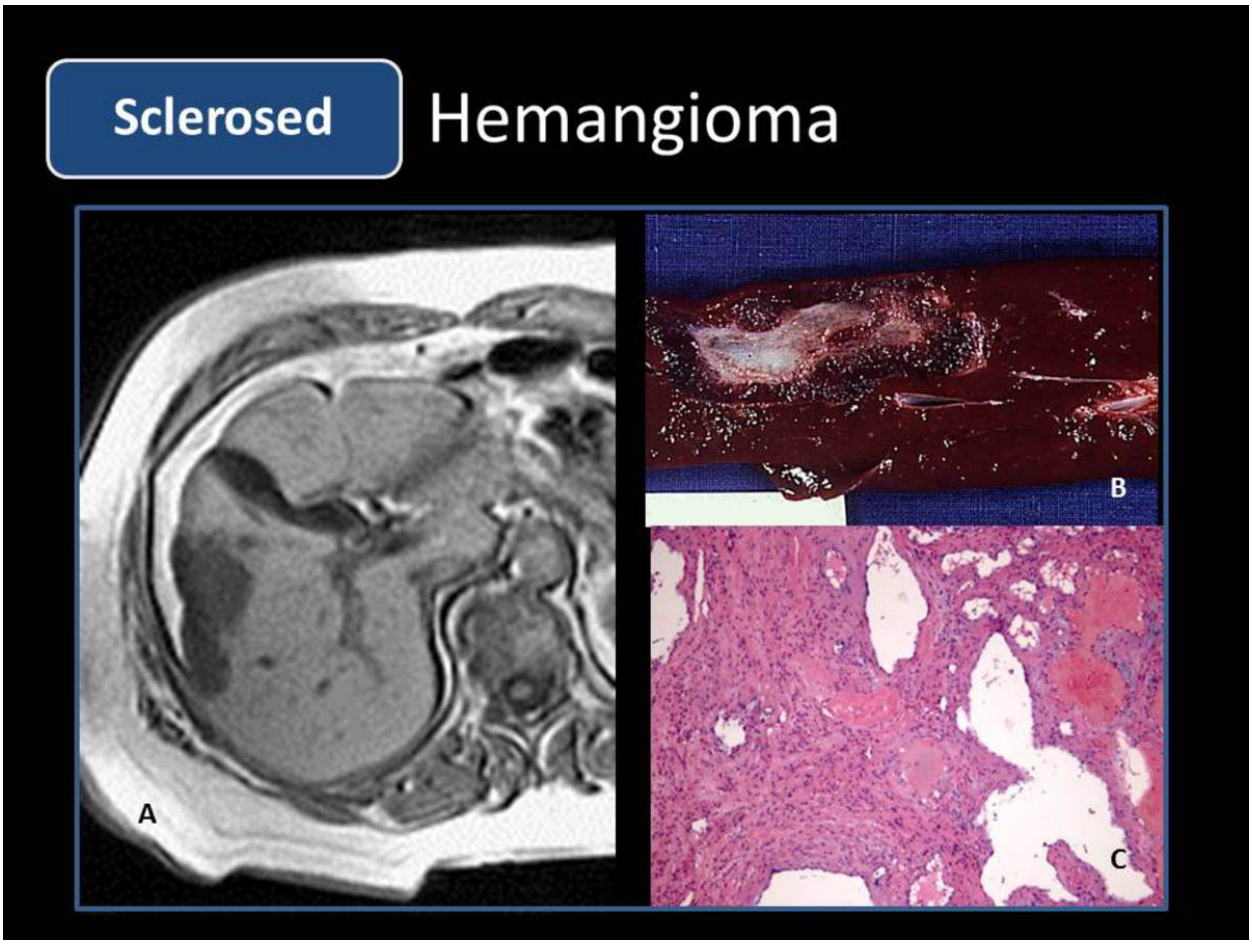

Fig. 13: 80 year-old woman with chronic-liver disease and a long- term liver mass. A. T1-weighted MR image shows lobulated liver with an irregular hypointense mass. B. Hyalinised fibrotic tissue (considered the end-stage of involution of a haemangioma). C. Photomicrograph shows dilated vessels with fibrosis
References: M. L. O. O. Coelho; radioogia, Porto, PORTUGAL

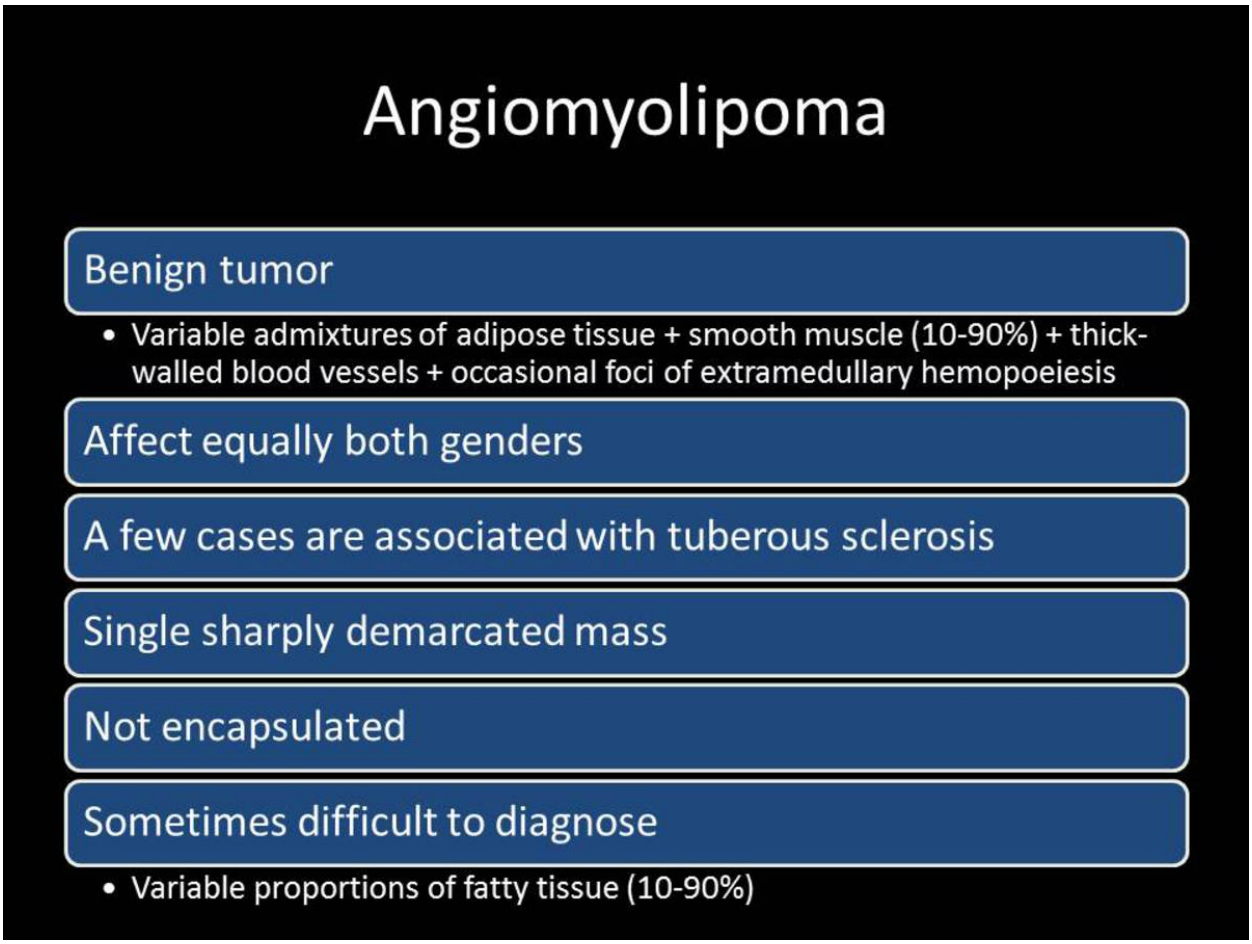

Fig. 14: 14
References: M. L. O. O. Coelho; radioogia, Porto, PORTUGAL

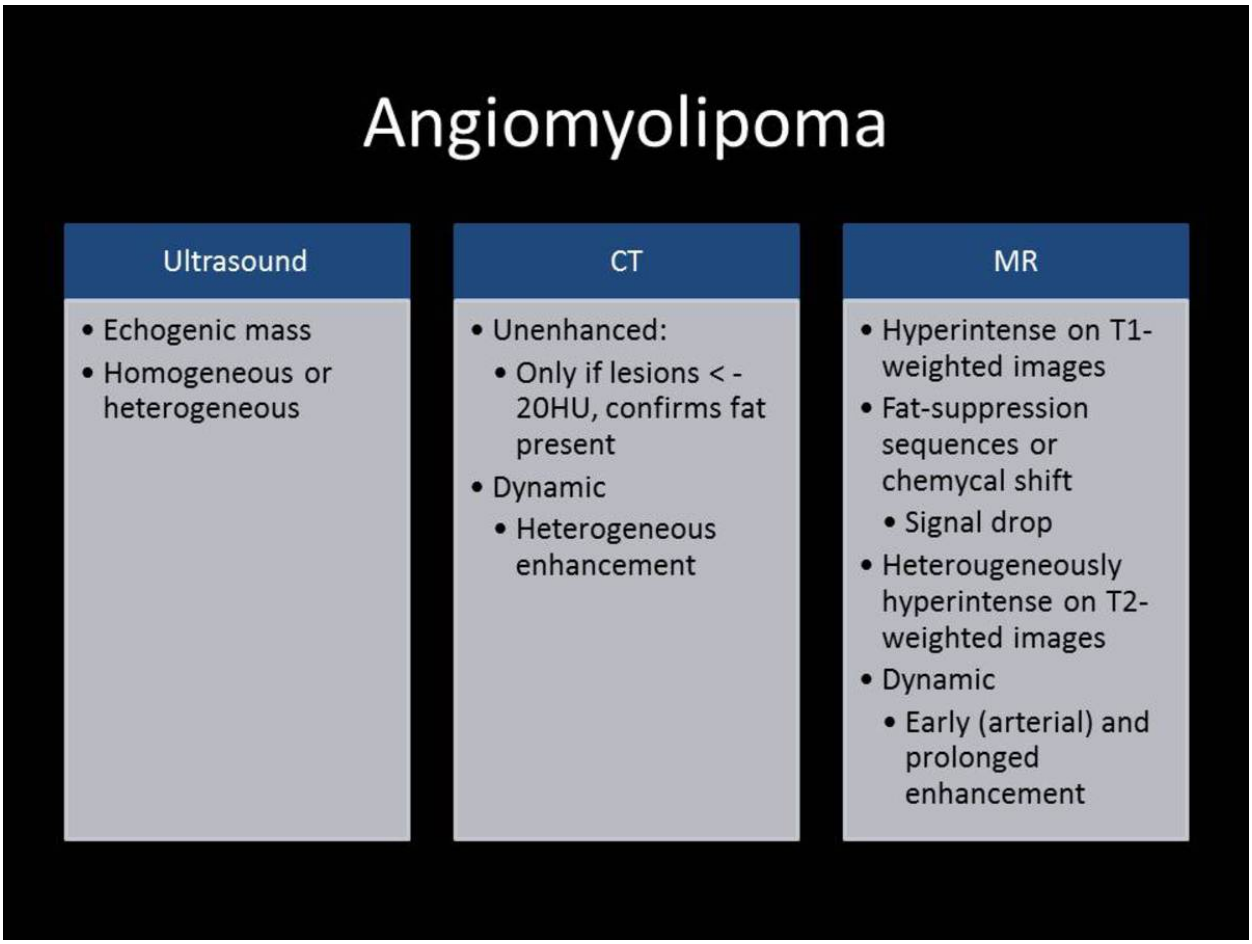

Fig. 15: 15
References: M. L. O. O. Coelho; radioogia, Porto, PORTUGAL

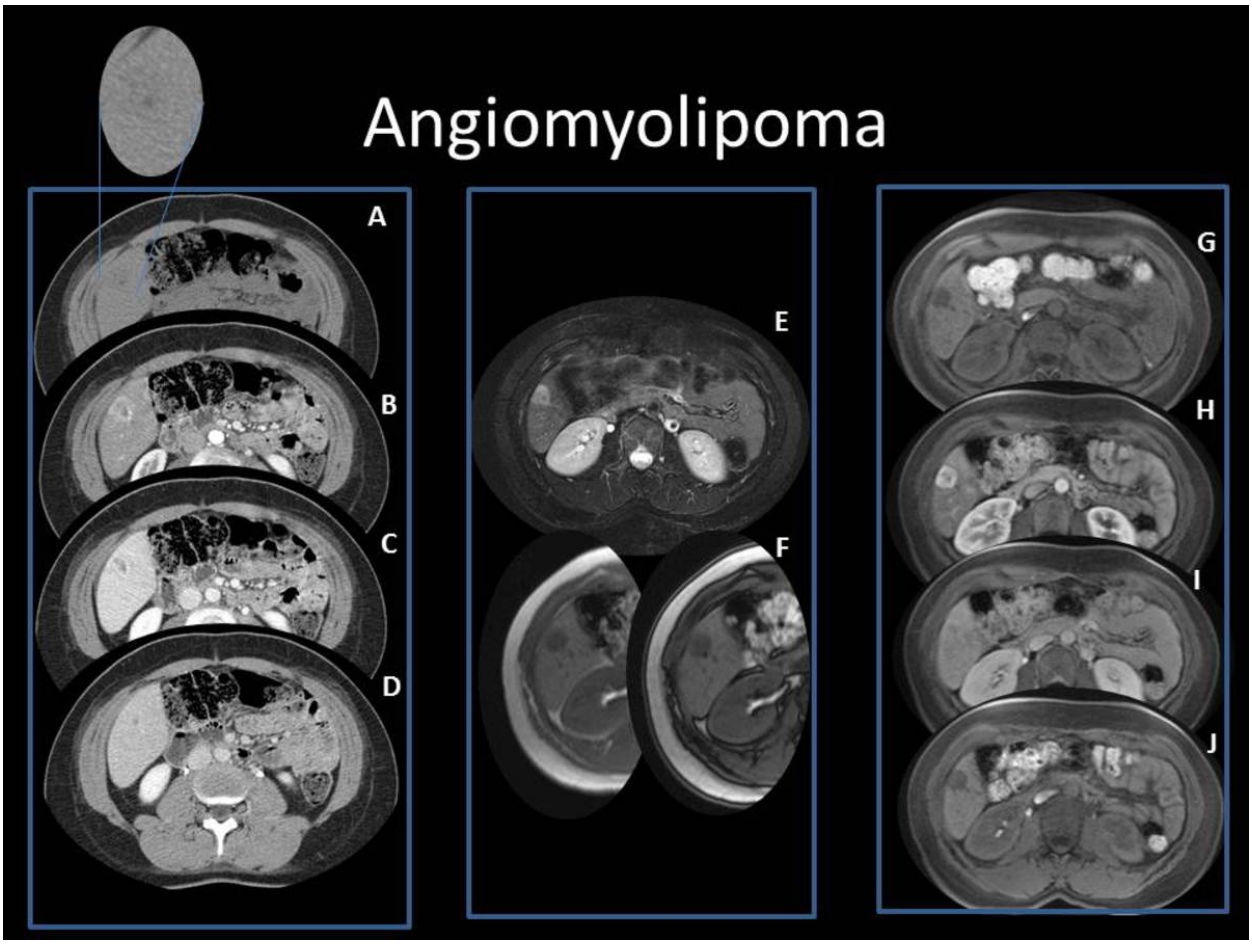

Fig. 16: A - Unenhanced CT image shows a hypoattenuating lesion with an area of fat attenuation. Arterial phase scan (B) shows marked enhancement. C, D - Slight hyperattenuation compared with the surrounding parenchyma during venous and late phase scan of the nonfat component. E - T2 weighted axial MR images shows a hyperintense mass. Axial T1 weighted MR images (F) shows that only a small spot of the lesion reveals drop signal on out-of-phase image. G - Unhenhanced axial T1 weighted MR image. H, I, J - Gd-EOB-DTPA-enhanced images: arterial phase shows marked enhancement, but at the hepatobiliary phase the lesion becomes hypointense (it does not have hepatocytes).

References: M. L. O. O. Coelho; radioogia, Porto, PORTUGAL

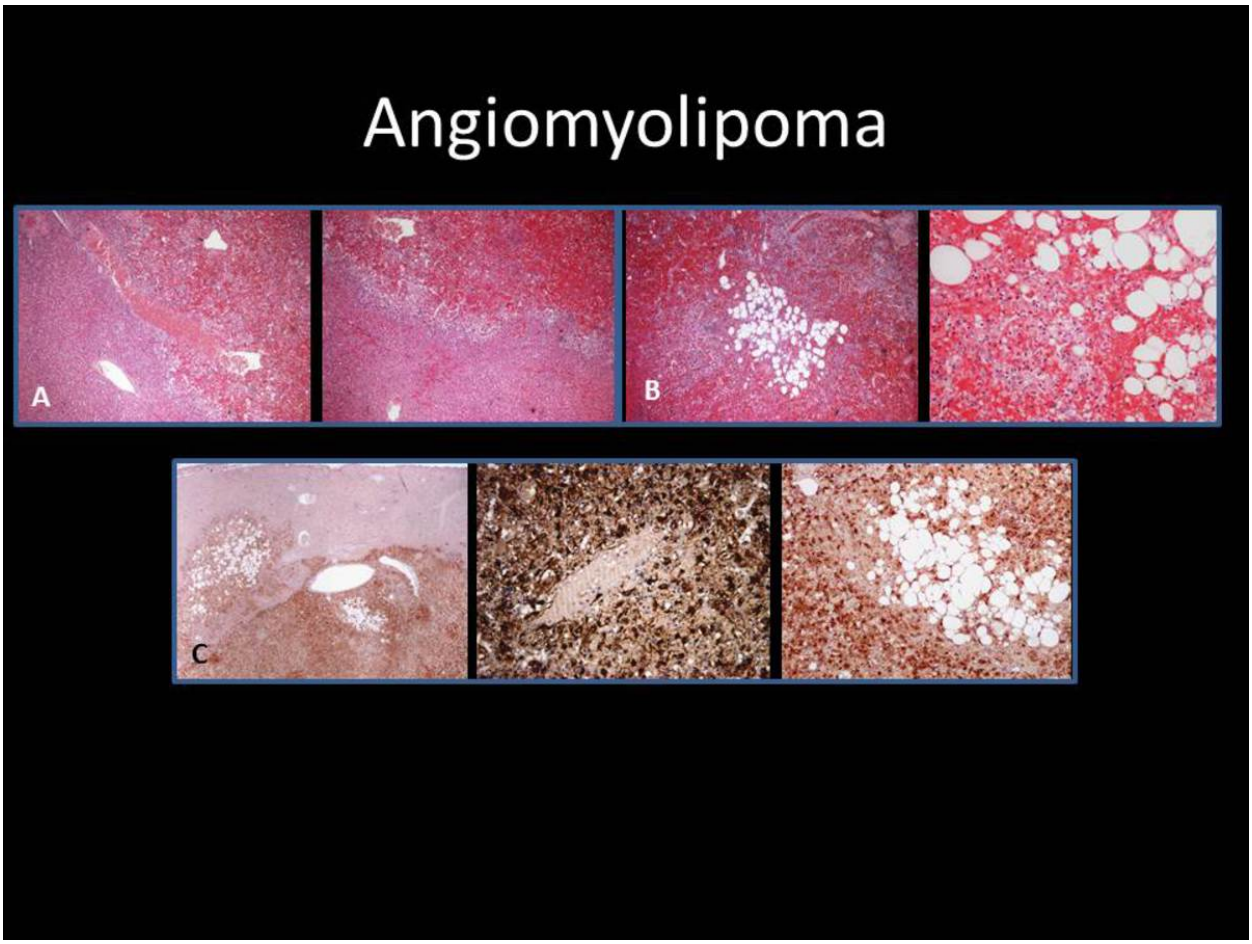

Fig. 17: A. Photomicrographs: show the well demarcated limits of the lesion; B. - High-power photomicrographs show the components of the lesion: adipose tissue, epithelioid (muscular component) and blood vessels. C. High-power photomicrograph immunohistochemical studies show positivity for human melanocyte-specific antibody HMB45, supporting the diagnosis (different magnifications).
References: M. L. O. O. Coelho; radioogia, Porto, PORTUGAL

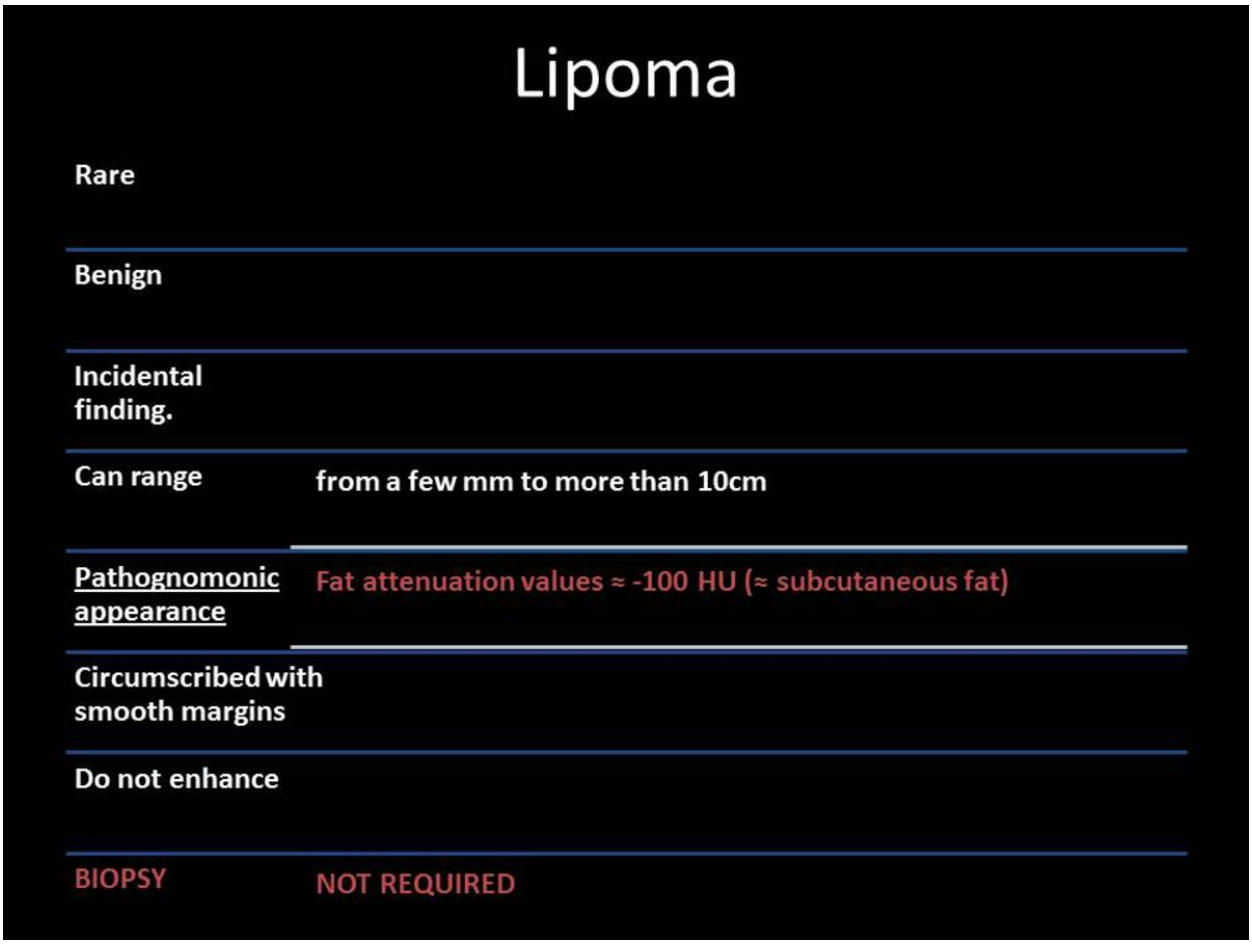

Fig. 18: 18
References: M. L. O. O. Coelho; radioogia, Porto, PORTUGAL

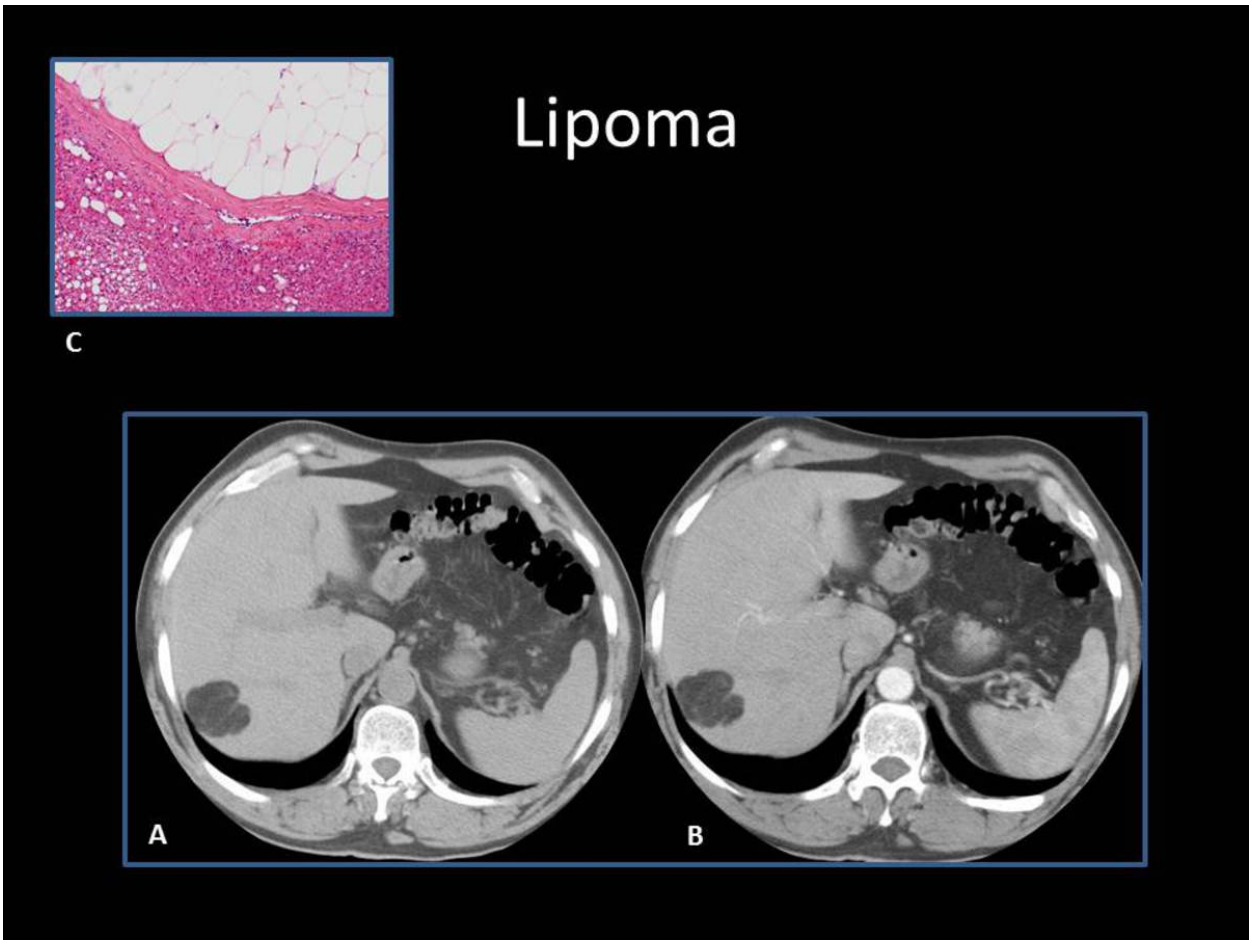

Fig. 19: A. Unenhanced-CT shows a fat density hypoattenuating mass in the right liver lobe. B. In enhanced-CT study the lesion shows no enhancement. C. - High-power photomicrograph shows fat cells limited by a capsule.
References: M. L. O. O. Coelho; radioogia, Porto, PORTUGAL

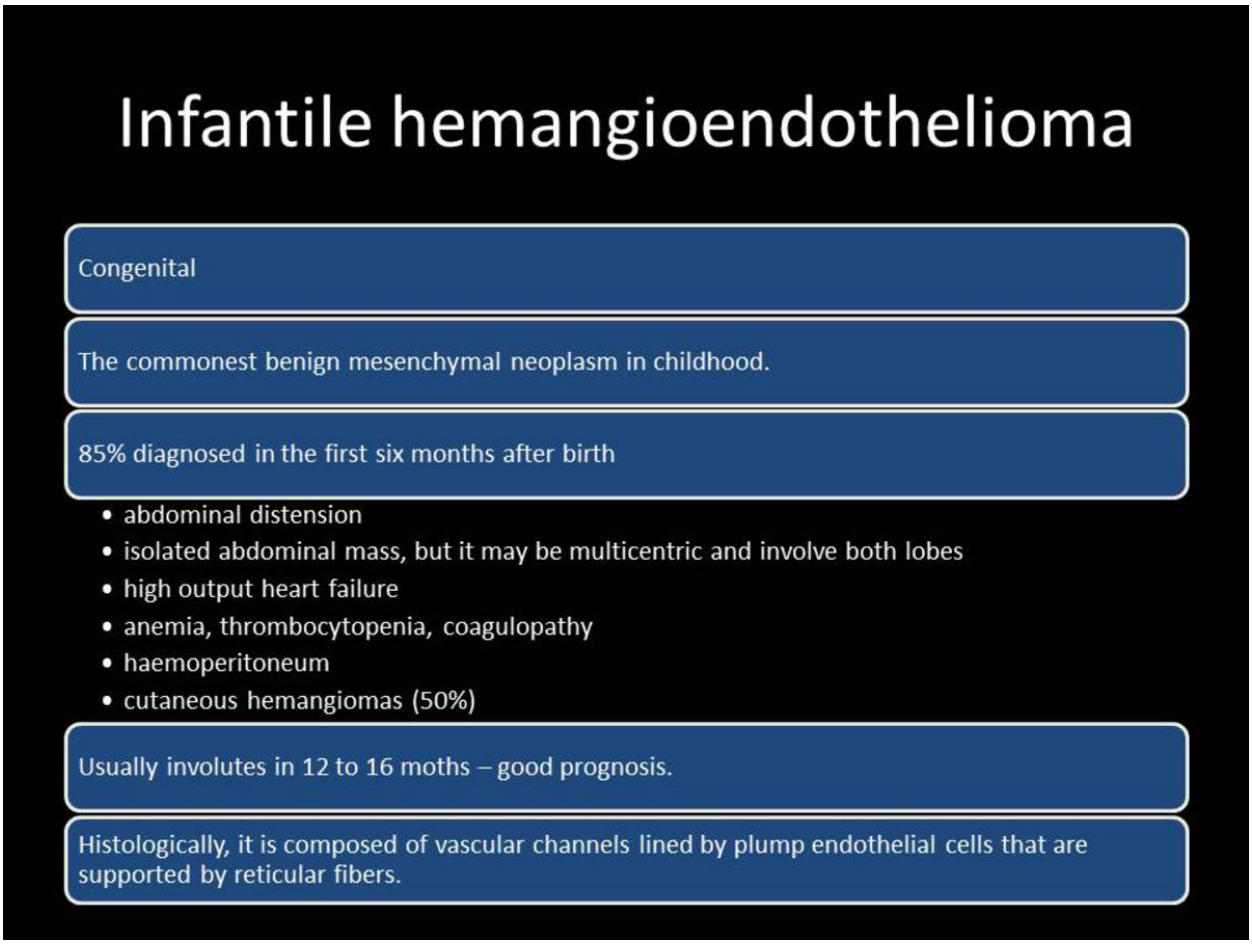

Fig. 20: 20
References: M. L. O. O. Coelho; radioogia, Porto, PORTUGAL

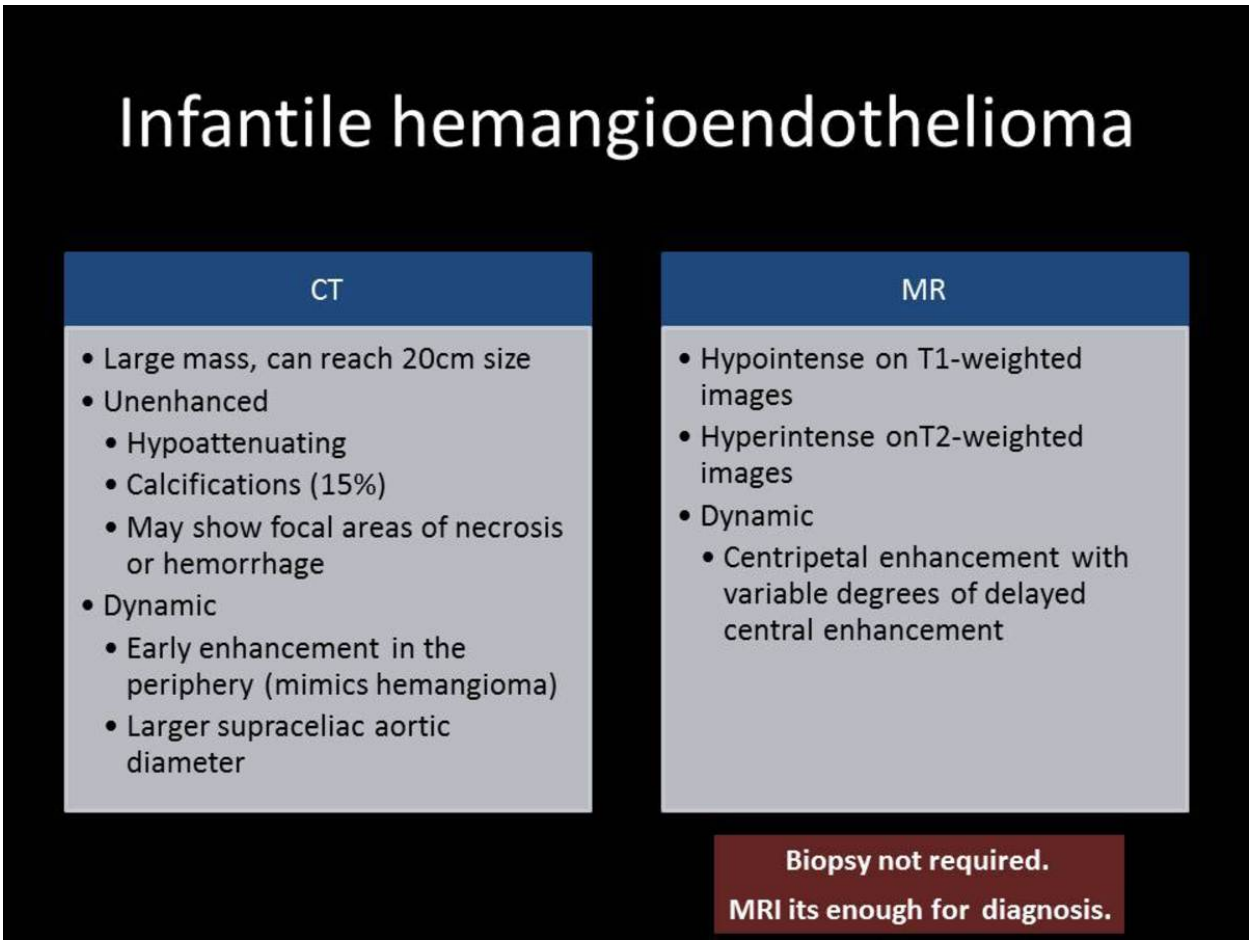

Fig. 21: 21
References: M. L. O. O. Coelho; radioogia, Porto, PORTUGAL

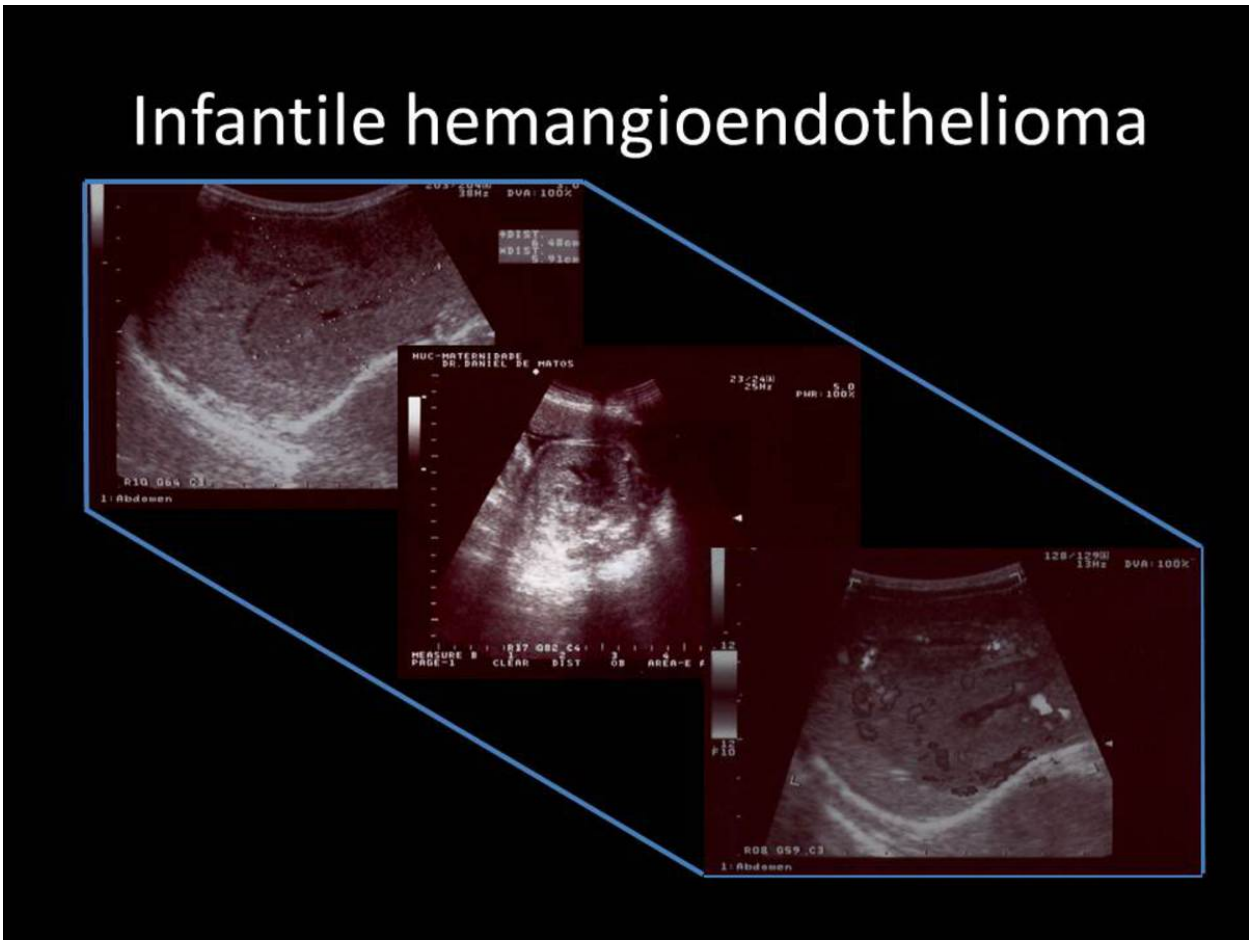

Fig. 22: Obstetric US (26th week-gestation) shows a nodular hypoechoic lesion in the liver. B. After birth US confirms the right liver lobe mass with lobulated borders. C. US-Doppler demonstrates a hypervascular lesion.
References: M. L. O. O. Coelho; radioogia, Porto, PORTUGAL

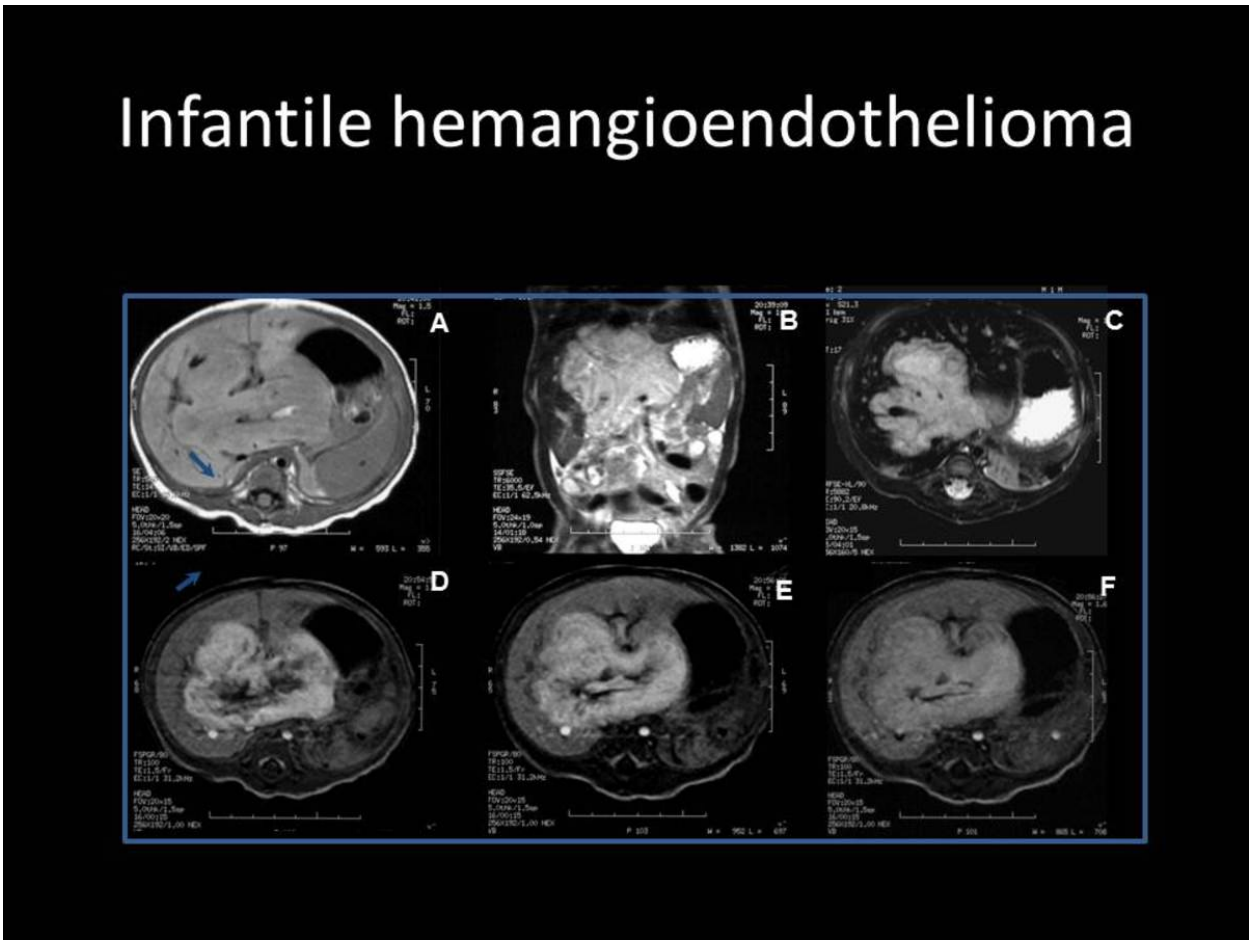

Fig. 23: A. On T1-weighted image the mass shows slight heterogeneous isointense signal and mild hyperintensity on the T2-WI (B,C). In Dynamic MR study (D-F) it shows a peripheral, ill-defined and irregular hyperenhancement. The signal intensity then decreases, until the late interstitial phase of liver enhancement, when the lesion is only slightly hyperintense. After 2 years of treatment with interferon the tumor completely disappeared.

References: M. L. O. O. Coelho; radioogia, Porto, PORTUGAL

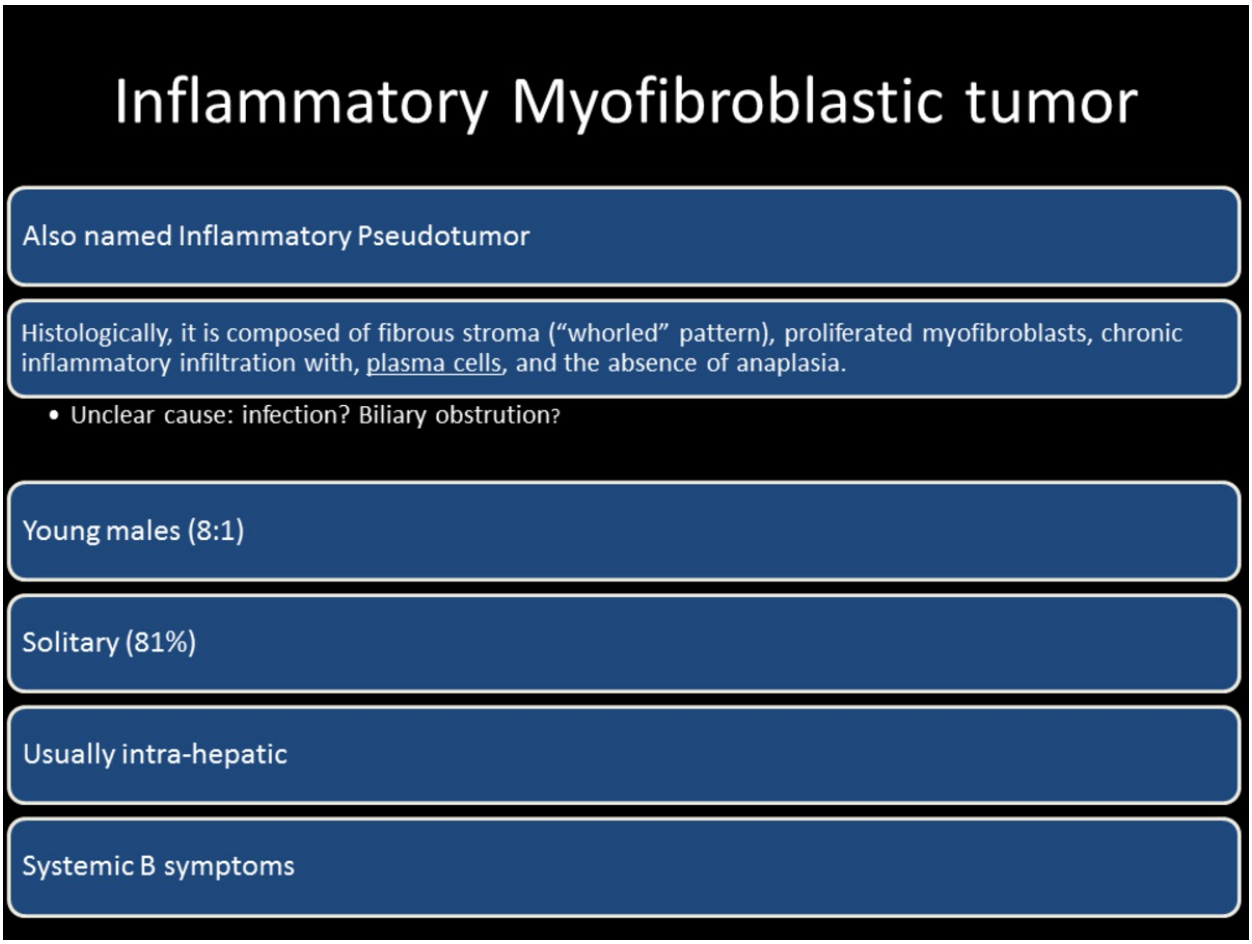

Fig. 24: 24
References: M. L. O. O. Coelho; radioogia, Porto, PORTUGAL

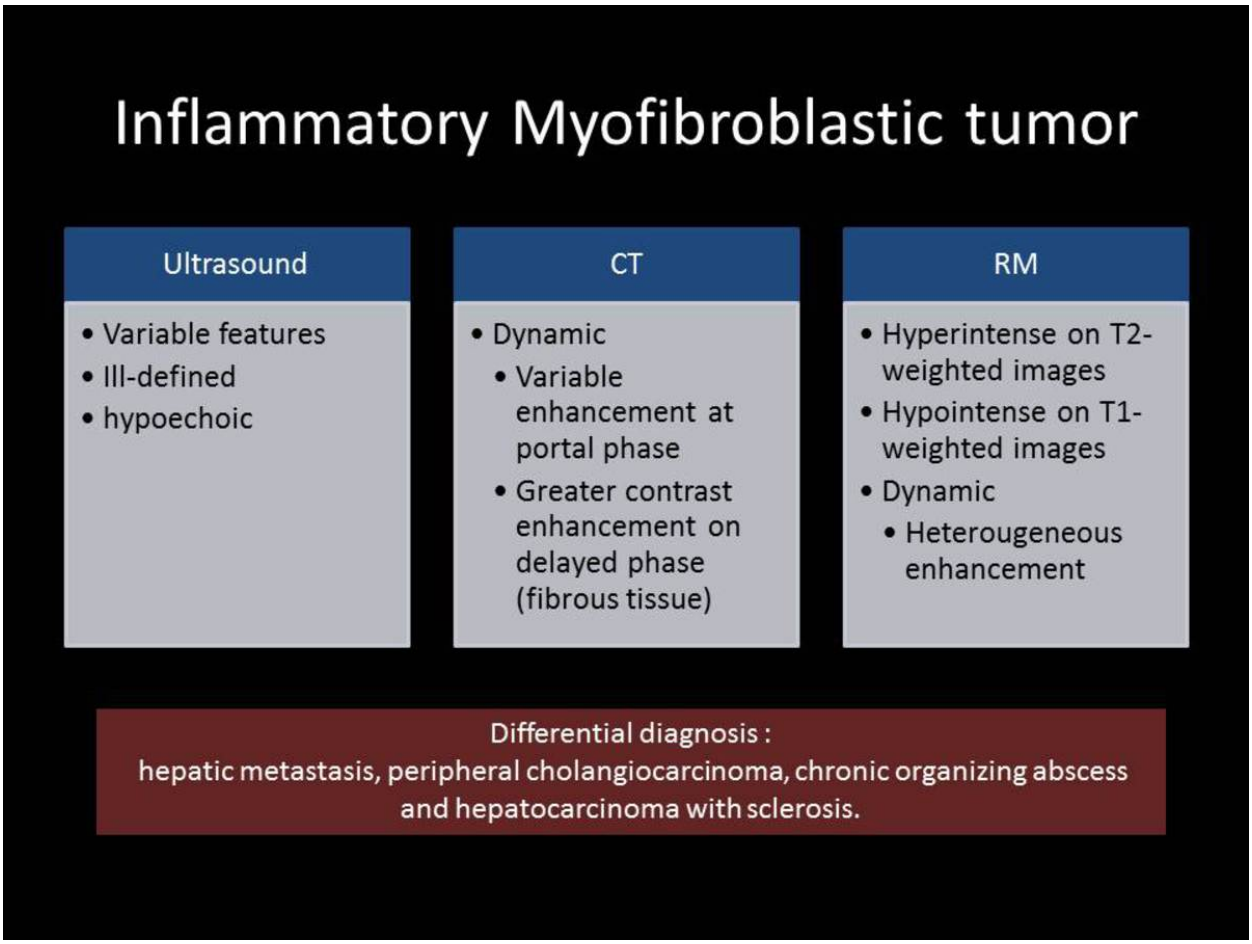

Fig. 25: 25
References: M. L. O. O. Coelho; radioogia, Porto, PORTUGAL

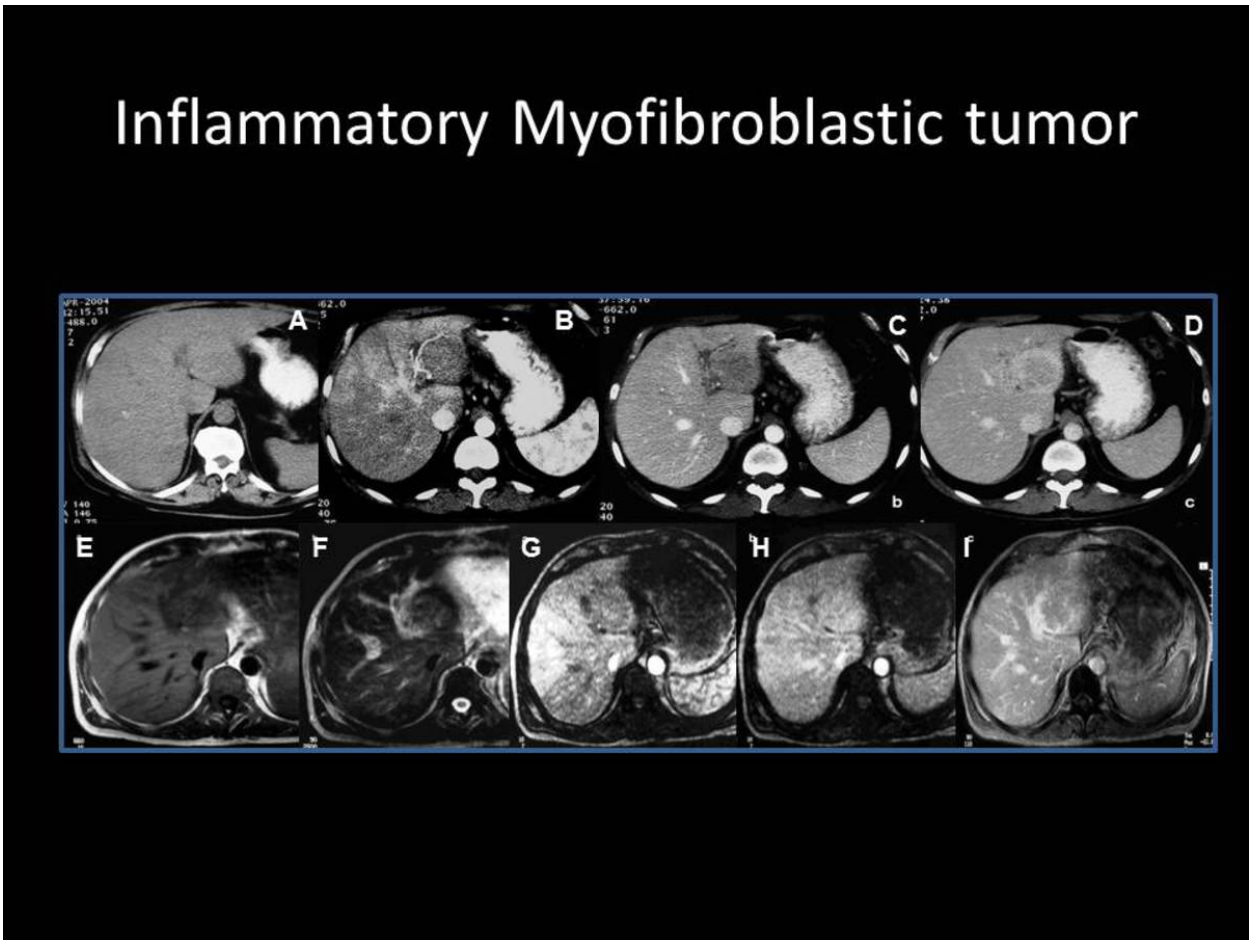

Fig. 26: 53 year-old man presented after 3 months with low grade fever, weight loss, general fatigue and upper abdominal pain. A. Unenhanced CT shows an isoattenuating mass in the left liver lobe. B-D. In dynamic CT study the lesion is heterogeneously hypodense at the arterial and portal venous phases of the dynamic liver study. In the delayed phase, a broad peripheral hyperdense halo was noted. E, F In T1-weighted image the mass appears heterogeneous with slight hyperintensity on the T2-WI. G-I. In Dynamic MR study it shows hypovascularity, with a peripheral ill-defined and irregular rim noted on the late interstitial phase of liver enhancement.
References: M. L. O. O. Coelho; radioogia, Porto, PORTUGAL

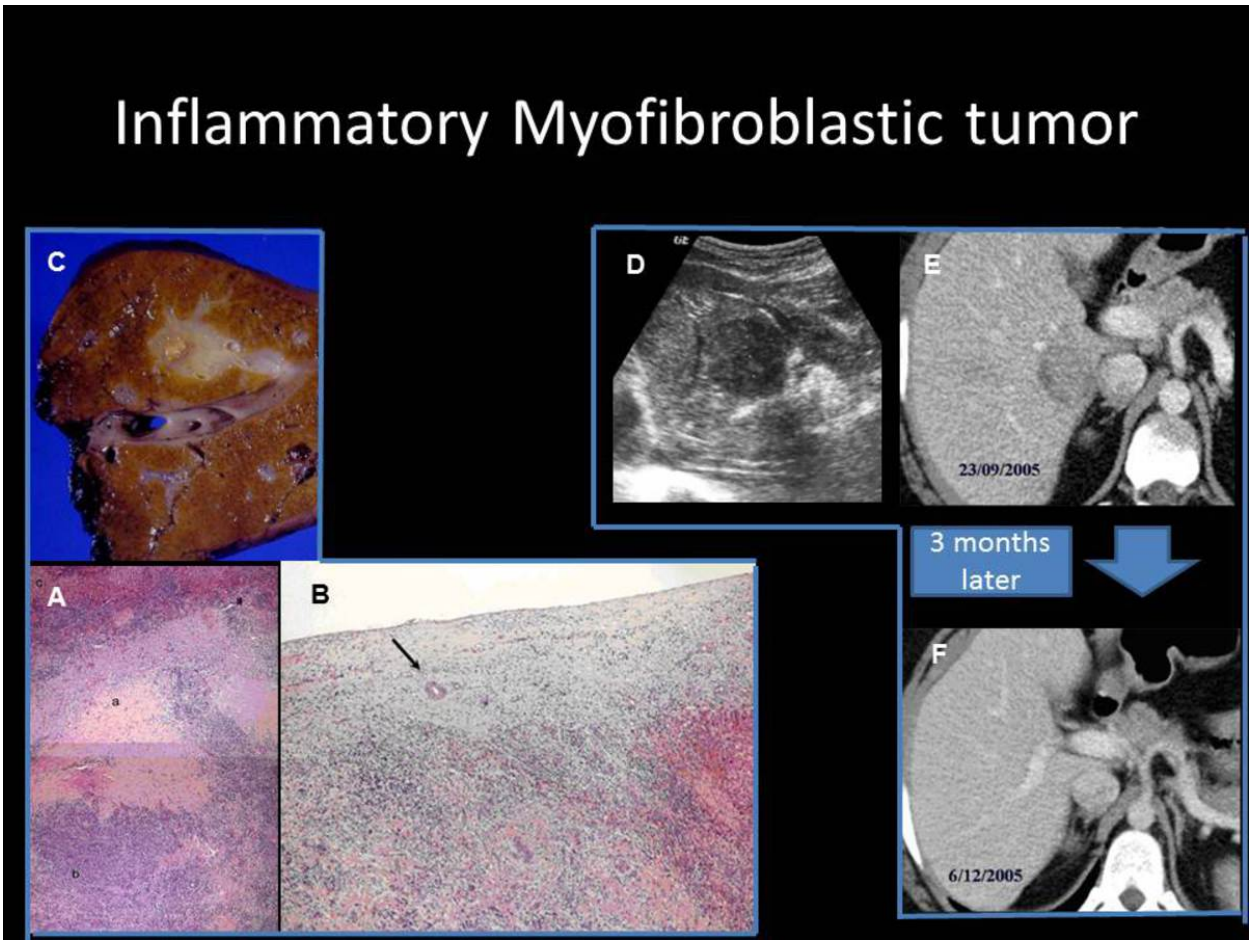

Fig. 27: A. Composed high-power photomicrograph shows prominent fibrosis and proliferating myofibroblasts at the periphery of the mass (a) contrasting with a cellular lymphoplasmocytic infiltrate central core (b). The liver parenchyma away from the disease process has normal arquitecture (c). B. High-power photomicrograph. Portal tracts are expanded by fibrosis and granulation tissue, with occlusive phlebitis (arrow). C. Pathologic specimen showing a tender heterogeneous mass with a yellowish, smooth core surrounded by an ill-defined hyperemic halo. D. US: the mass is relatively well-defined, heterogeneous and hypoechoic. E, F: A follow-up CT scan 2 months later performed after a course of antibiotics and anti-inflammatory drugs, showed complete resolution of the lesions.

References: M. L. O. O. Coelho; radioogia, Porto, PORTUGAL

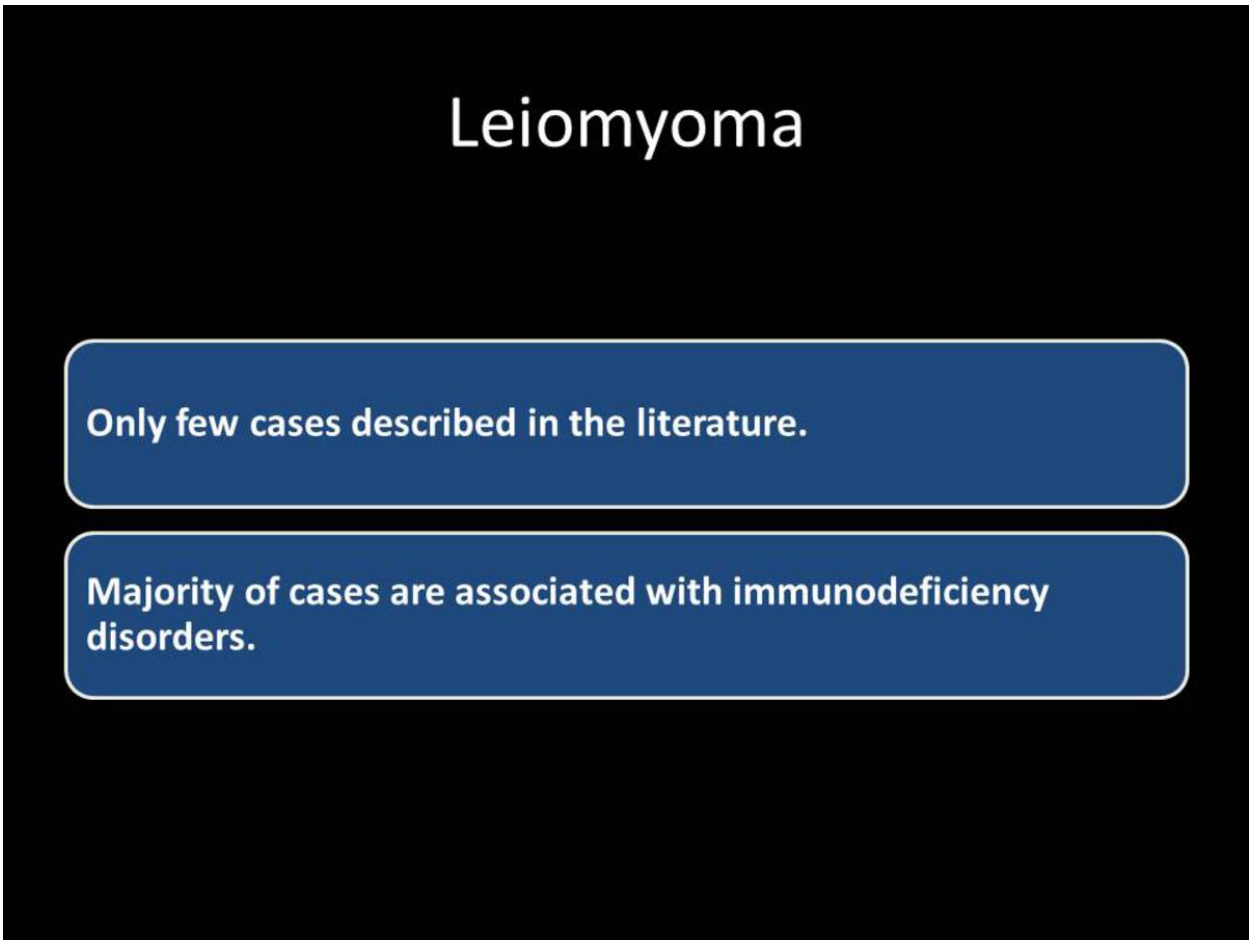

Fig. 28: 28
References: M. L. O. O. Coelho; radioogia, Porto, PORTUGAL

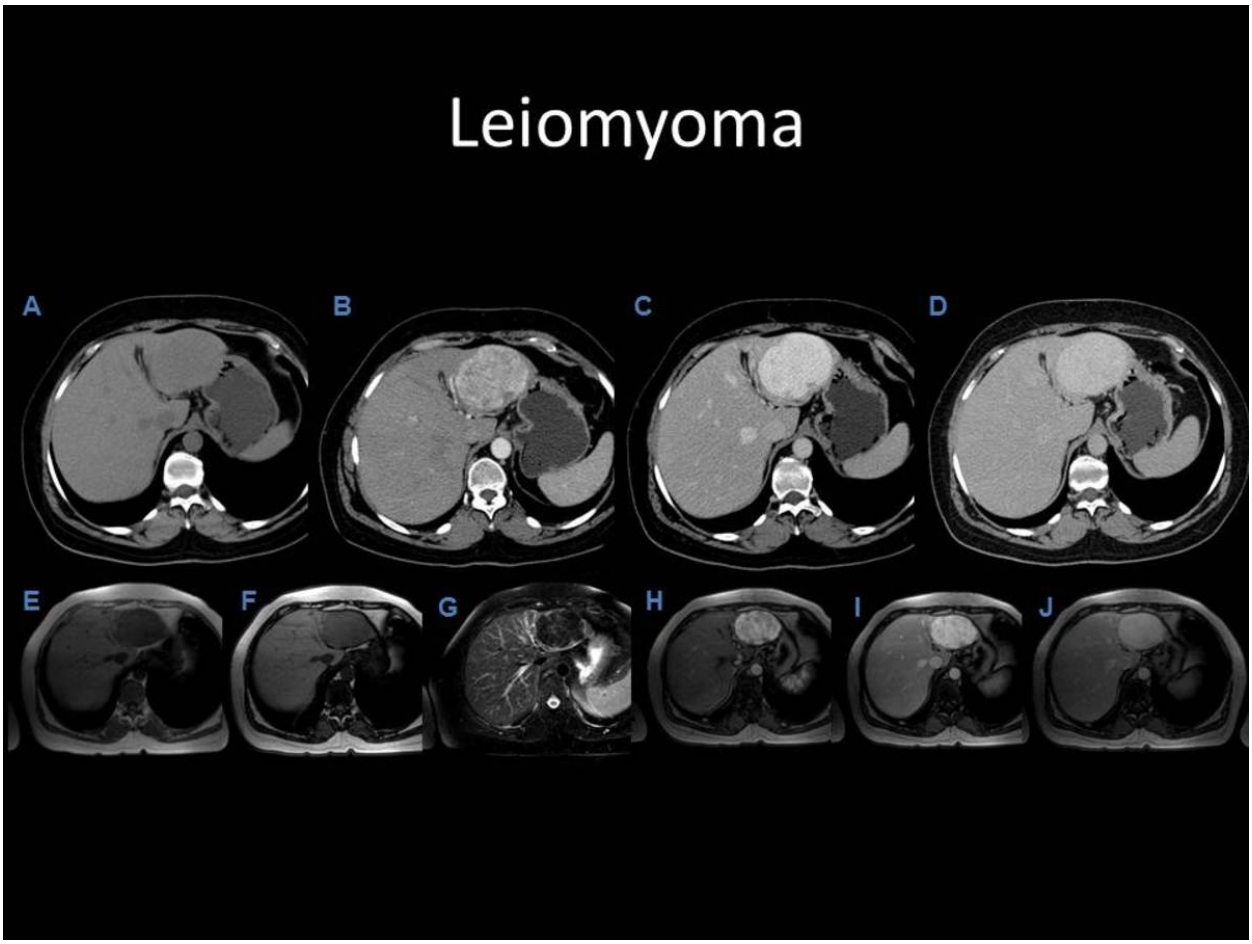

Fig. 29: 61-year old woman with an asymptomatic epigastric mass. A. Unenhanced CT shows an isoattenuating left lobe mass. B-D. In dynamic CT study it shows a marked, progressive and homogeneous enhancement throughout the liver enhancement phases. E,F Axial T1 weighted in-phase and out-of-phase MR images show low signal intensity. G. T2 fat-saturated weighted axial MR image shows also low signal intensity. H-J. In Dynamic MR study the lesion shows identical behaviour as on the CT scan.

References: M. L. O. O. Coelho; radioogia, Porto, PORTUGAL

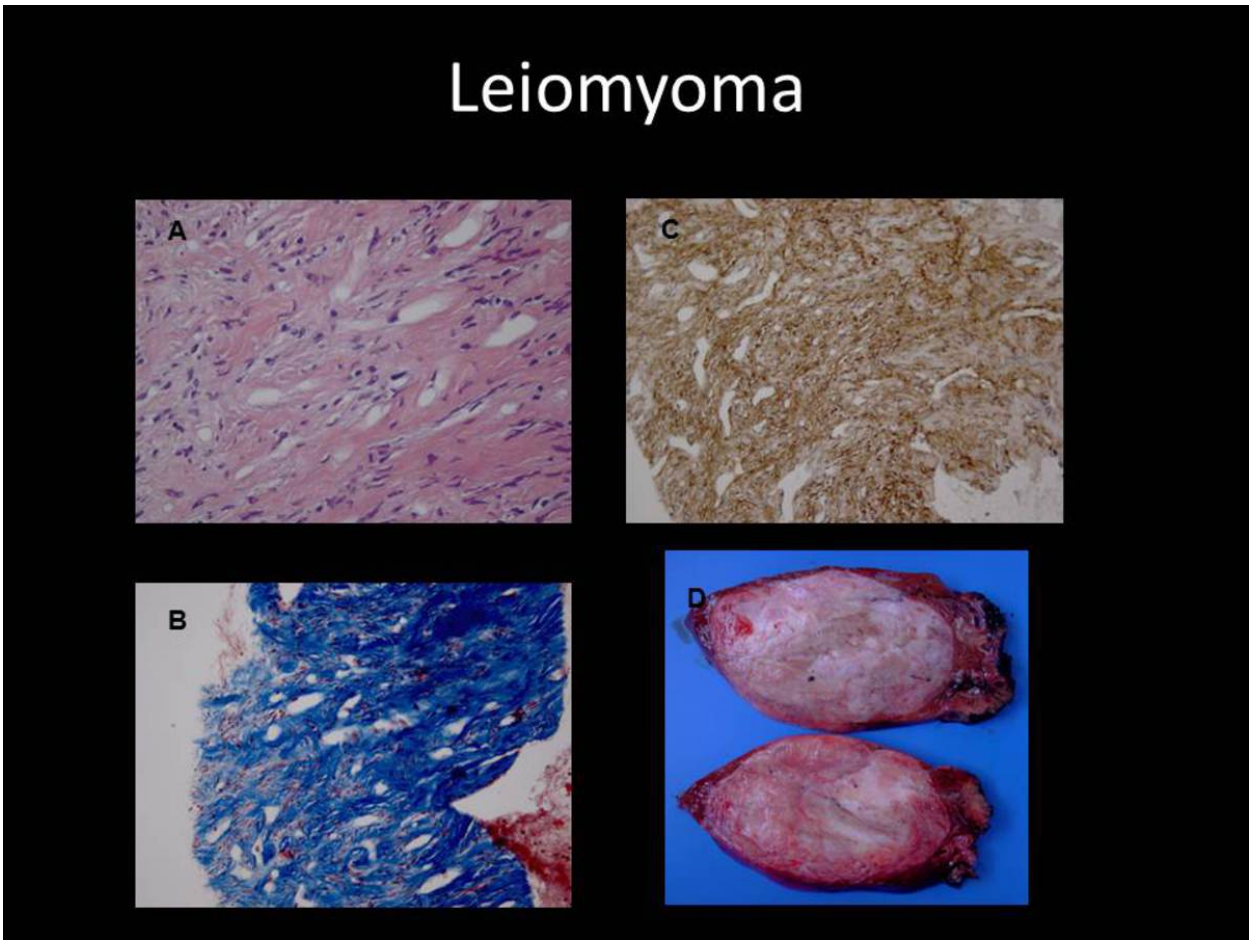

Fig. 30: High-power photomicrographs. A. Smooth muscle fibers without atypia. Histochemical study positive for trichrome (B) and for smooth muscle actin (C). D. Pathologic specimen the left liver lobe mass.
References: M. L. O. O. Coelho; radioogia, Porto, PORTUGAL

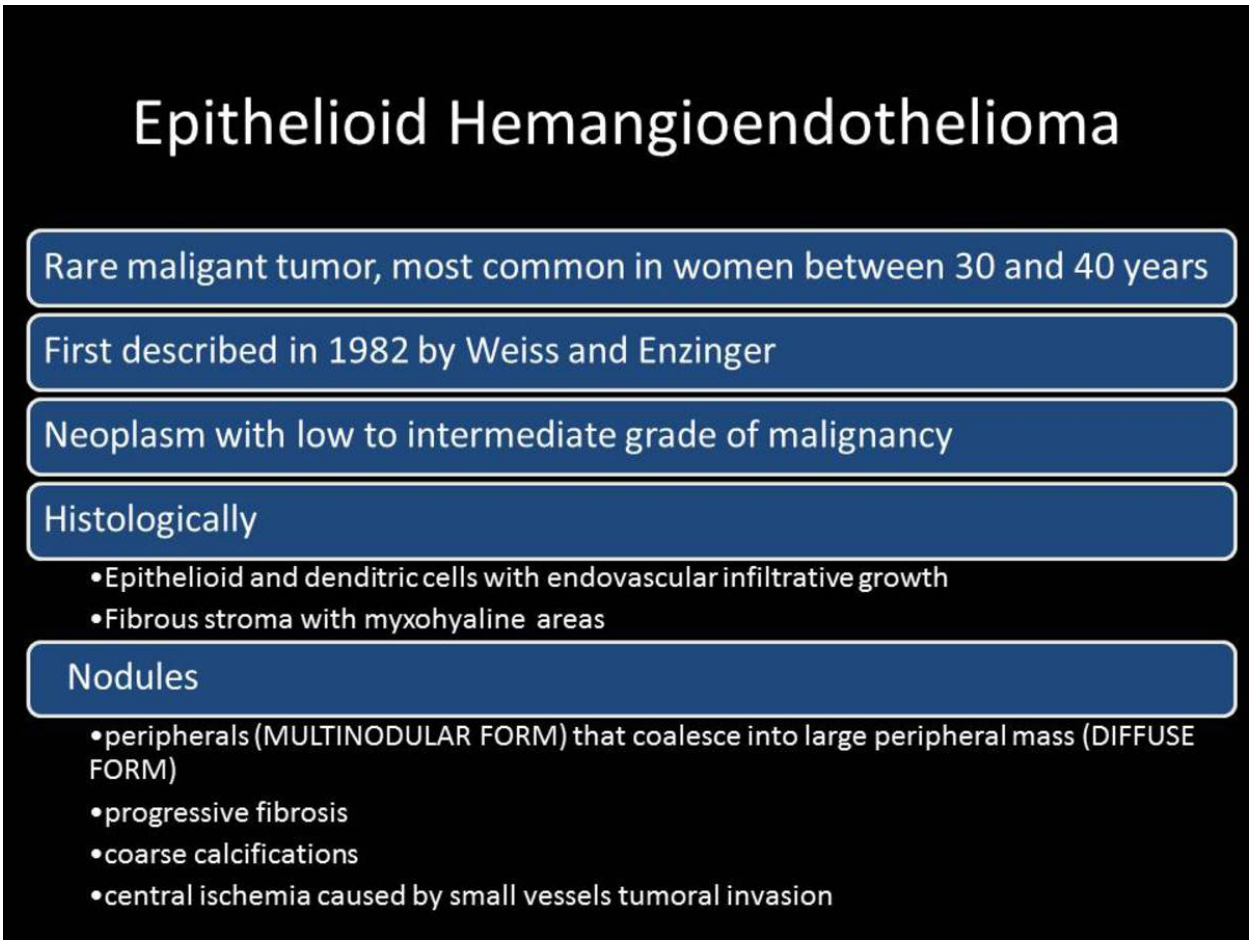

Fig. 31: 31
References: M. L. O. O. Coelho; radioogia, Porto, PORTUGAL

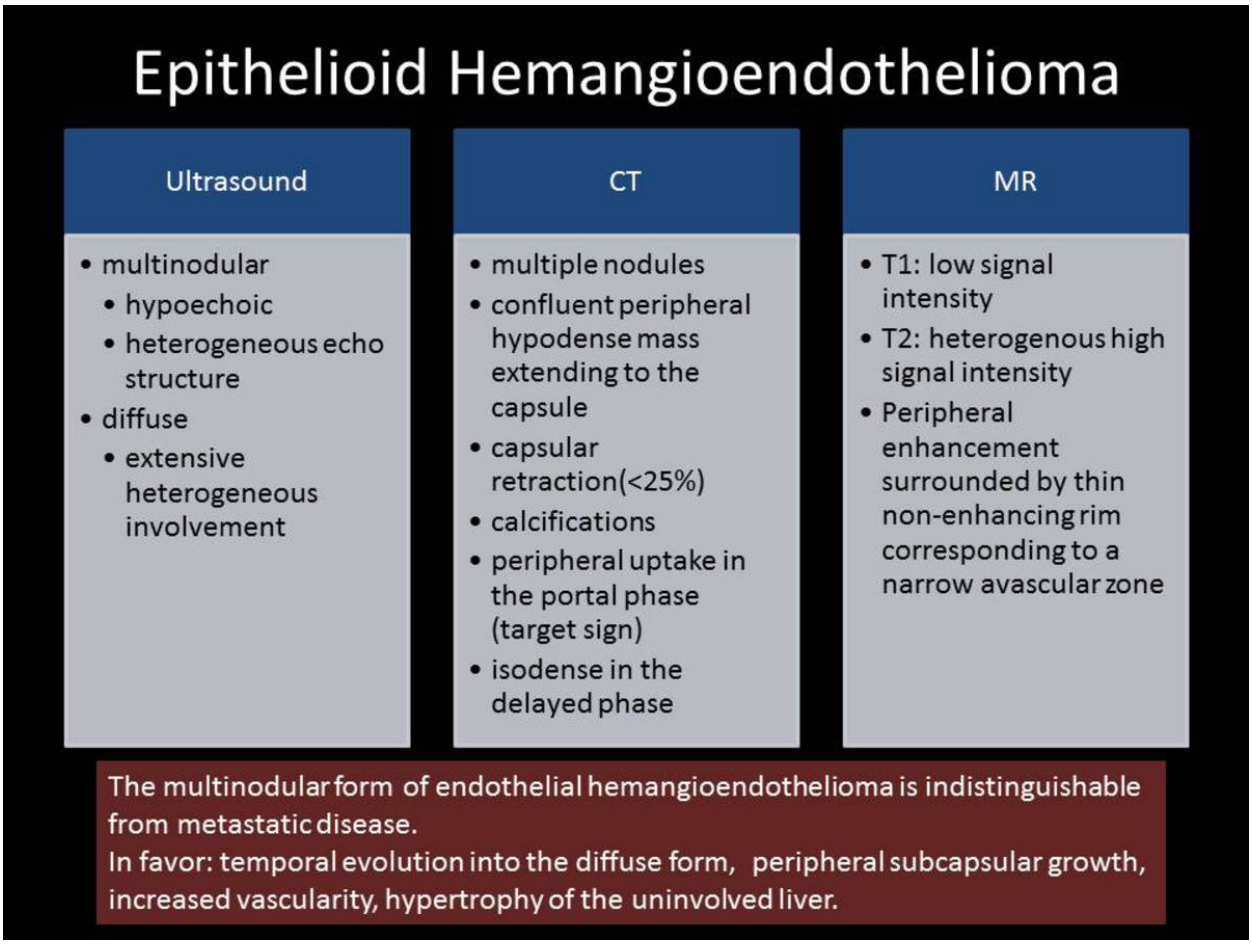

Fig. 32: 32
References: M. L. O. O. Coelho; radioogia, Porto, PORTUGAL

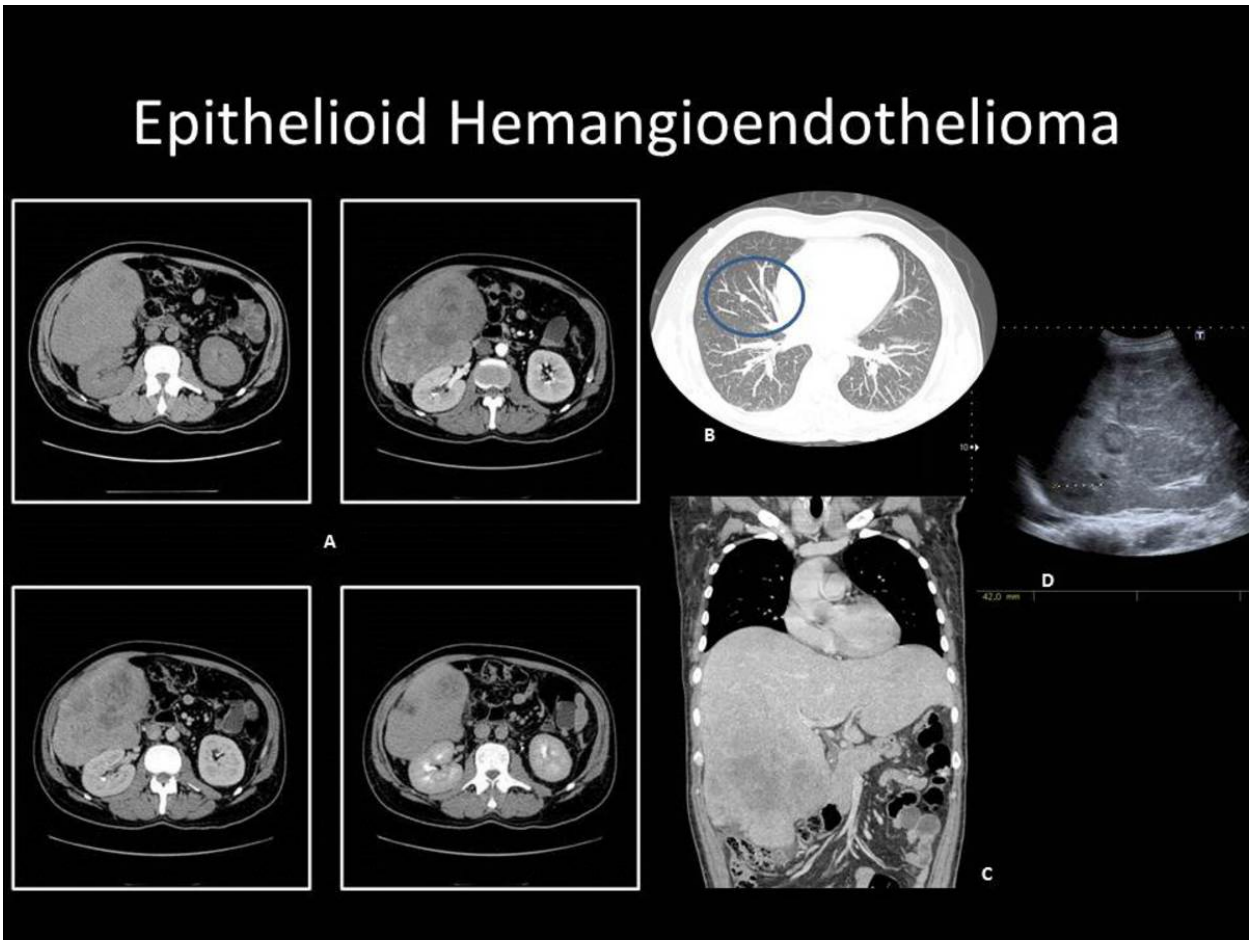

Fig. 33: A - Axial abdominal CT images: lobulated liver contour, with capsular shrinkage and exophytic nodules. There are peripheral areas that suffer moderate enhancement on arterial phase, with centripetal progression in later stages (becoming partly isoattenuating). The larger lesion has 16 x 12cm, and keeps hypodense central areas at all phases. B - Axial Lung CT images (MIP): Lung metastasis. C - Coronal CT image: Heterogeneous hepatomegaly. D - Ultrasonography: multiple small, sometimes confluent, nodules with target appearance.
References: M. L. O. O. Coelho; radioogia, Porto, PORTUGAL

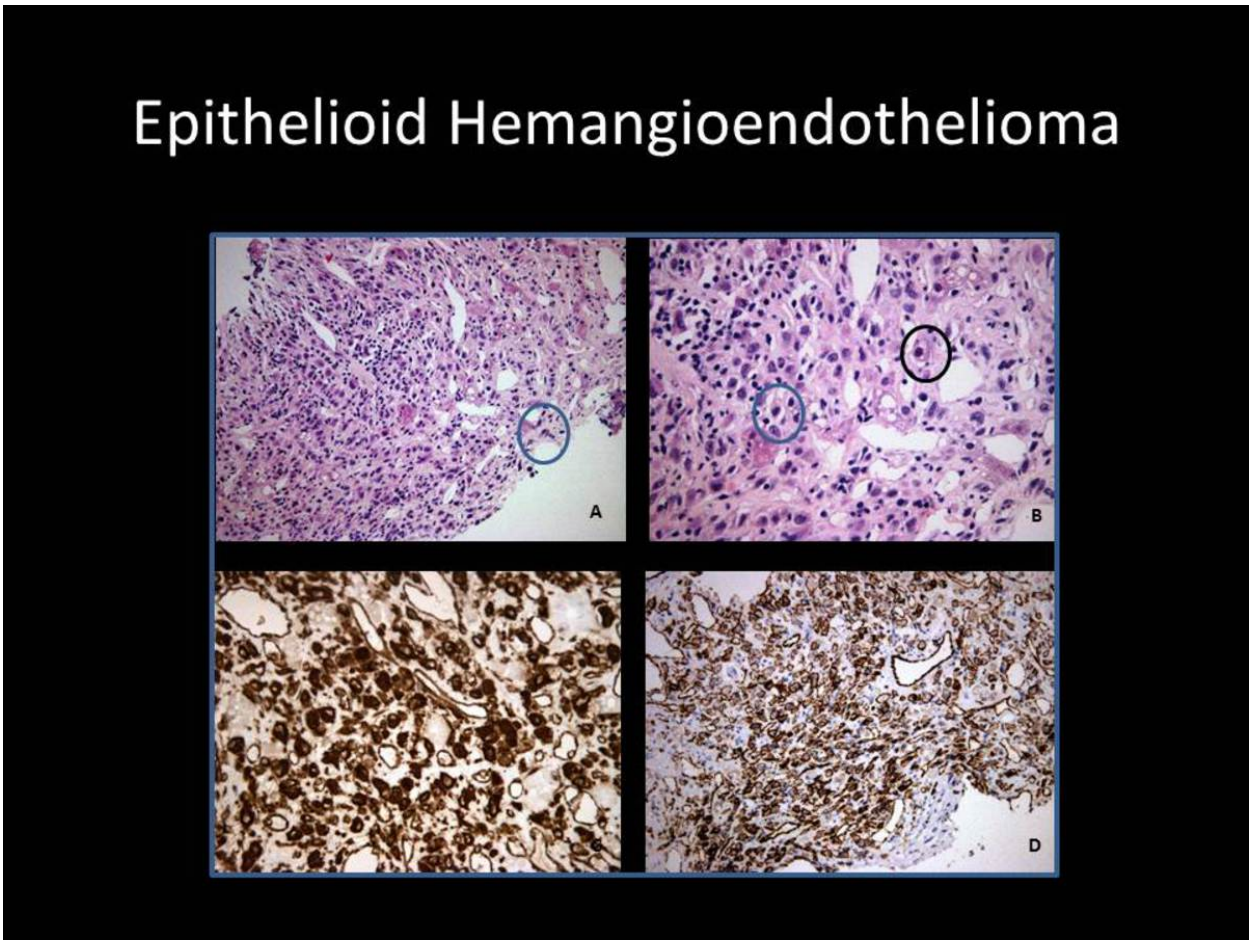

Fig. 34: A - High-power photomicrograph shows epithelioid tumor cells sccattered in fibrohyaline stroma. B - High-power photomicrograph shows epithelioid cells with intracytoplasmatic vacuoles (black circumference). C - Immunohistochemical staining, tumor cells show positivity for vimentin. D - Immunohistochemical staining, tumor cells show positivity for CD31.
References: M. L. O. O. Coelho; radioogia, Porto, PORTUGAL

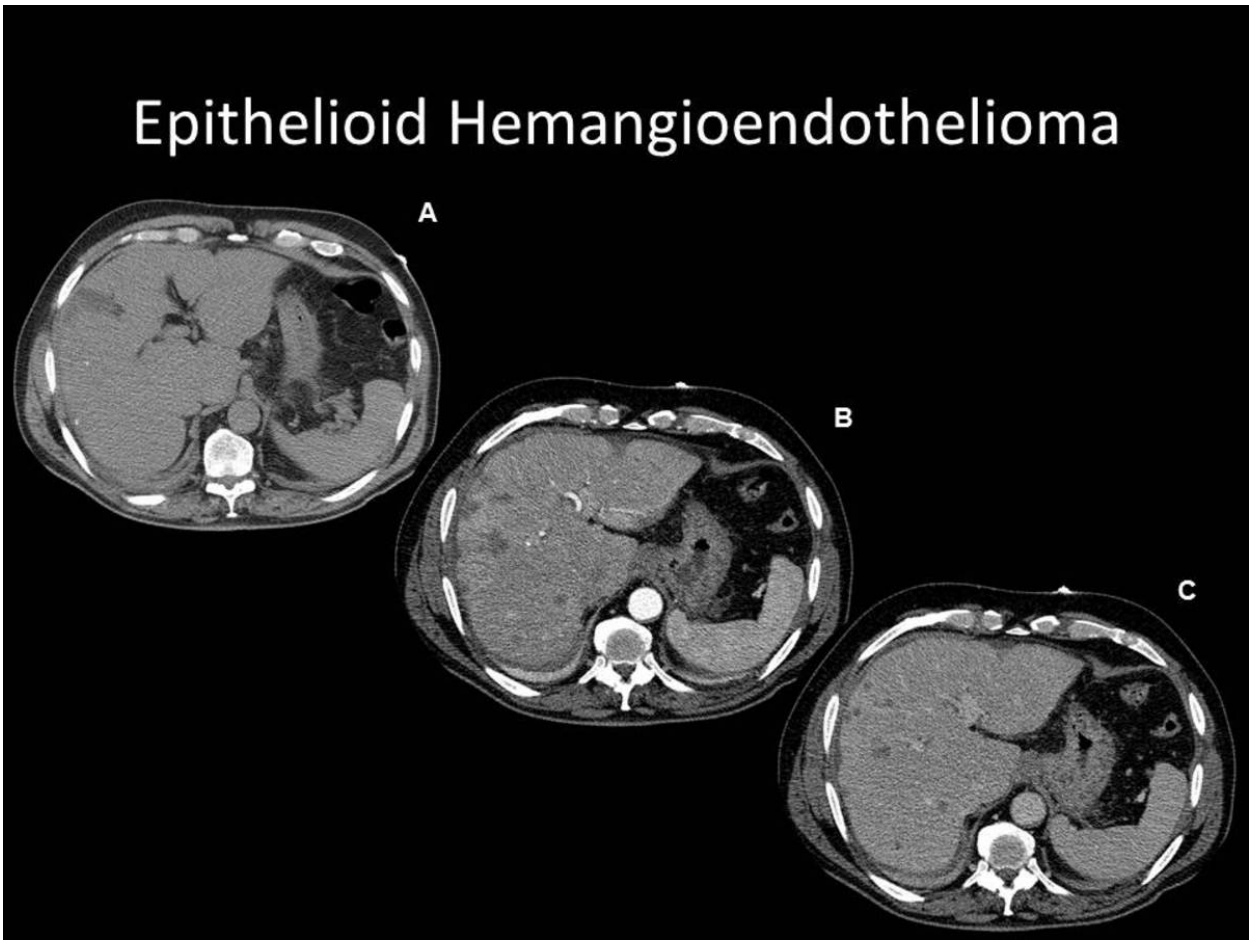

Fig. 35: A. Unenhanced CT image shows hepatomegaly with some calcifications visible in the right lobe. B. Enhanced-CT (arterial phase) shows multiple liver nodules in the right and caudate lobes: most are hipodense, but some show peripheral. B. The portal phase image demonstrate gradual centripetal enhancement progression. Note irregular liver border associated with the nodules suggesting capsular retraction.
References: M. L. O. O. Coelho; radioogia, Porto, PORTUGAL

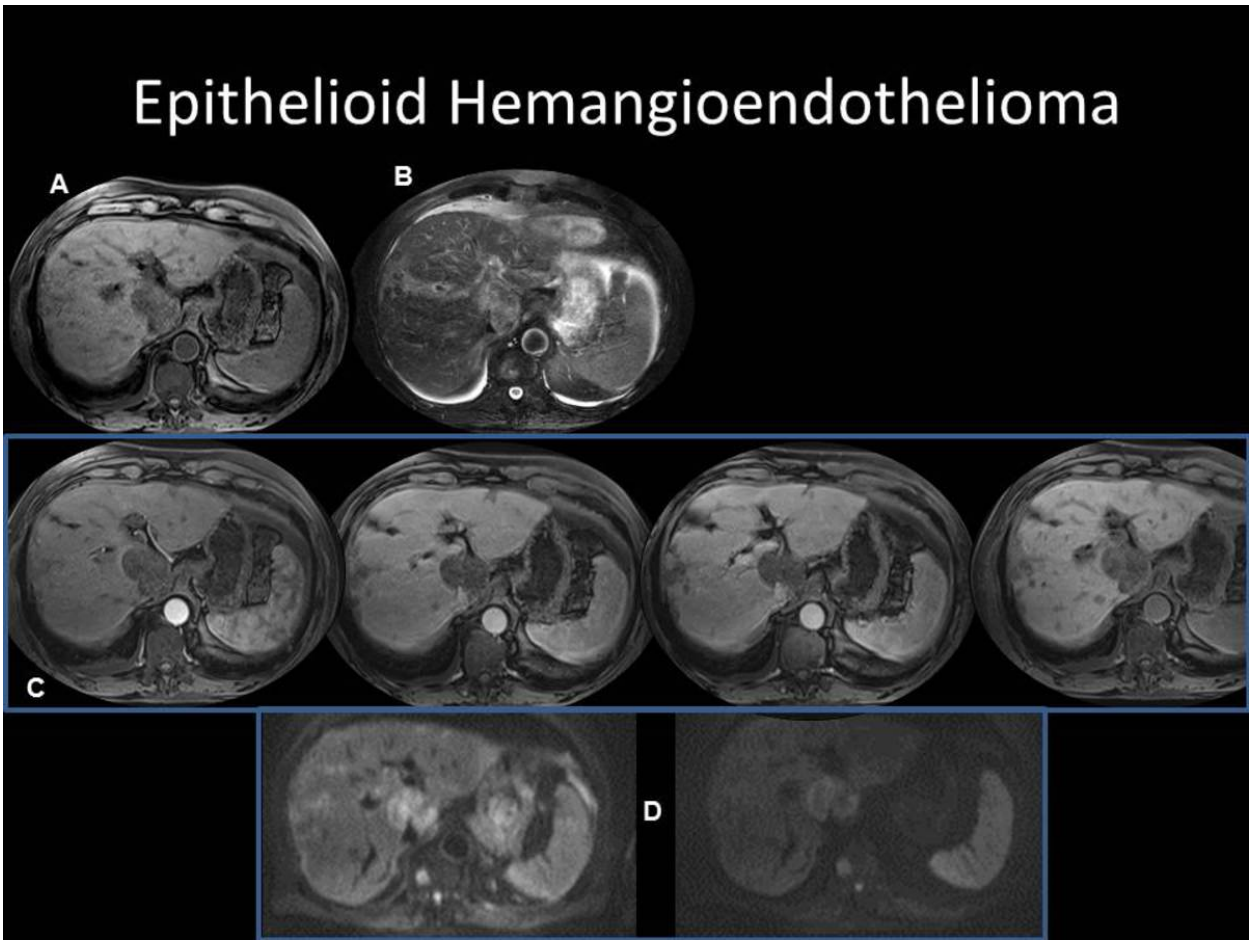

Fig. 36: A. T1-weighted image: hypointense large mass in the caudate lobe and small nodules in the right and left lobes. B. The mass is slightly hyperintense on T2-weighted MR images, but the small nodules show an hypointense rim. C. Gd-EOB-DTPA-enhanced images: only the mass in the caudate lobe slightly enhances in the hepatobiliary phase. D - In the diffusion-weighted study the lesion has no diffusion restriction.

References: M. L. O. O. Coelho; radioogia, Porto, PORTUGAL

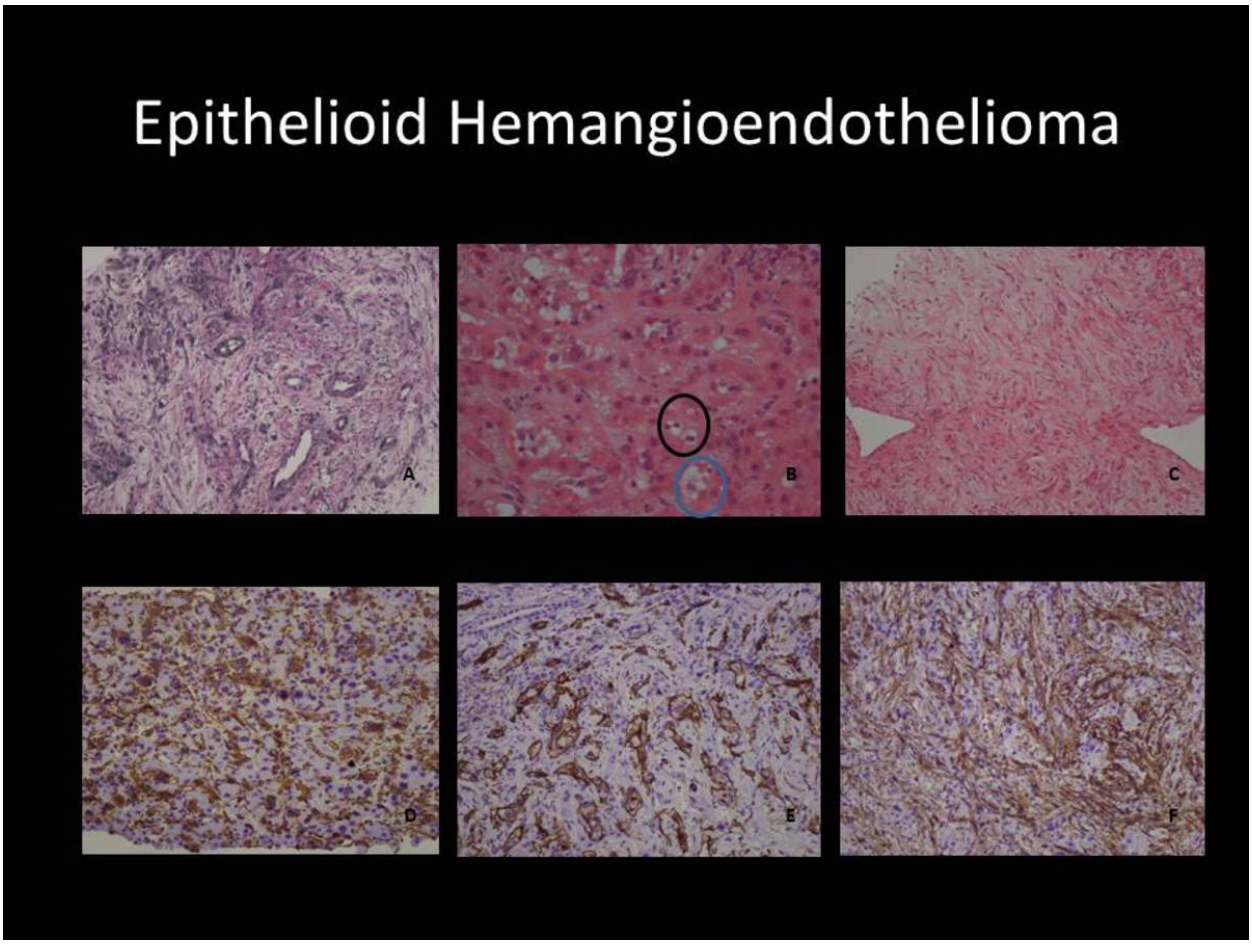

Fig. 37: A - High-power photomicrograph shows epiethelioid cells growing along preformed vessels B - High-power photomicrograph shows some cells with intracytoplasmatic vacuoles (blue circumference: cell with intracytoplasmatic vacuoles containing red blood cells). C - High-power photomicrograph shows spindle tumor cells sccattered in fibromyxoid stroma. D - Immunohistochemical staining, tumor cells show positivity for vimentin. D - Immunohistochemical staining, tumor cells show positivity for CD34. E - Immunohistochemical staining, tumor cells show positivity for CD31.
References: M. L. O. O. Coelho; radioogia, Porto, PORTUGAL

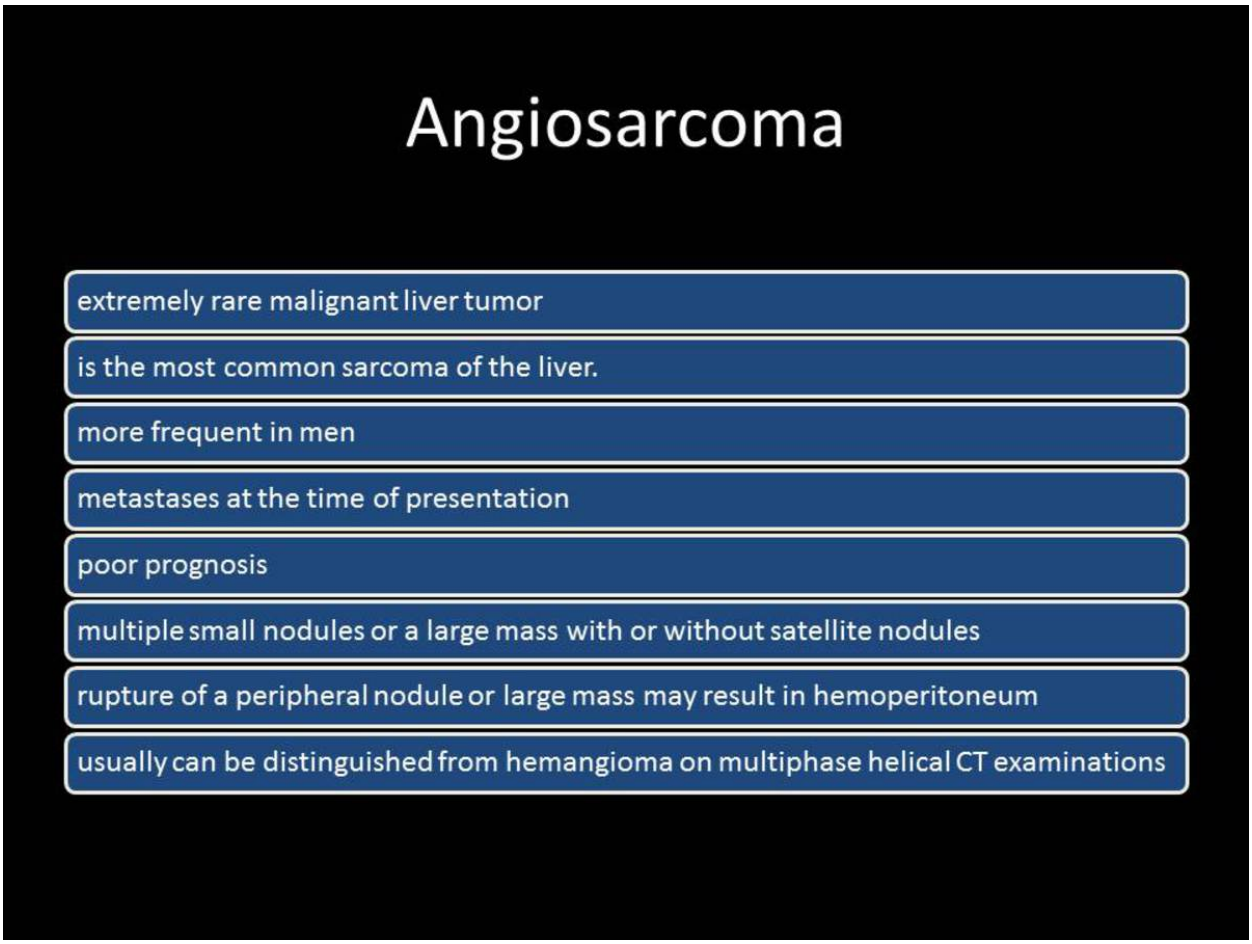

Fig. 38: 38
References: M. L. O. O. Coelho; radioogia, Porto, PORTUGAL

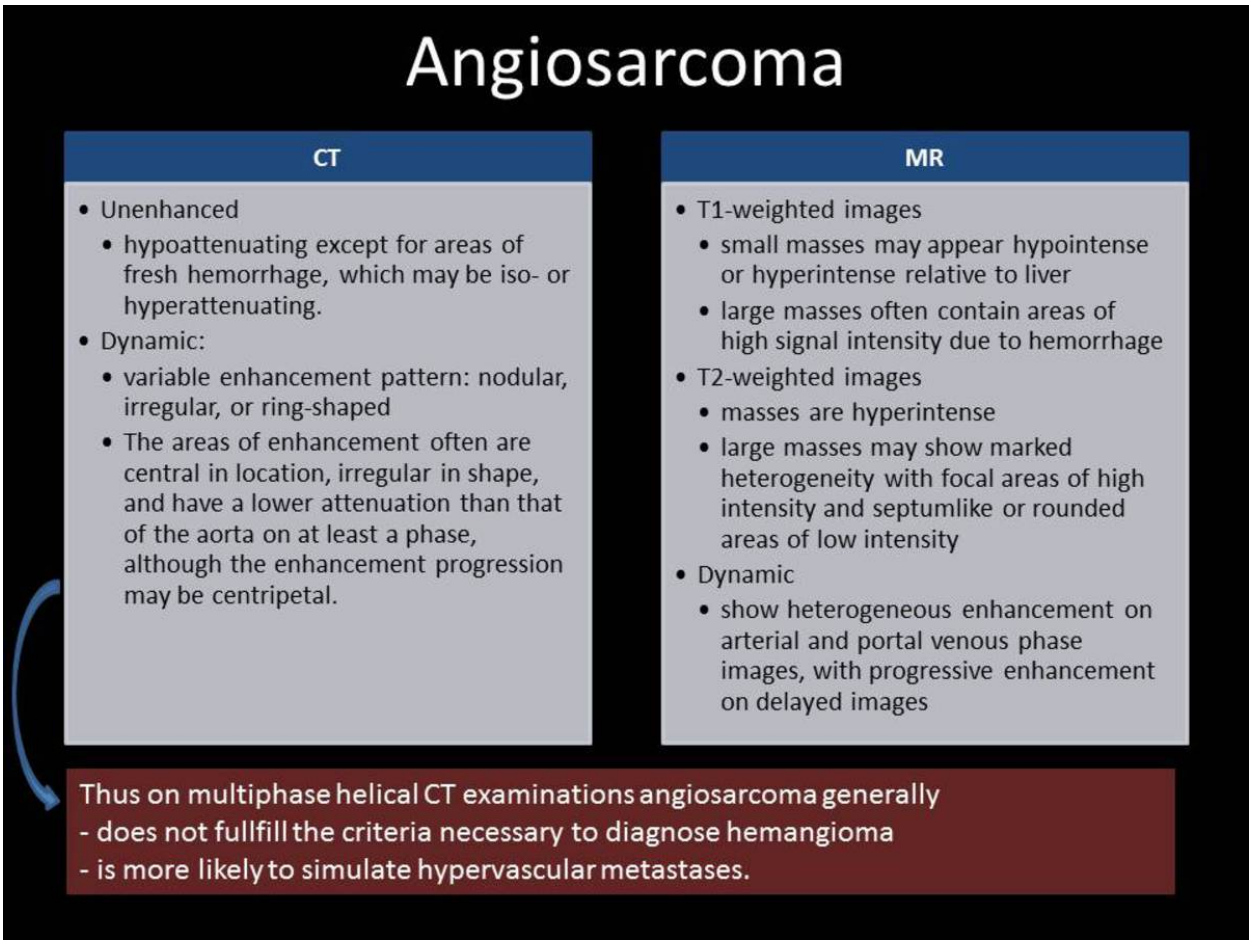

Fig. 39: 39
References: M. L. O. O. Coelho; radioogia, Porto, PORTUGAL

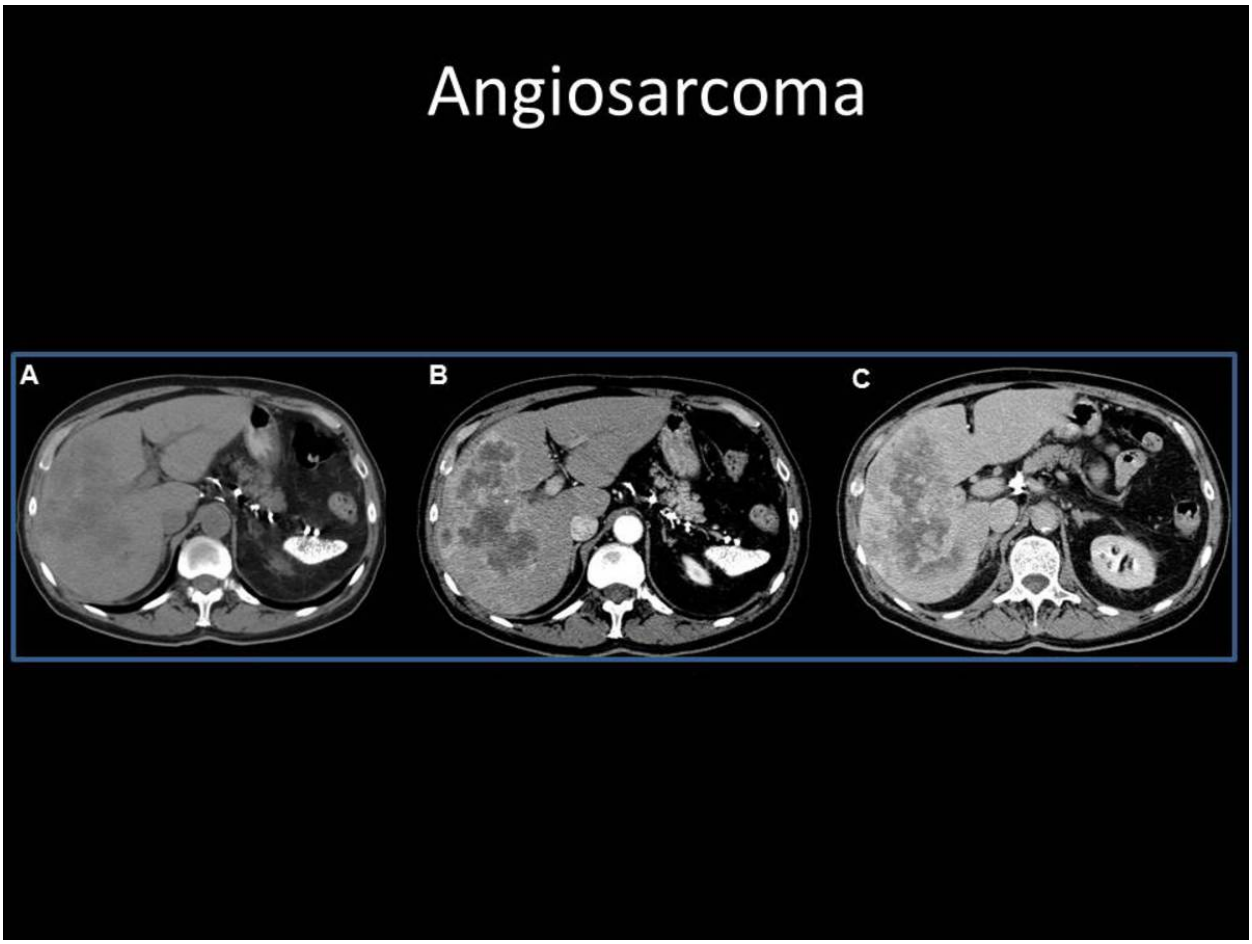

Fig. 40: 72-year old man with history of Thorotrast exposure. A. Unenhanced CT shows an heterogeneous hypoattenuating mass. B. Enhanced-CT (arterial phase) shows a bizarre shaped mass with hypervascular heterogeneous enhancement and central areas of low attenuation representing old hemorrhage. C. Progressive and heterogeneous enhancement is shown in venous phase.
References: M. L. O. O. Coelho; radioogia, Porto, PORTUGAL

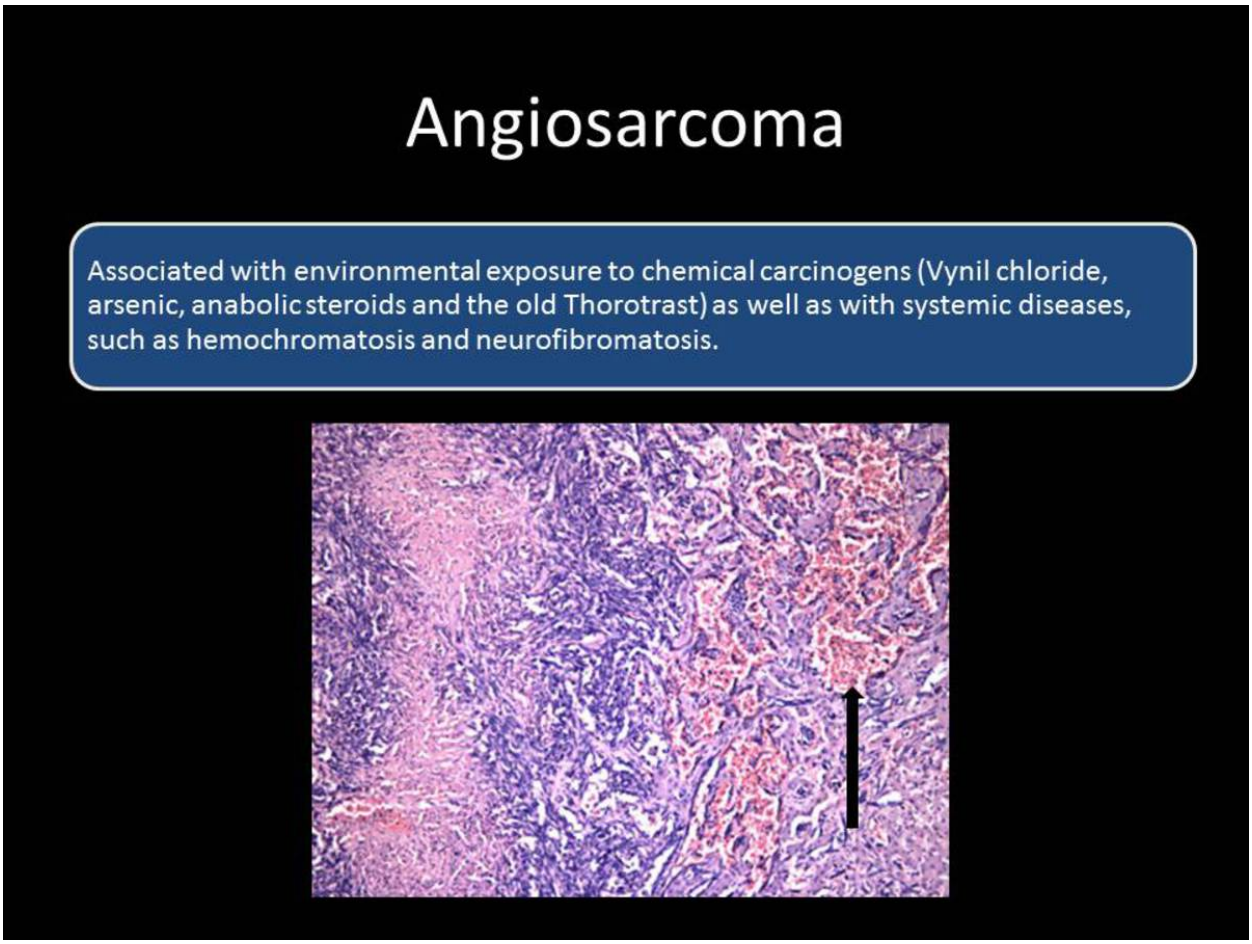

Fig. 41: High-power photomicrograph shows malignant spindle and pleomorphic cells. These cells origin new sinusoidal vessels (arrow).
References: M. L. O. O. Coelho; radioogia, Porto, PORTUGAL

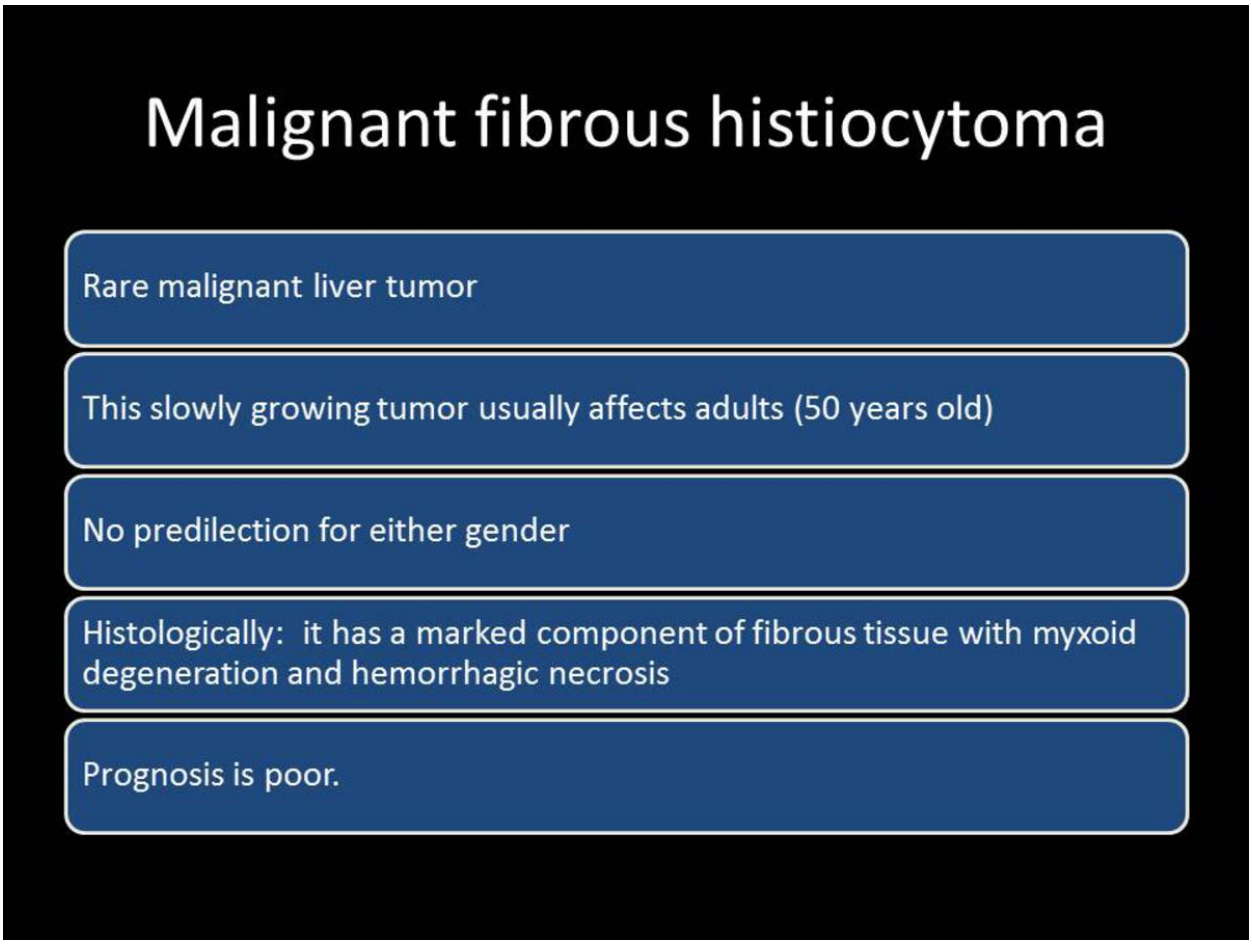

Fig. 42: 42
References: M. L. O. O. Coelho; radioogia, Porto, PORTUGAL

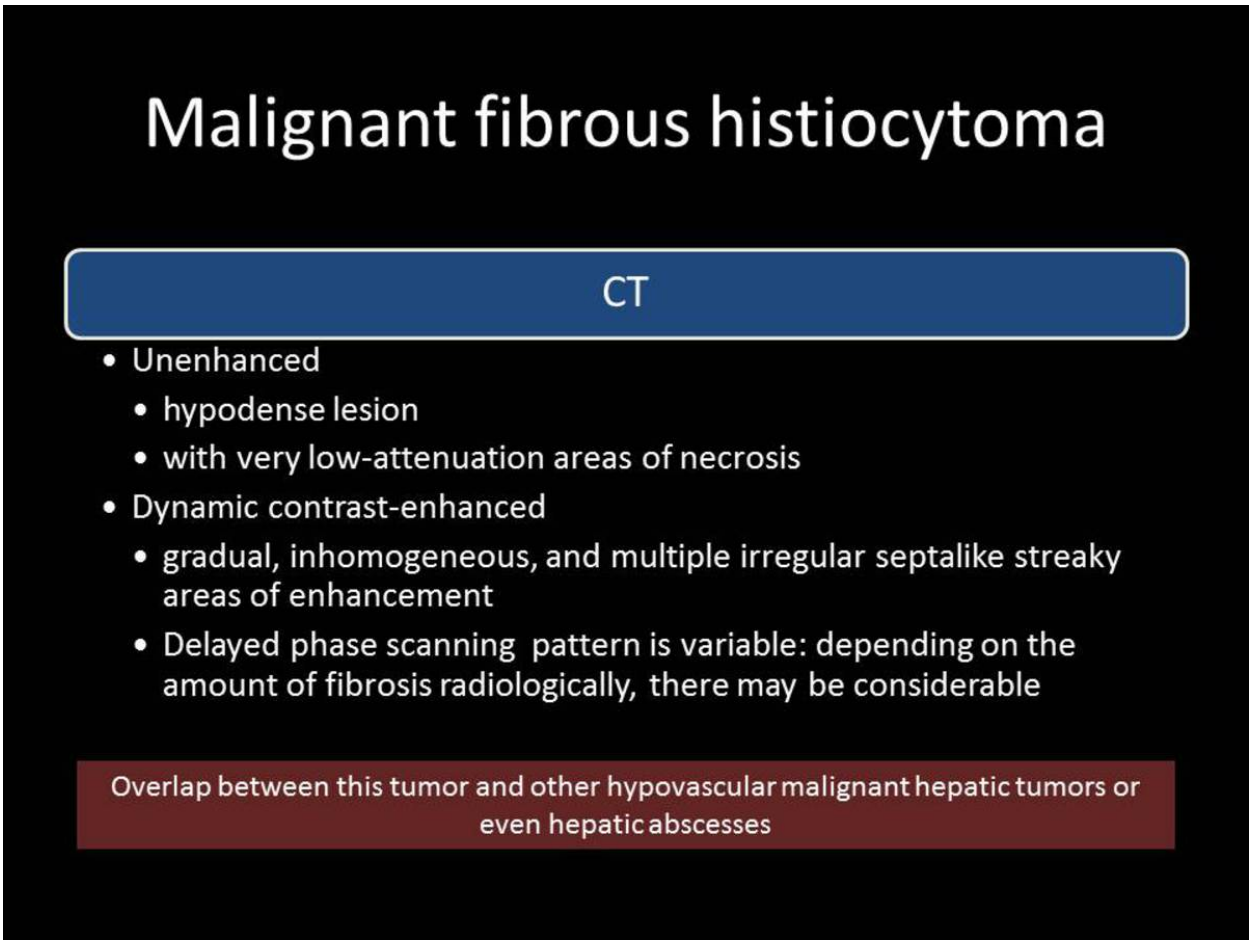

Fig. 43: 43
References: M. L. O. O. Coelho; radioogia, Porto, PORTUGAL

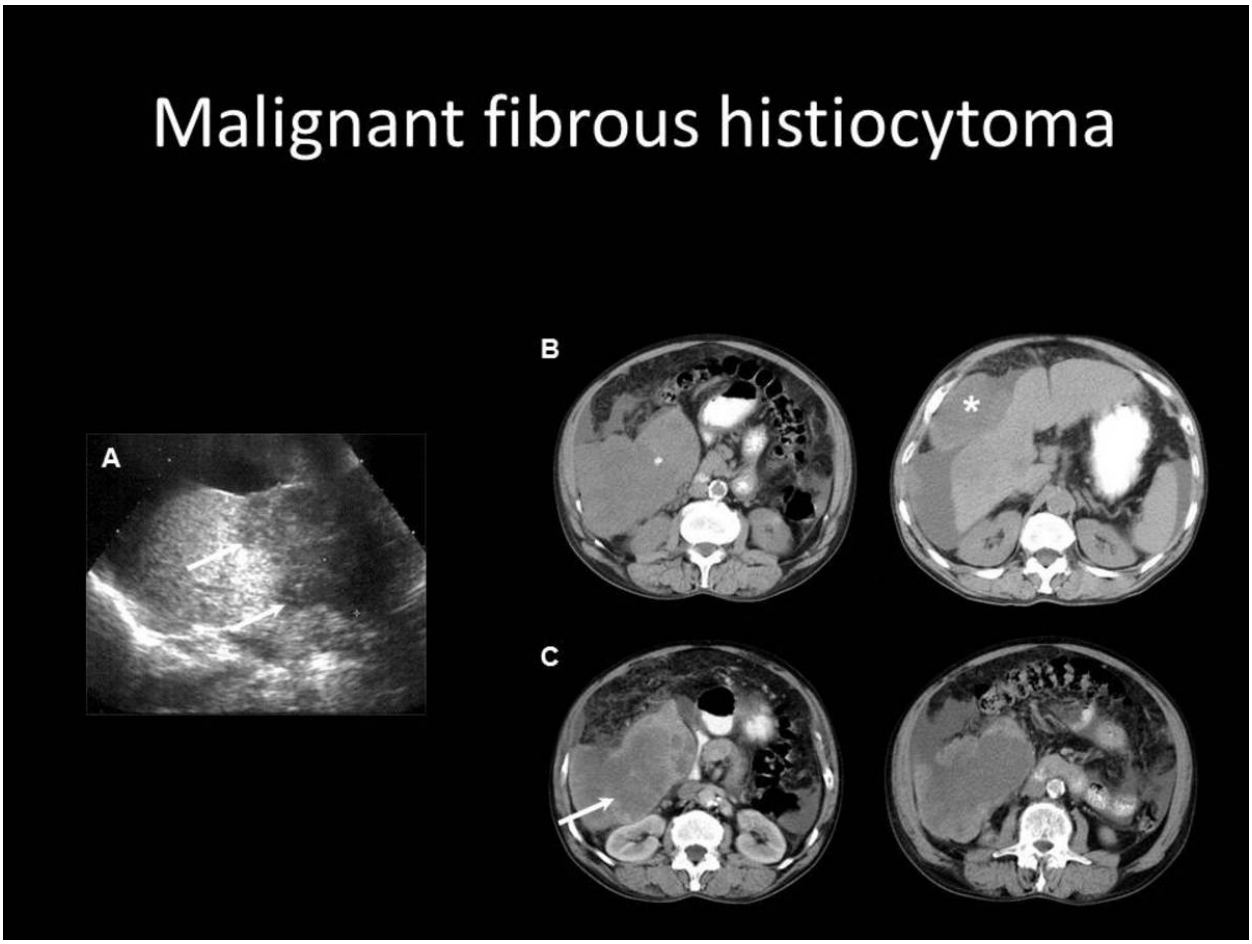

Fig. 44: 63-year-old man with progressive weight loss and distended abdomen.
A. Ultrasound shows an heterogeneous hypoechogenic liver mass (arrows). B. Unenhanced CT shows a low- attenuation soft tissue liver mass with a calcification. It is also shown peritoneal tumor metastasis (arrow-head). C. Enhanced CT (portal phase) confirms the heterogeneity and the marked low attenuation of the mass representing necrosis. There is also ascites. Delayed phase (not shown) enhancement depends on the amount of fibrosis.
References: M. L. O. O. Coelho; radioogia, Porto, PORTUGAL

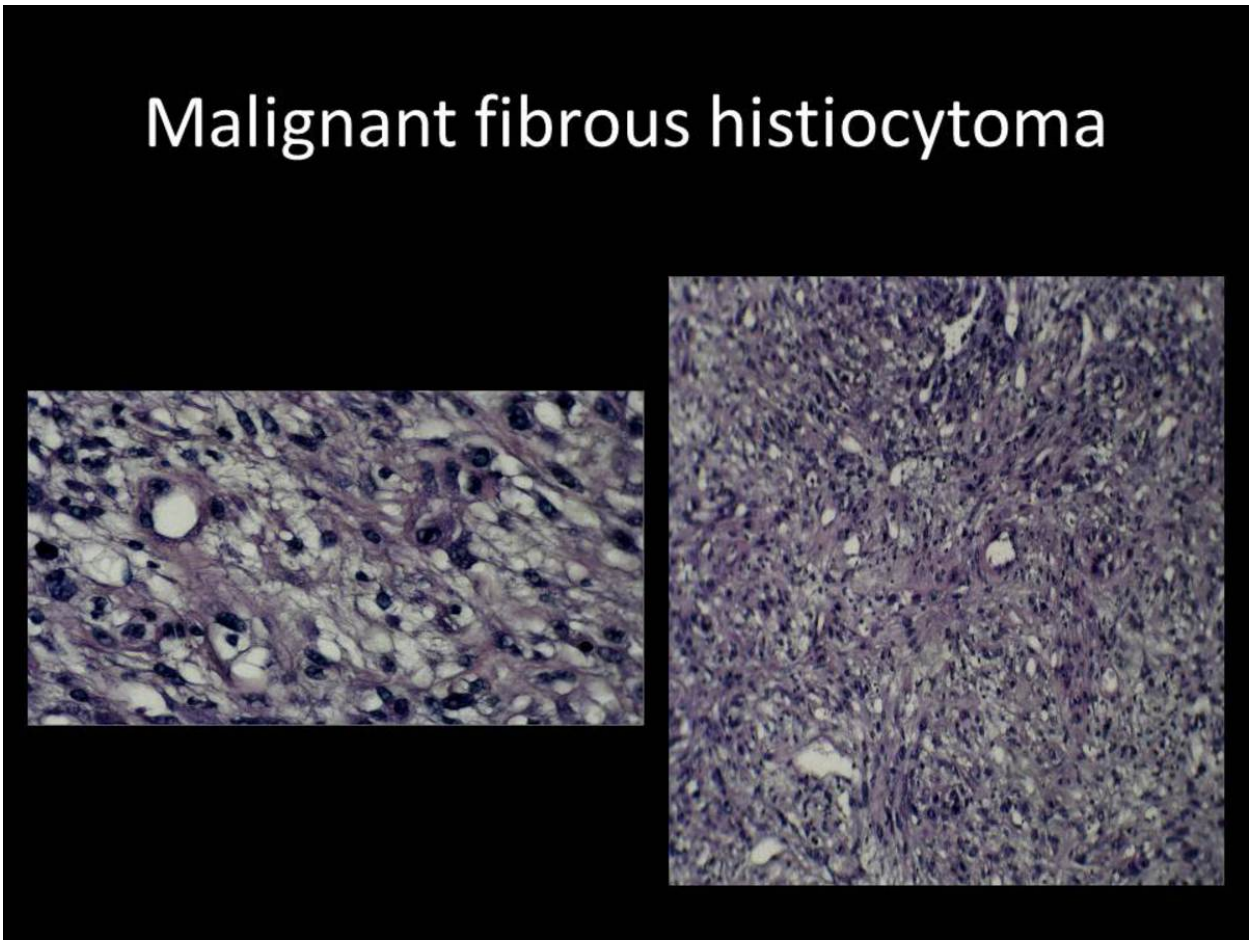

Fig. 45: High-power photomicrographs show a pleomorphic-storiform pattern with giant cells.
References: M. L. O. O. Coelho; radioogia, Porto, PORTUGAL

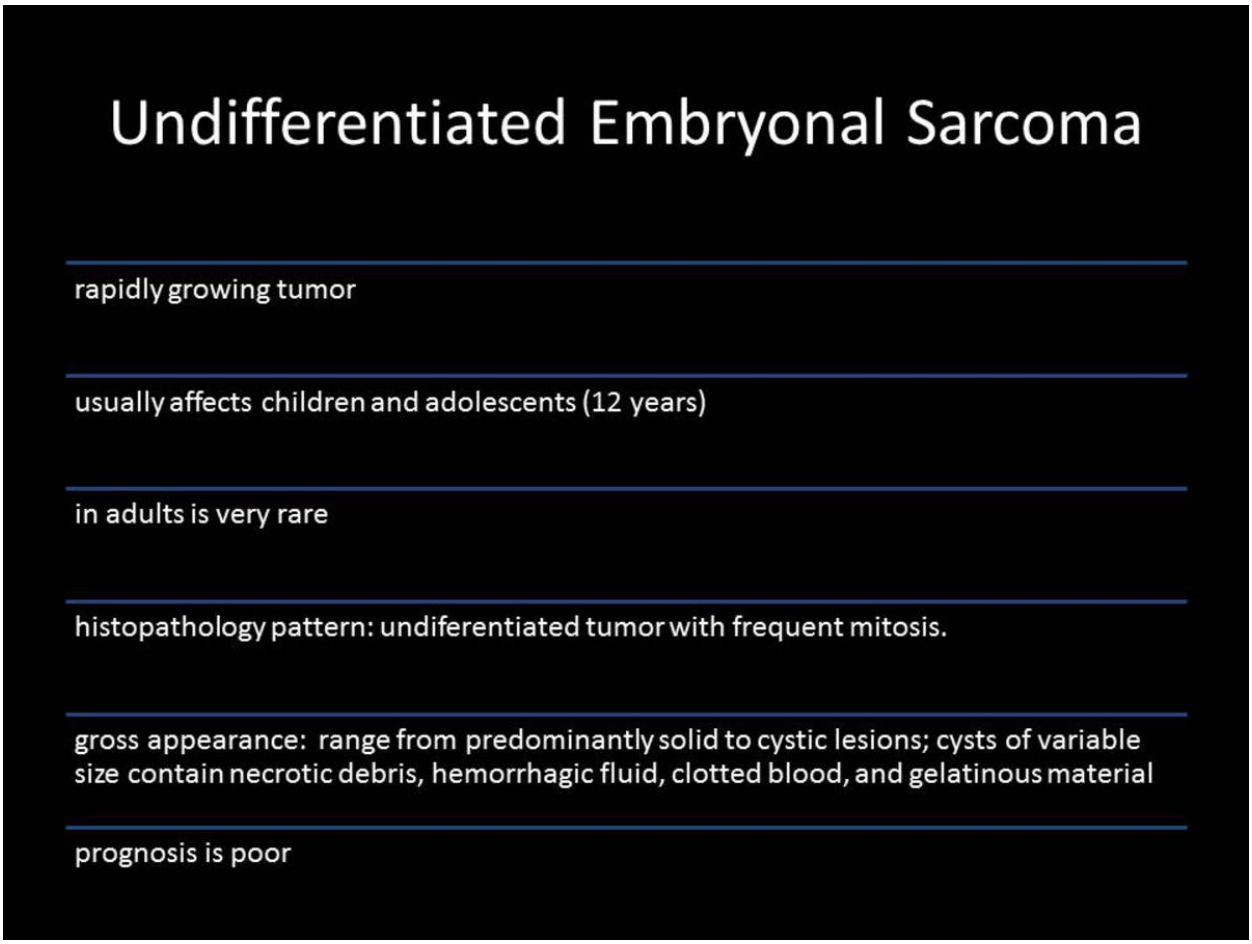

Fig. 46: 46
References: M. L. O. O. Coelho; radioogia, Porto, PORTUGAL

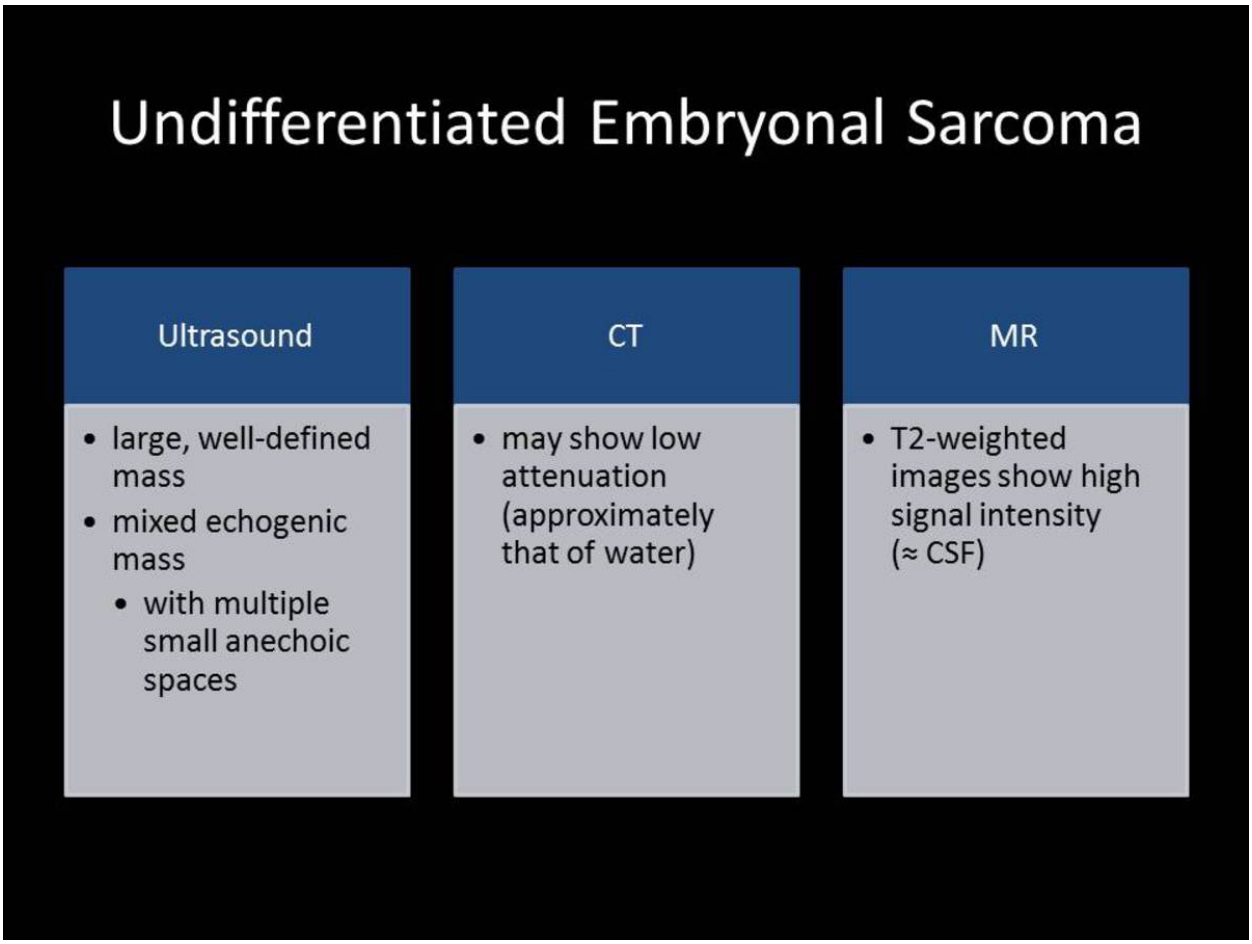

Fig. 47: 47
References: M. L. O. O. Coelho; radioogia, Porto, PORTUGAL

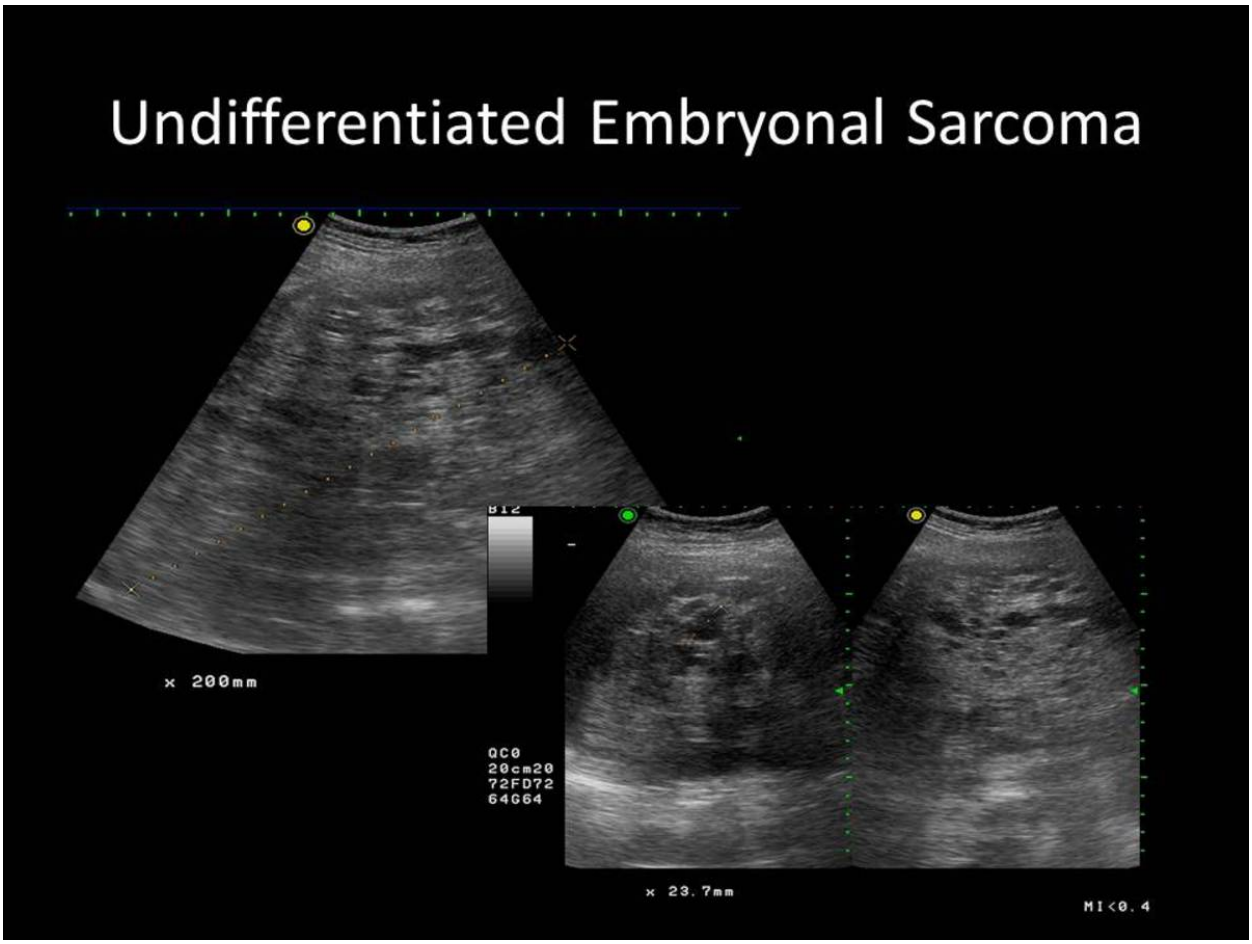

Fig. 48: Ultrasound shows an heterogeneous echogenic liver mass with several anechogenic areas, of different sizes.
References: M. L. O. O. Coelho; radioogia, Porto, PORTUGAL

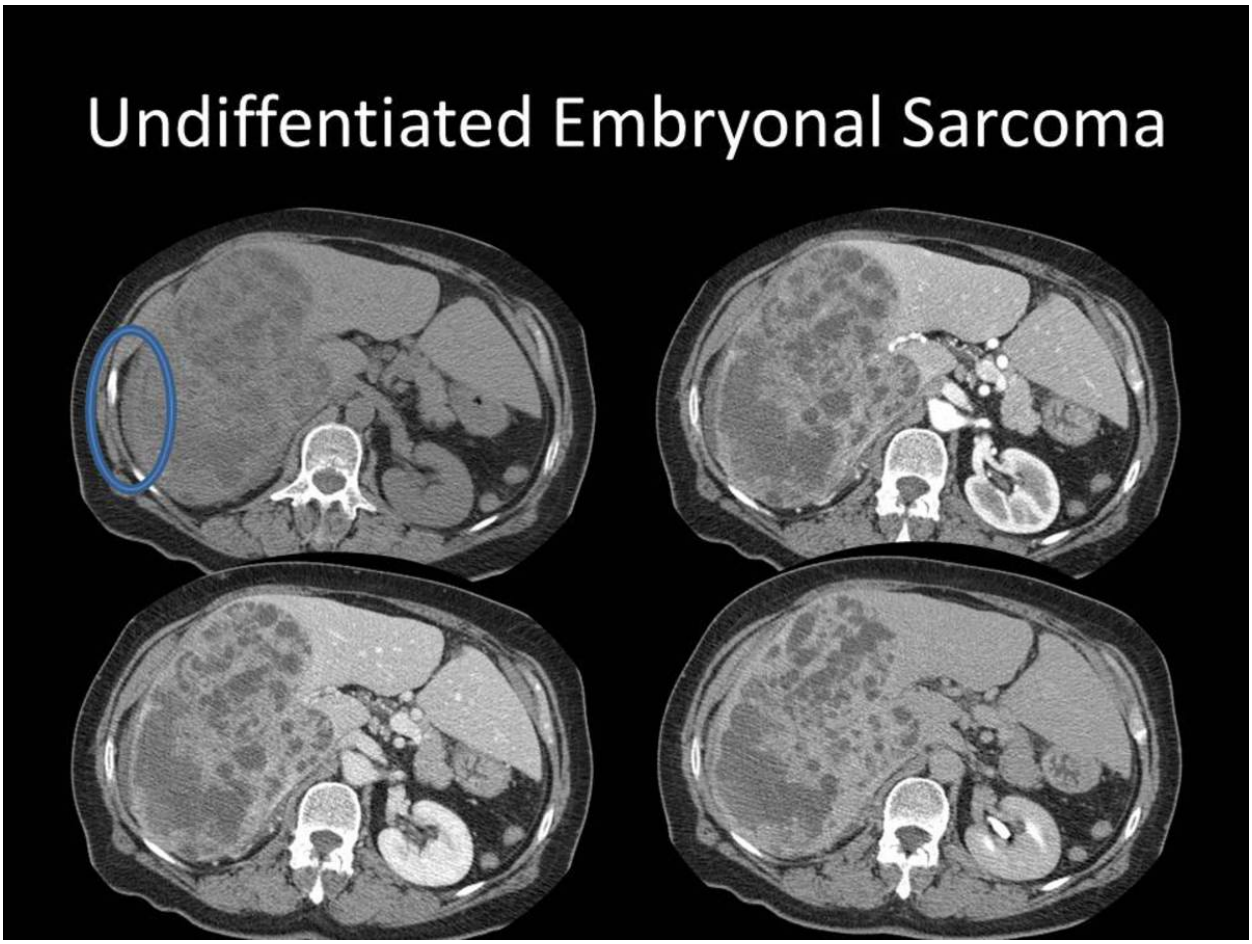

Fig. 49: A. Unenhanced CT shows a soft tissue mass with multiple low attenuation areas. A focal spot of peritoneal hemorrhage is also shown (blue circumference). C-E. Dynamic study demonstrates the multiple cystic components of the mass. Other areas represent necrotic debris, clotted blood and hemorrhagic fluid
References: M. L. O. O. Coelho; radioogia, Porto, PORTUGAL

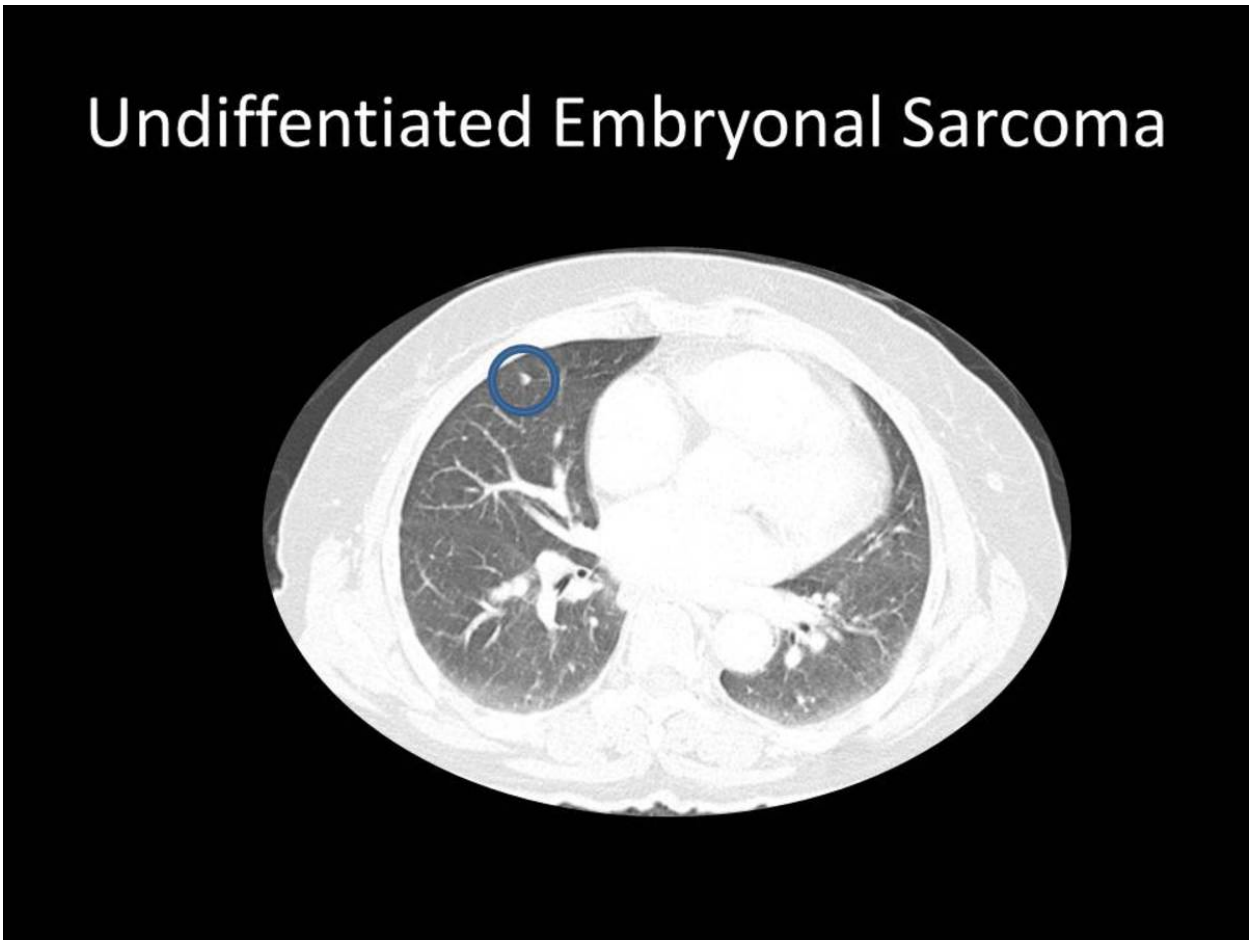

Fig. 50: C - Thoracic axial computed image, lung window: Right superior lobe metastasis (1cm).
References: M. L. O. O. Coelho; radioogia, Porto, PORTUGAL

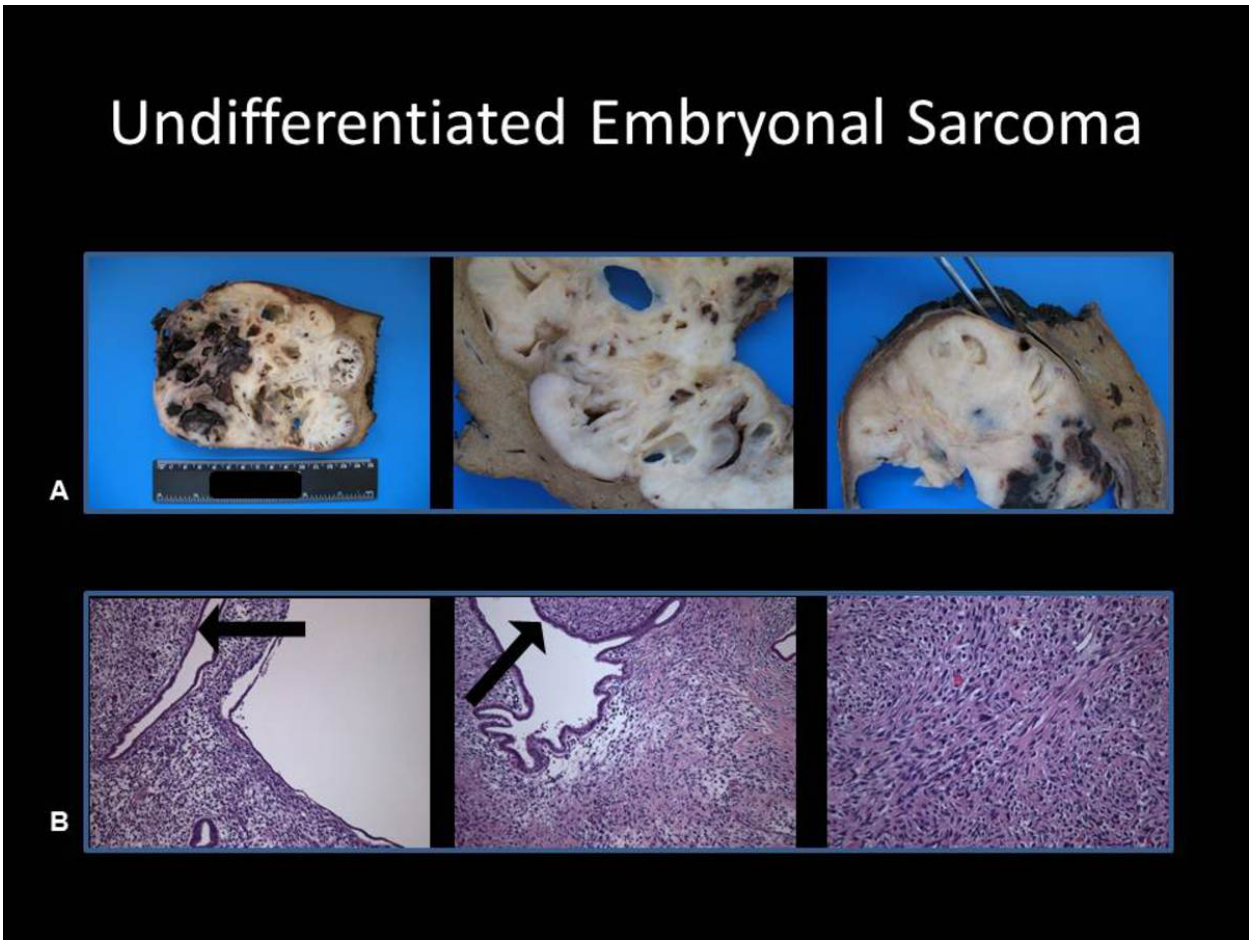

Fig. 51: A. Pathologic specimen shows the tumor huge size and several areas with necrotic debris and clotted blood distending the billiary tree in the hilar region but without infiltration. The third image depicts its pseudocapsule. B. High-power photomicrographs show malignant stellate and spindle shaped cells and benign embrional epithelium lining glandular cystic spaces. The epithelial lining of the cysts (arrow) is spared.
References: M. L. O. O. Coelho; radioogia, Porto, PORTUGAL

Images for this section:

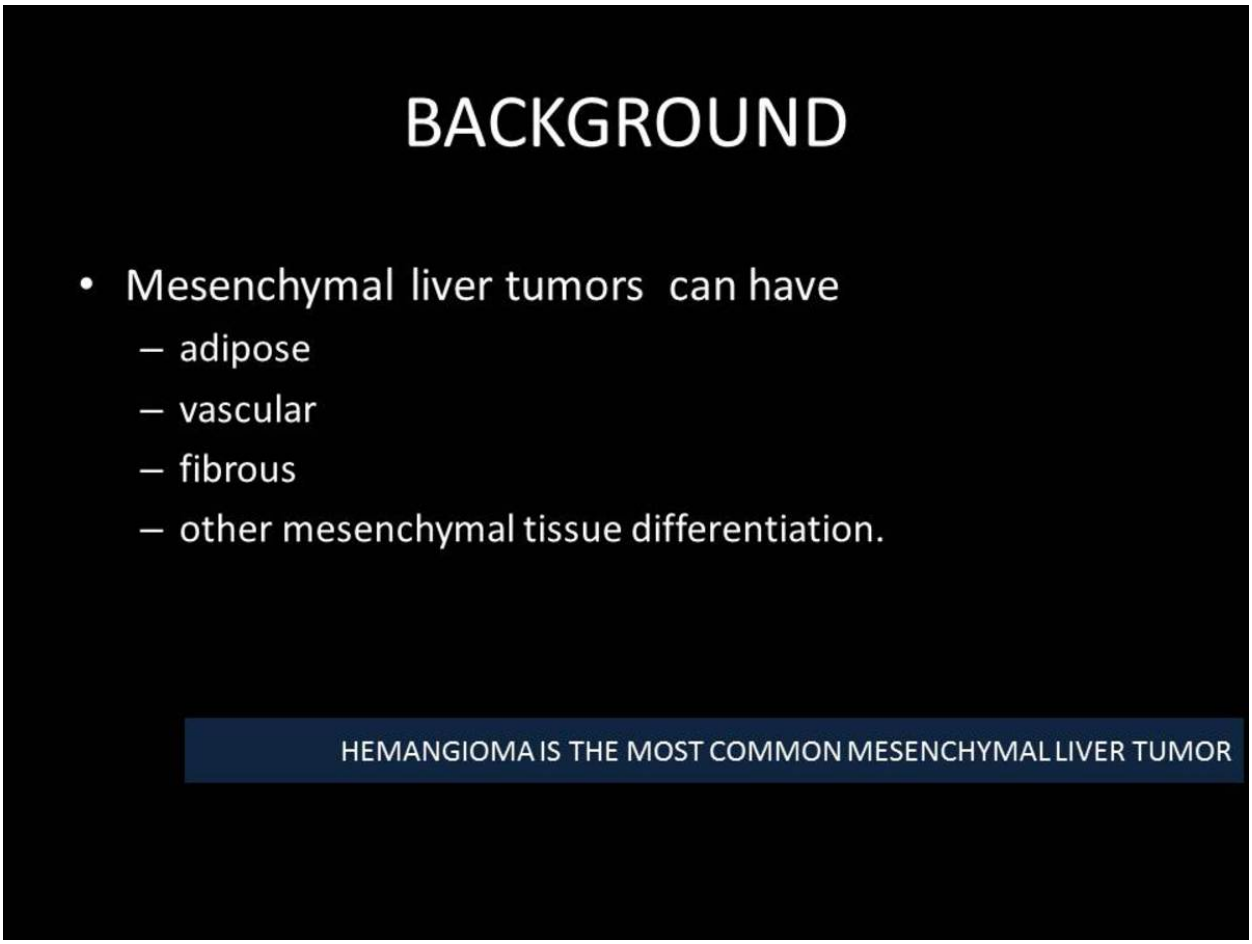
BACKGROUND
• Mesenchymal liver tumors can have
– adipose
– vascular
– fibrous
– other mesenchymal tissue differentiation.
HEMANGIOMA IS THE MOST COMMON MESENCHYMAL LIVER TUMOR

Fig. 1: 1

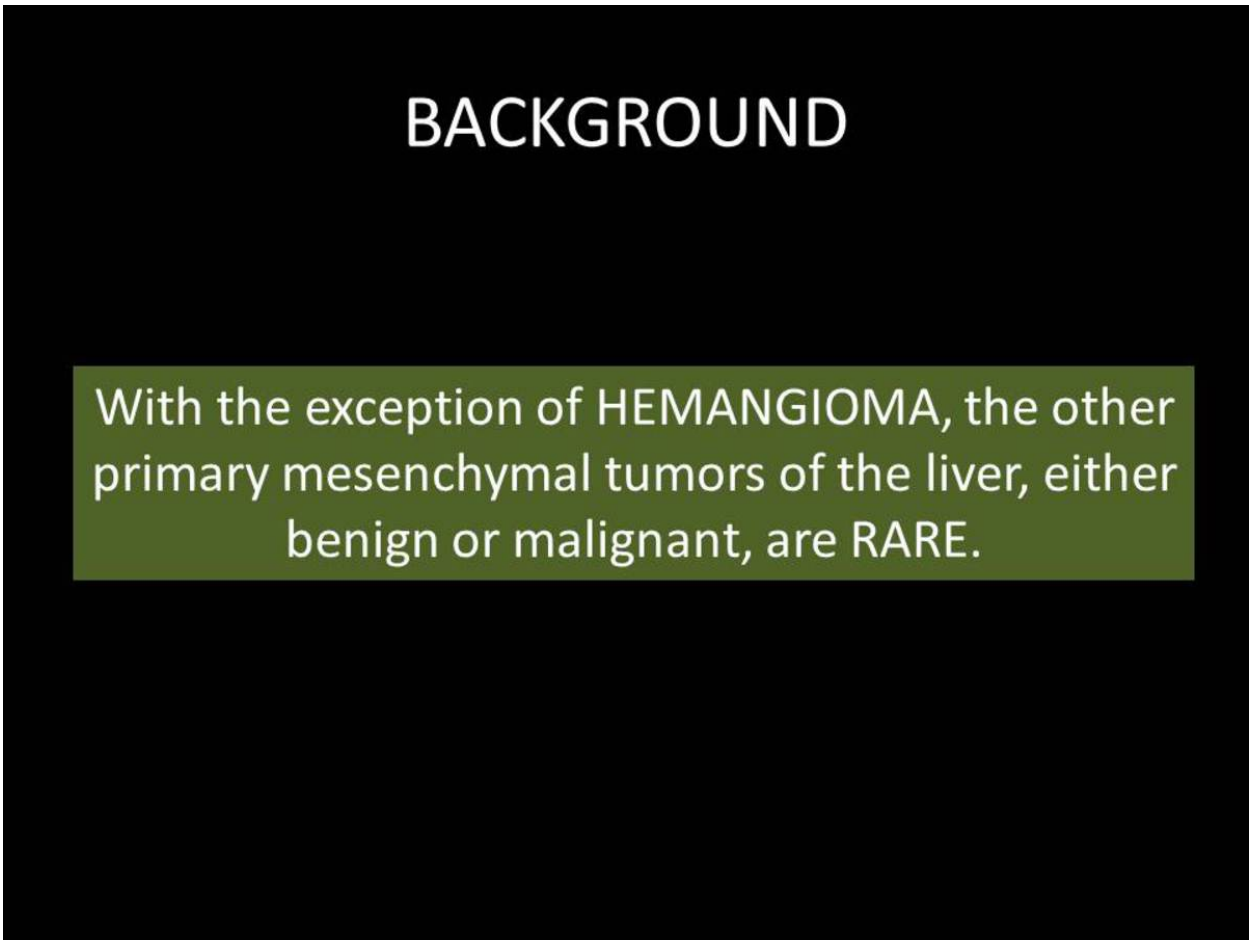
BACKGROUND
With the exception of HEMANGIOMA, the other primary mesenchymal tumors of the liver, either benign or malignant, are RARE.

Fig. 4: 4

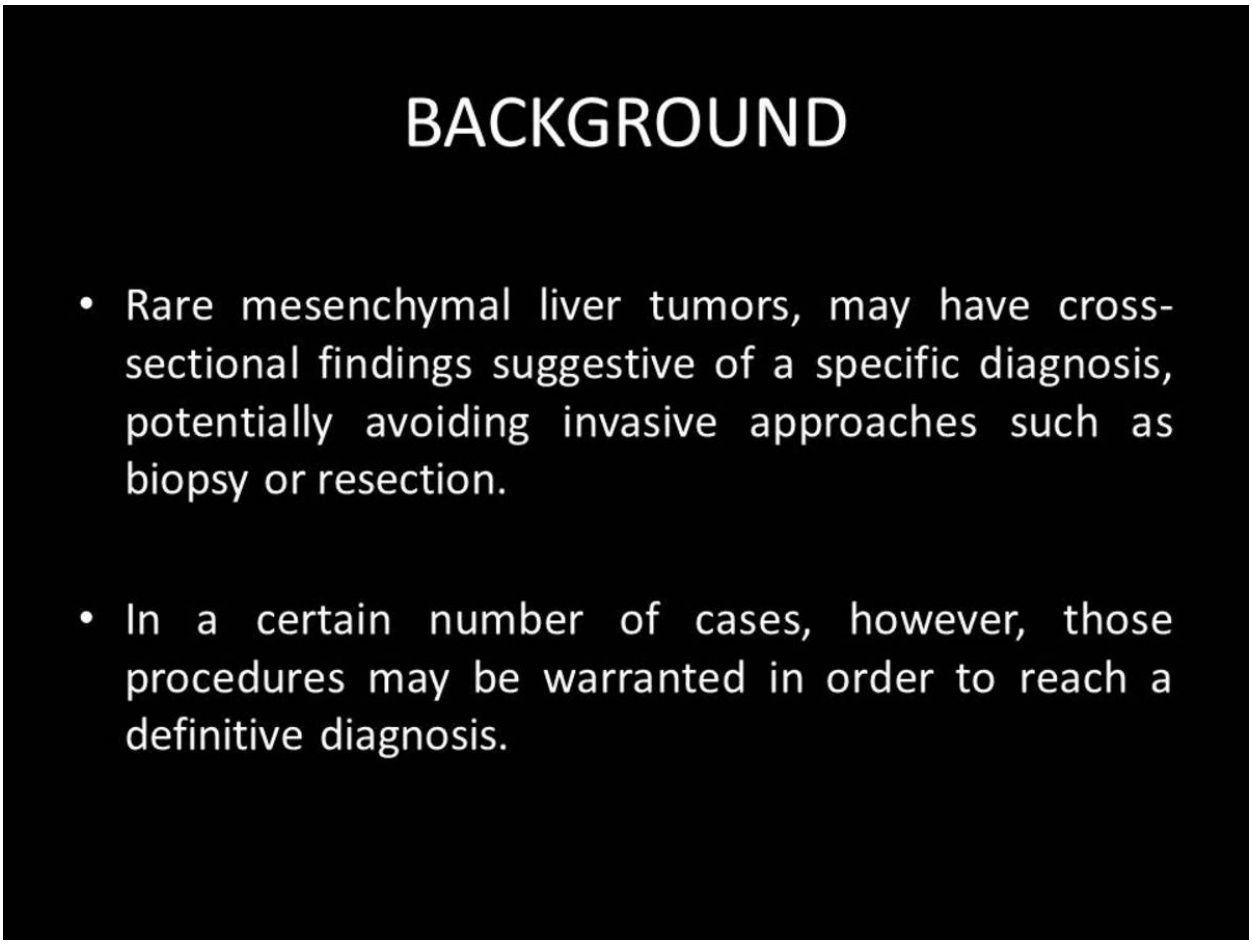
BACKGROUND
• Rare mesenchymal liver tumors, may have cross-sectional findings suggestive of a specific diagnosis, potentially avoiding invasive approaches such as biopsy or resection.
• In a certain number of cases, however, those procedures may be warranted in order to reach a definitive diagnosis.

Fig. 5: 5

Lipoma

Rare	
Benign	
Incidental finding.	
Can range	from a few mm to more than 10cm
Pathognomonic appearance	Fat attenuation values ≈ -100 HU (≈ subcutaneous fat)
Circumscribed with smooth margins	
Do not enhance	
BIOPSY	NOT REQUIRED

Fig. 18: 18

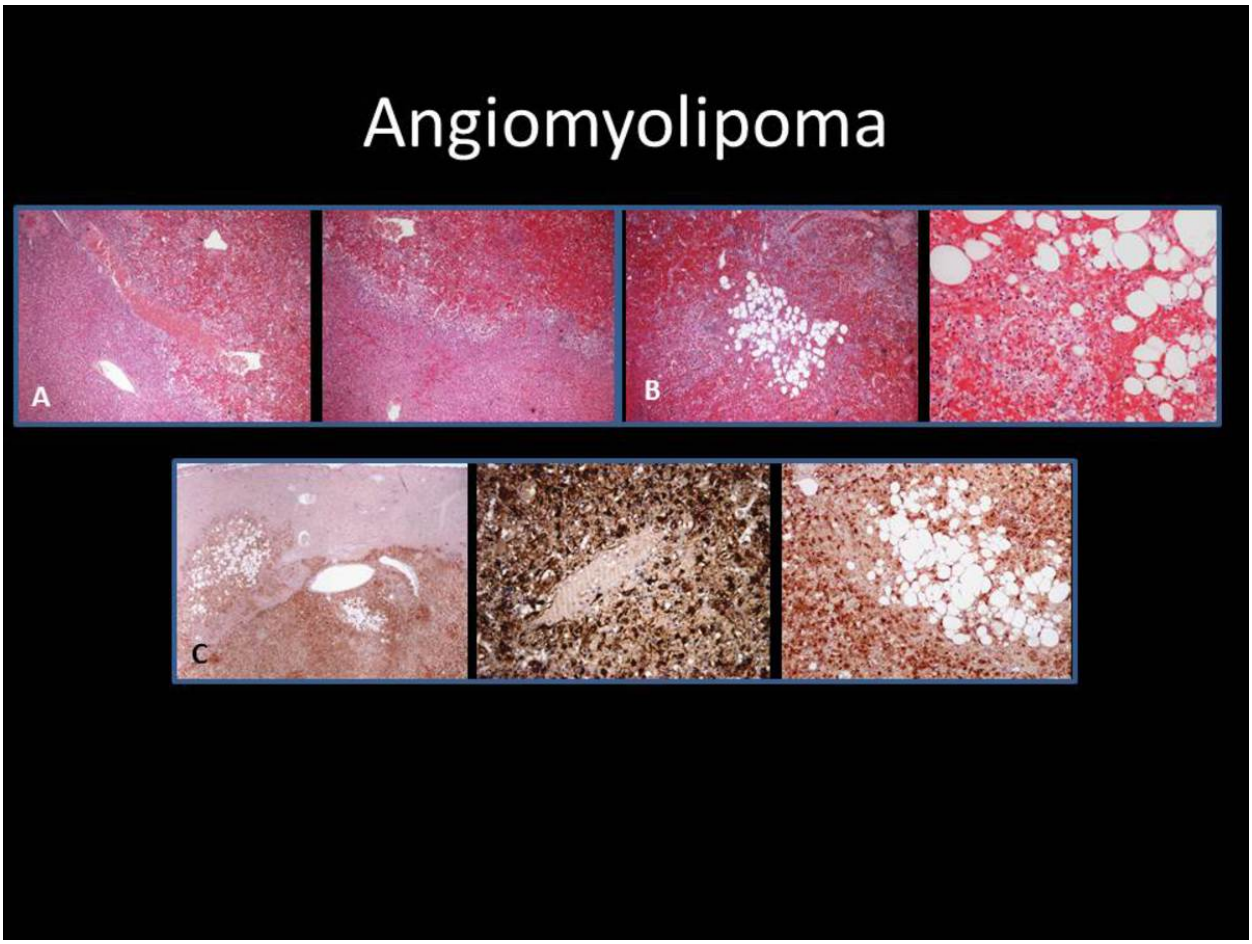

Fig. 17: A. Photomicrographs: show the well demarcated limits of the lesion; B. - High-power photomicrographs show the components of the lesion: adipose tissue, epithelioid (muscular component) and blood vessels. C. High-power photomicrograph immunohistochemical studies show positivity for human melanocyte-specific antibody HMB45, supporting the diagnosis (different magnifications).

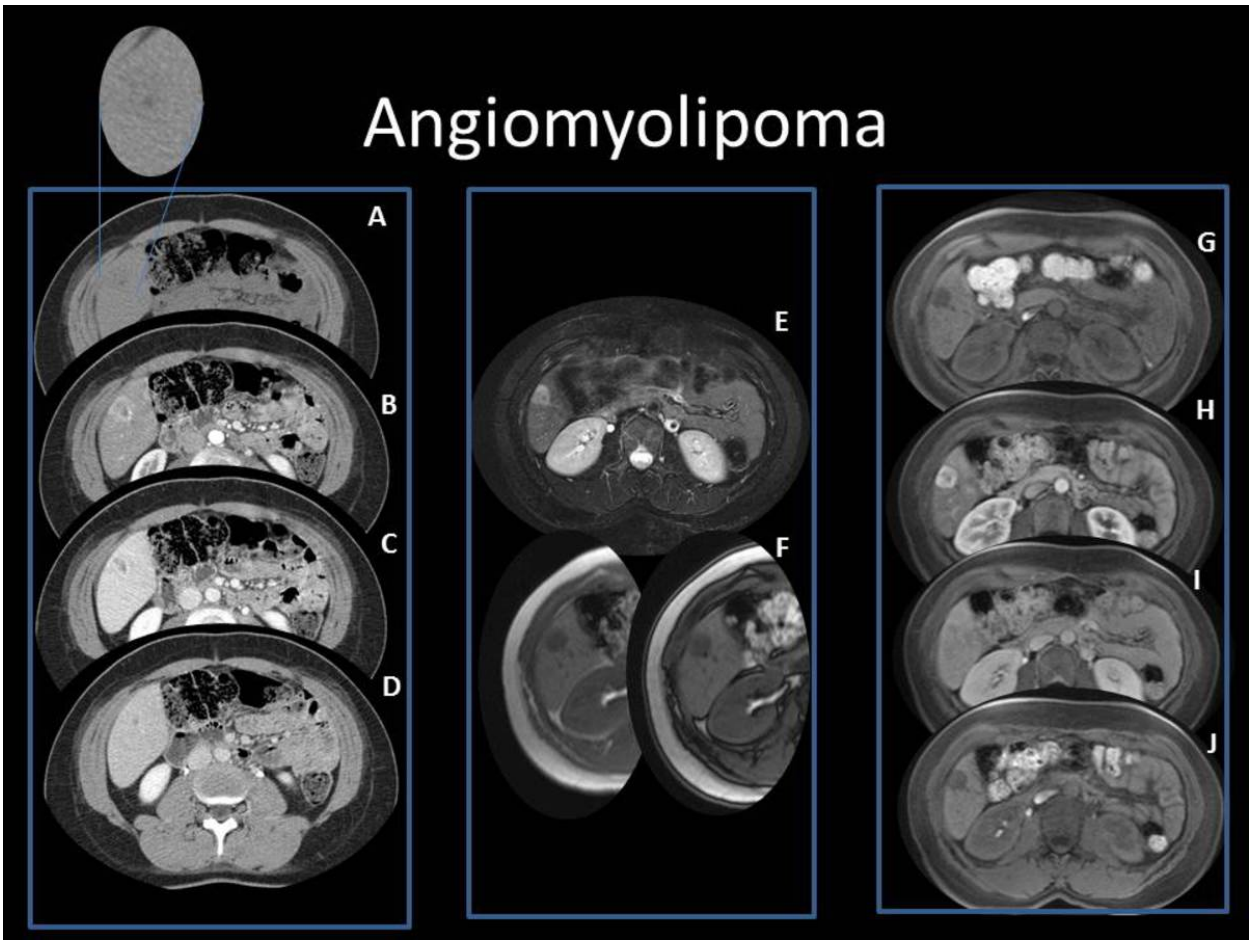

Fig. 16: A - Unenhanced CT image shows a hypoattenuating lesion with an area of fat attenuation. Arterial phase scan (B) shows marked enhancement. C, D - Slight hyperattenuation compared with the surrounding parenchyma during venous and late phase scan of the nonfat component. E - T2 weighted axial MR images shows a hyperintense mass. Axial T1 weighted MR images (F) shows that only a small spot of the lesion reveals drop signal on out-of-phase image. G - Unhenhanced axial T1 weighted MR image. H, I, J - Gd-EOB-DTPA-enhanced images: arterial phase shows marked enhancement, but at the hepatobiliary phase the lesion becomes hypointense (it does not have hepatocytes).

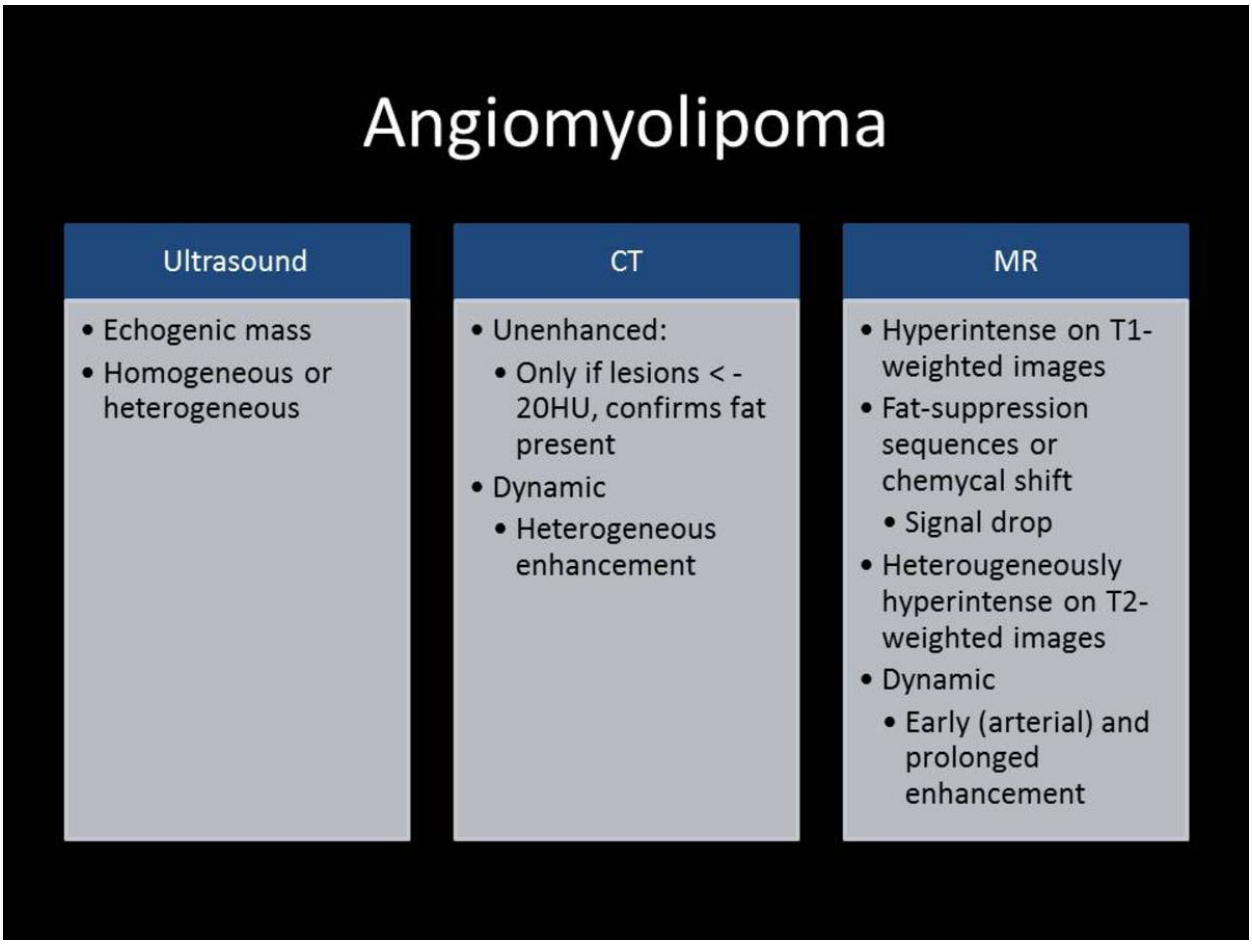
Angiomyolipoma
Ultrasound
• Echogenic mass
• Homogeneous or heterogeneous
CT
• Unenhanced:
• Only if lesions < -20HU, confirms fat present
• Dynamic
• Heterogeneous enhancement
MR
• Hyperintense on T1-weighted images
• Fat-suppression sequences or chemycal shift
• Signal drop
• Heterougeneously hyperintense on T2-weighted images
• Dynamic
• Early (arterial) and prolonged enhancement

Fig. 15: 15

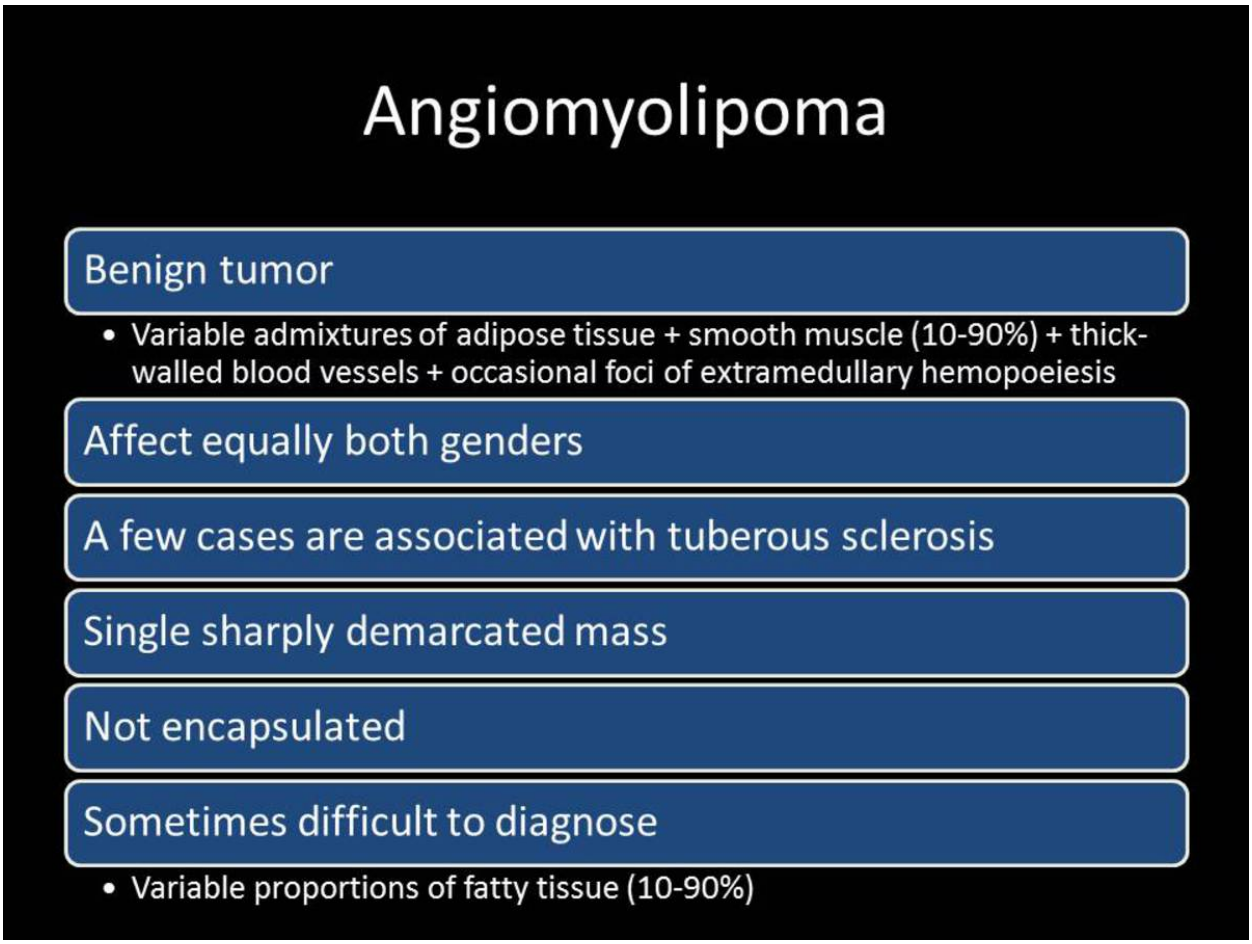
Angiomyolipoma
Benign tumor
• Variable admixtures of adipose tissue + smooth muscle (10-90%) + thick-walled blood vessels + occasional foci of extramedullary hemopoeiesis
Affect equally both genders
A few cases are associated with tuberous sclerosis
Single sharply demarcated mass
Not encapsulated
Sometimes difficult to diagnose
• Variable proportions of fatty tissue (10-90%)

Fig. 14: 14

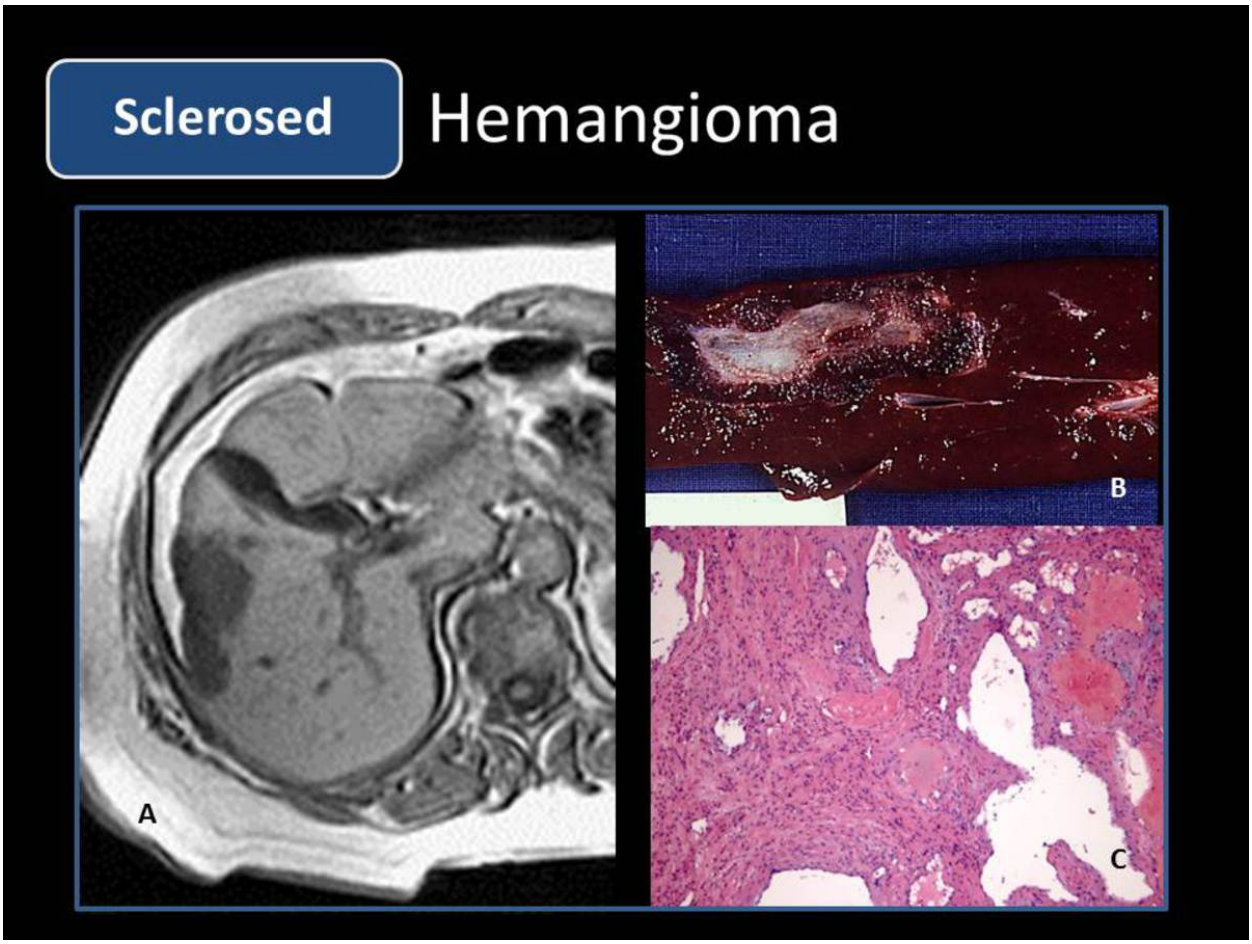

Fig. 13: 80 year-old woman with chronic-liver disease and a long- term liver mass. A. T1-weighted MR image shows lobulated liver with an irregular hypointense mass. B. Hyalinised fibrotic tissue (considered the end-stage of involution of a haemangioma). C. Photomicrograph shows dilated vessels with fibrosis

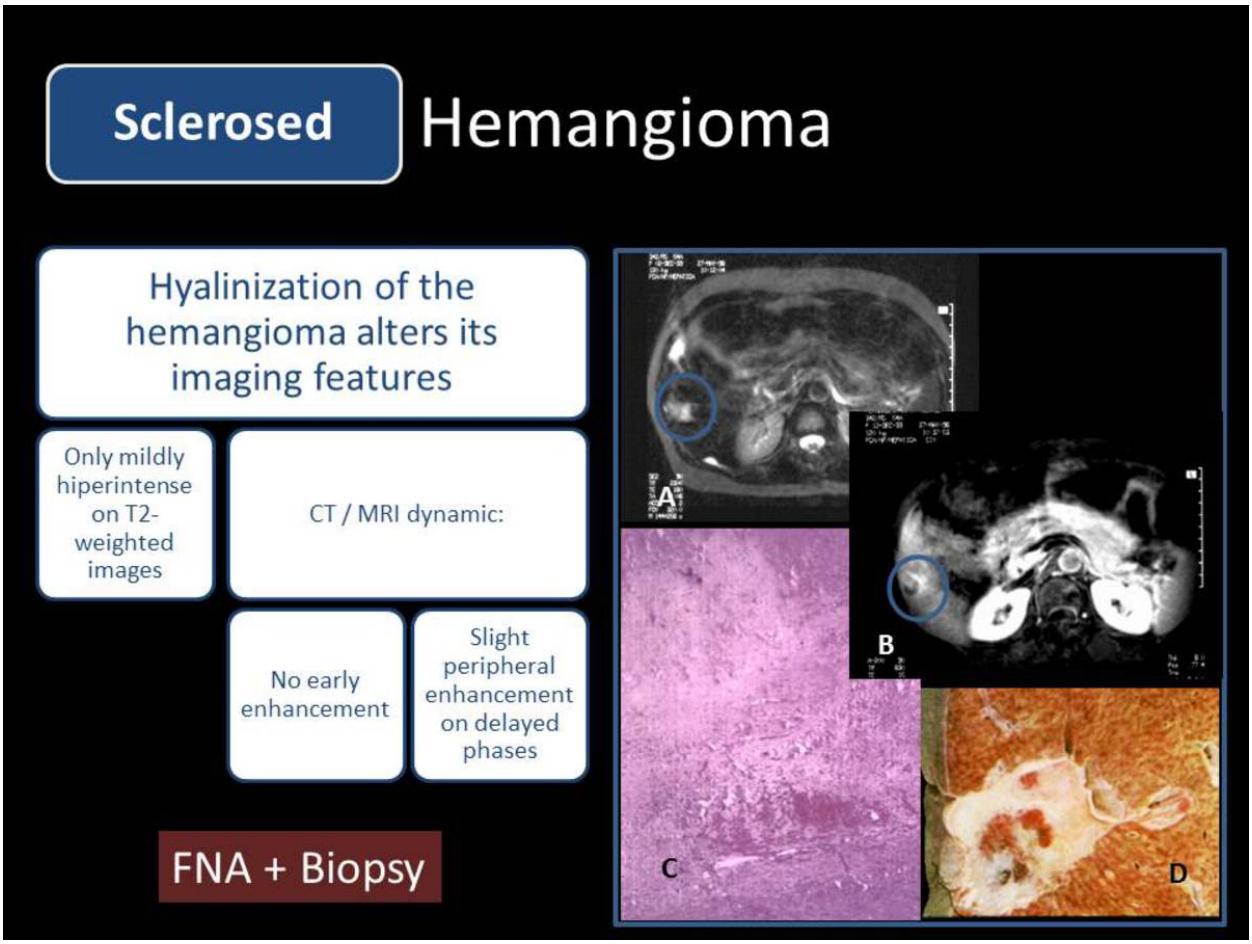

Fig. 12: A. T2-weighted MR image shows a heterogeneous lesion, less hyperintense than cerebrospinal fluid (as usual in typical hemangiomas). B. Dynamic gadolinium-enhanced T1-weighted MR image obtained at delayed phase shows peripheral enhancement. C. Photomicrograph shows dilated vessels with fibrosis. D. Hyalinised fibrotic tissue (considered the end-stage of involution of a haemangioma).

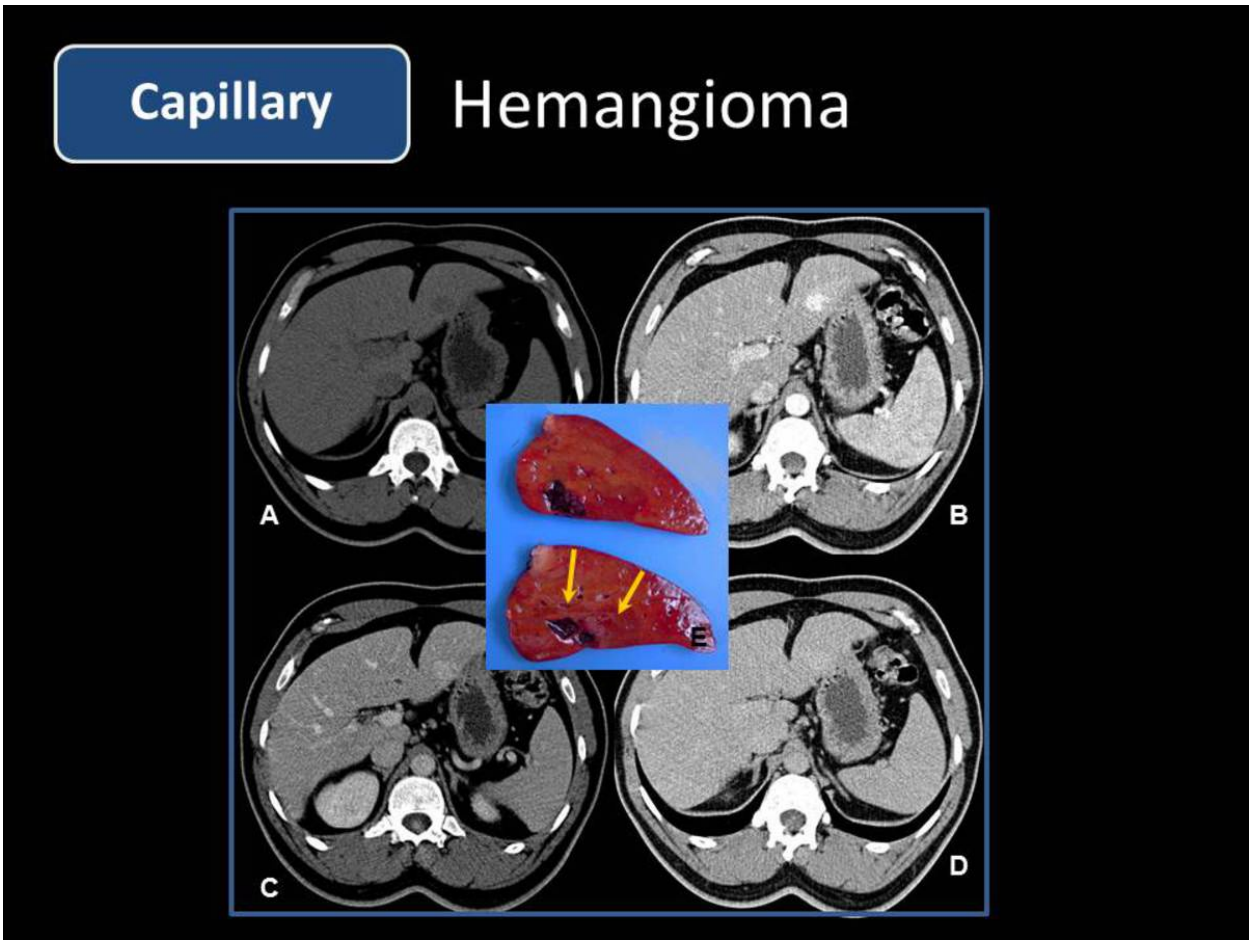

Fig. 11: A. Unenhanced CT shows slightly hypoattenuating nodule in left lobe (2cm). B. Flash-filling pattern in arterial scan phase. C. Slight hyperattenuation compared with the surrounding parenchyma during venous and late phase scan. E. Pathologic specimen shows a vascular lesion (arrows) with an eccentric thrombus within vascular spaces.

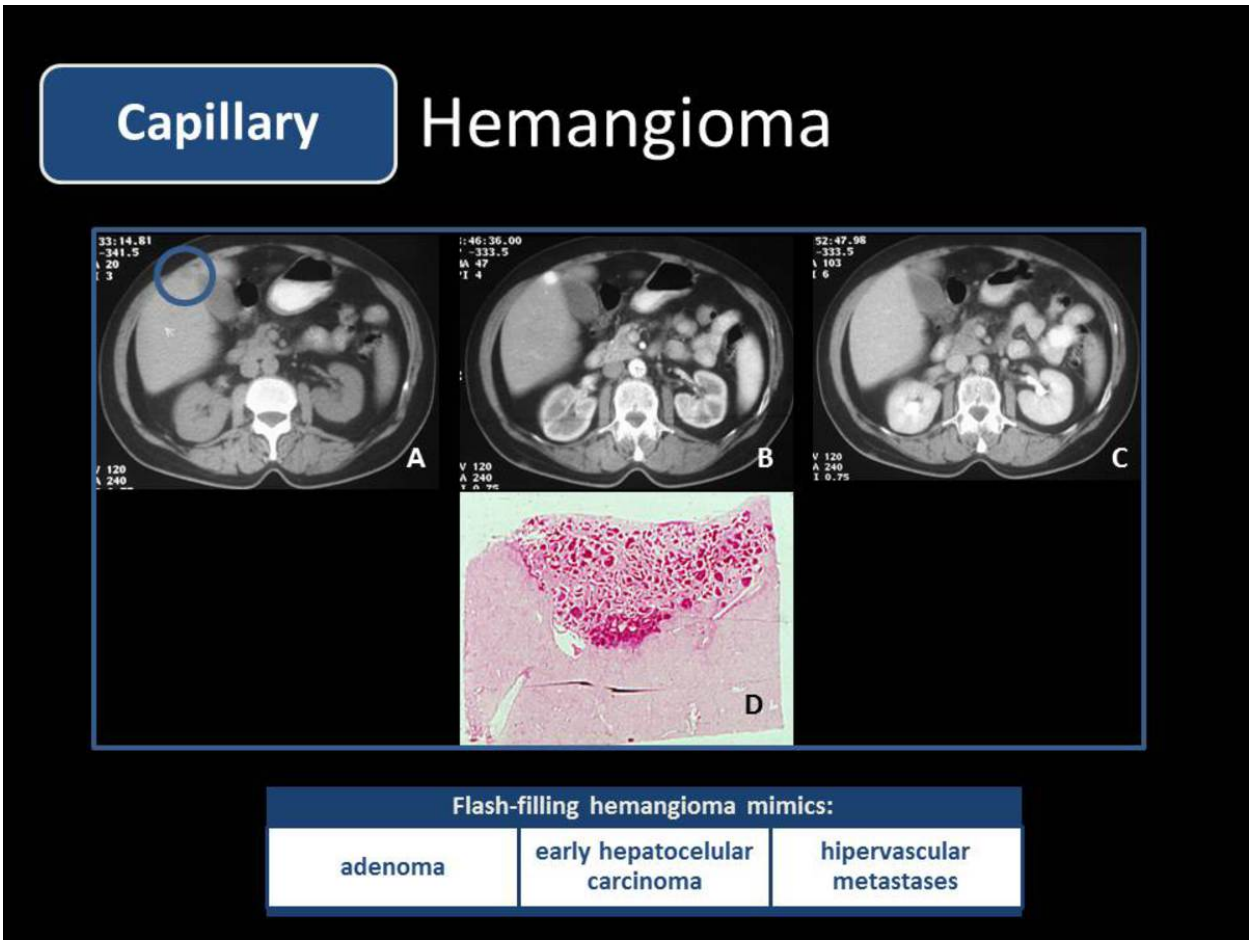

Fig. 10: A. Unenhanced CT shows slightly hypoattenuating subcapsular nodule in left lobe (1,5cm). B. Flash-filling pattern in arterial scan phase. C. Indistinct and iso-attenuating compared with the surrounding parenchyma during late phase scan. D. Microscopic appearance of capillary hemangioma.

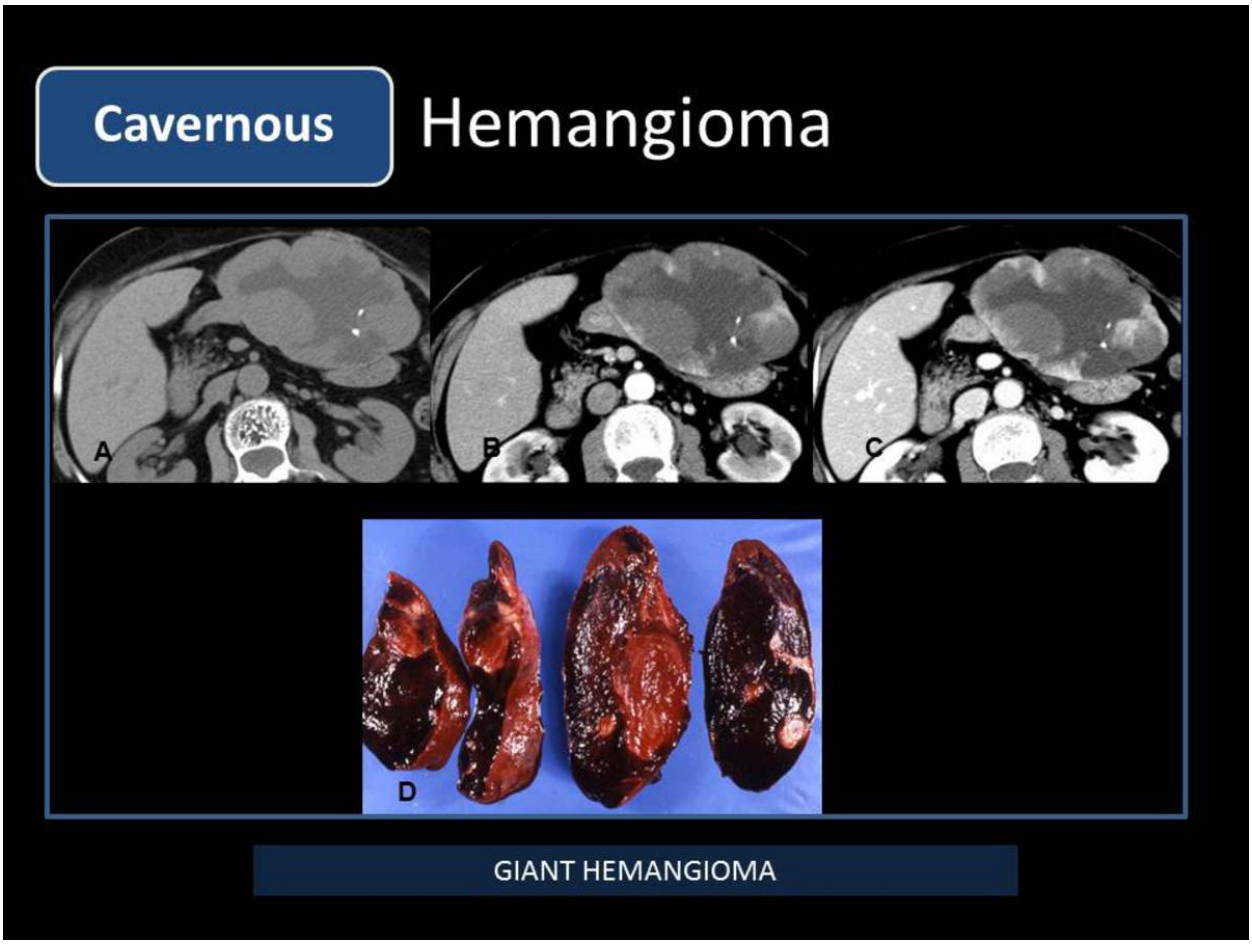

Fig. 9: A. Unenhanced CT shows a heterogeneous well-defined mass, with lobulated borders and some punctate calcifications (phleboliths) B-C. Dynamic study demonstrates progressive peripheral, globular and centripetal enhancement (arterial and venous phases) and a conspicuous central hypodense area (regressive changes) D. Pathologic specimen shows areas of internal necrosis and myxomatous degeneration

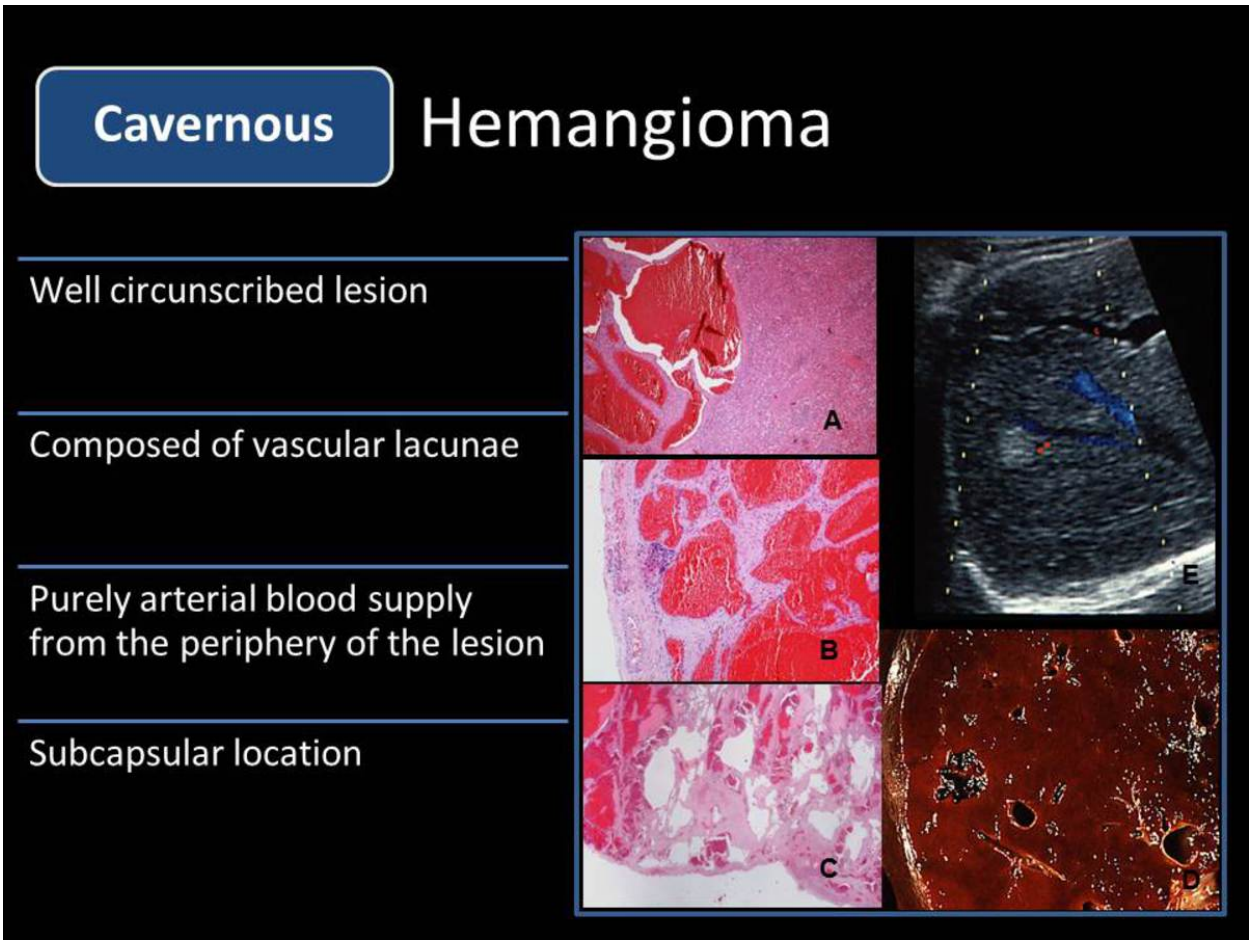

Fig. 8: A, B - Microscopic appearance: blood cells within vascular channels; C - Thin fibrous septations; D - Gross appearance: cut-section of a hemangioma demonstrates its well-defined borders. E - Ultrasound: homogeneous, hyperechoic, well defined nodule.

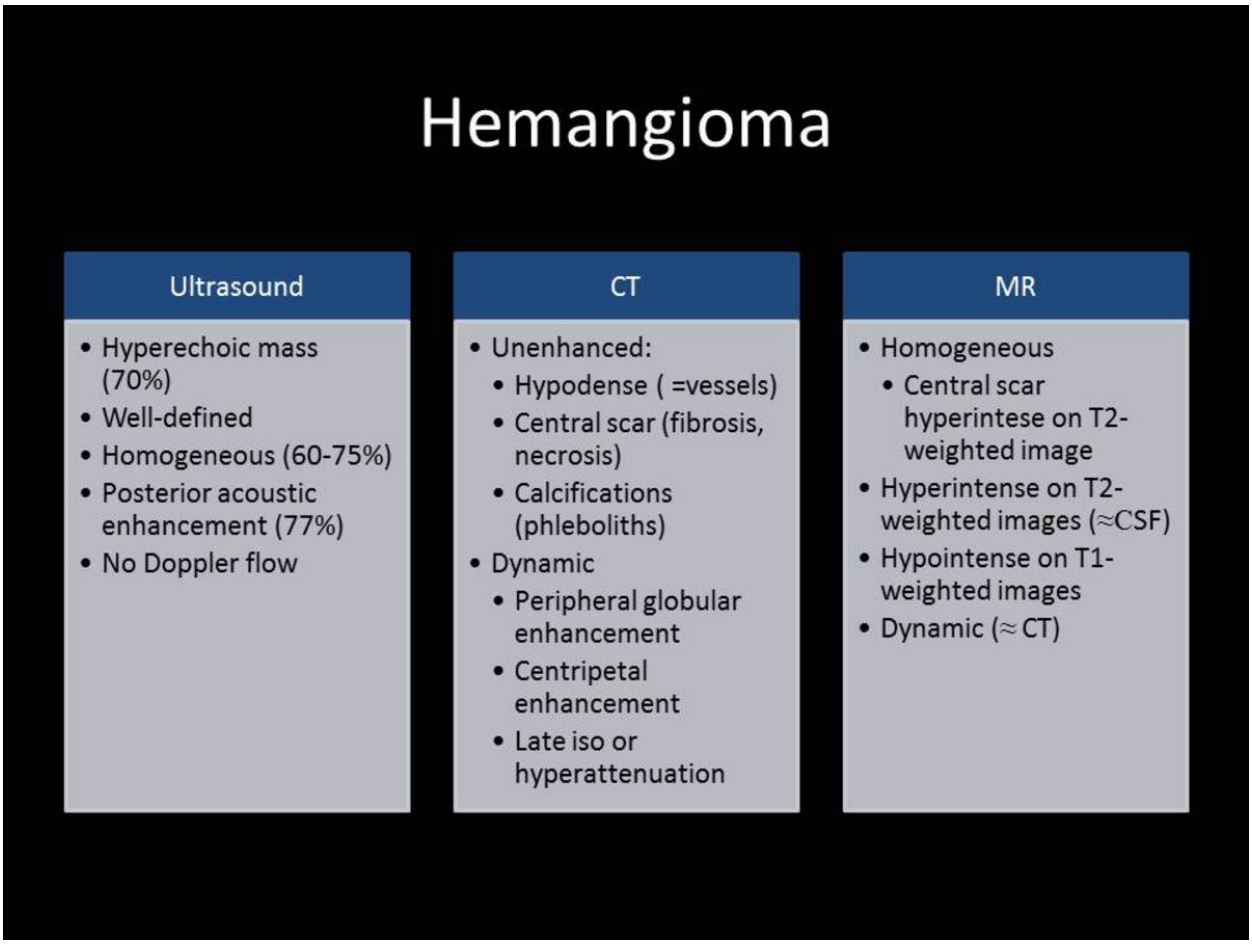
Hemangioma
Ultrasound
• Hyperechoic mass (70%)
• Well-defined
• Homogeneous (60-75%)
• Posterior acoustic enhancement (77%)
• No Doppler flow
CT
• Unenhanced:
• Hypodense (=vessels)
• Central scar (fibrosis, necrosis)
• Calcifications (phleboliths)
• Dynamic
• Peripheral globular enhancement
• Centripetal enhancement
• Late iso or hyperattenuation
MR
• Homogeneous
• Central scar hyperintese on T2-weighted image
• Hyperintense on T2-weighted images (≈CSF)
• Hypointense on T1-weighted images
• Dynamic (≈ CT)

Fig. 7: 7

IMAGING FINDINGS OR PROCEDURE DETAILS

- Primary mesenchymal liver tumors have a wide range of imaging appearances:
  - some similar to those appearing in epithelial tumors, metastasis or even abscesses
  - other are characteristic and can guide us to the diagnosis.

Fig. 6: 6

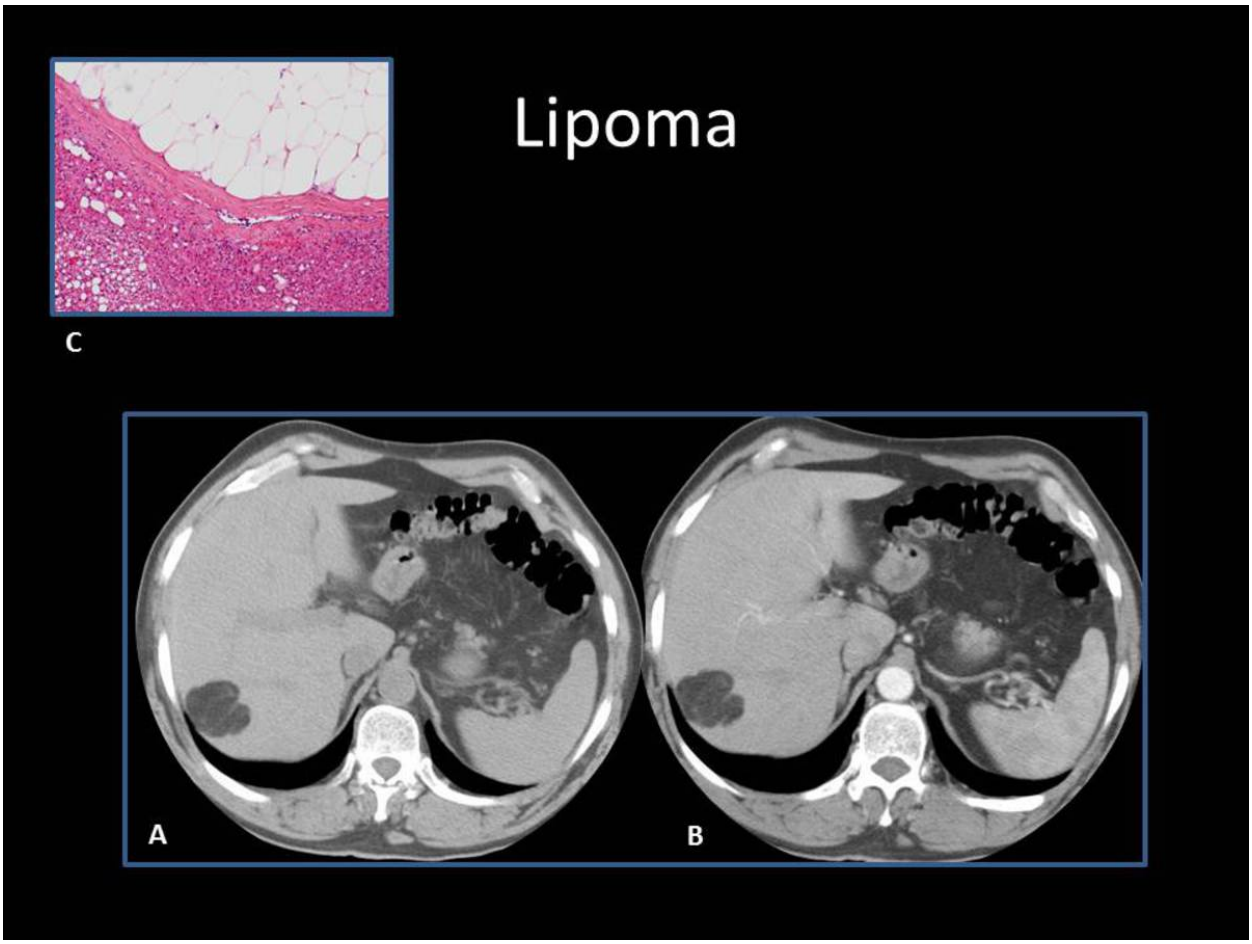

Fig. 19: A. Unenhanced-CT shows a fat density hypoattenuating mass in the right liver lobe. B. In enhanced-CT study the lesion shows no enhancement. C. - High-power photomicrograph shows fat cells limited by a capsule.

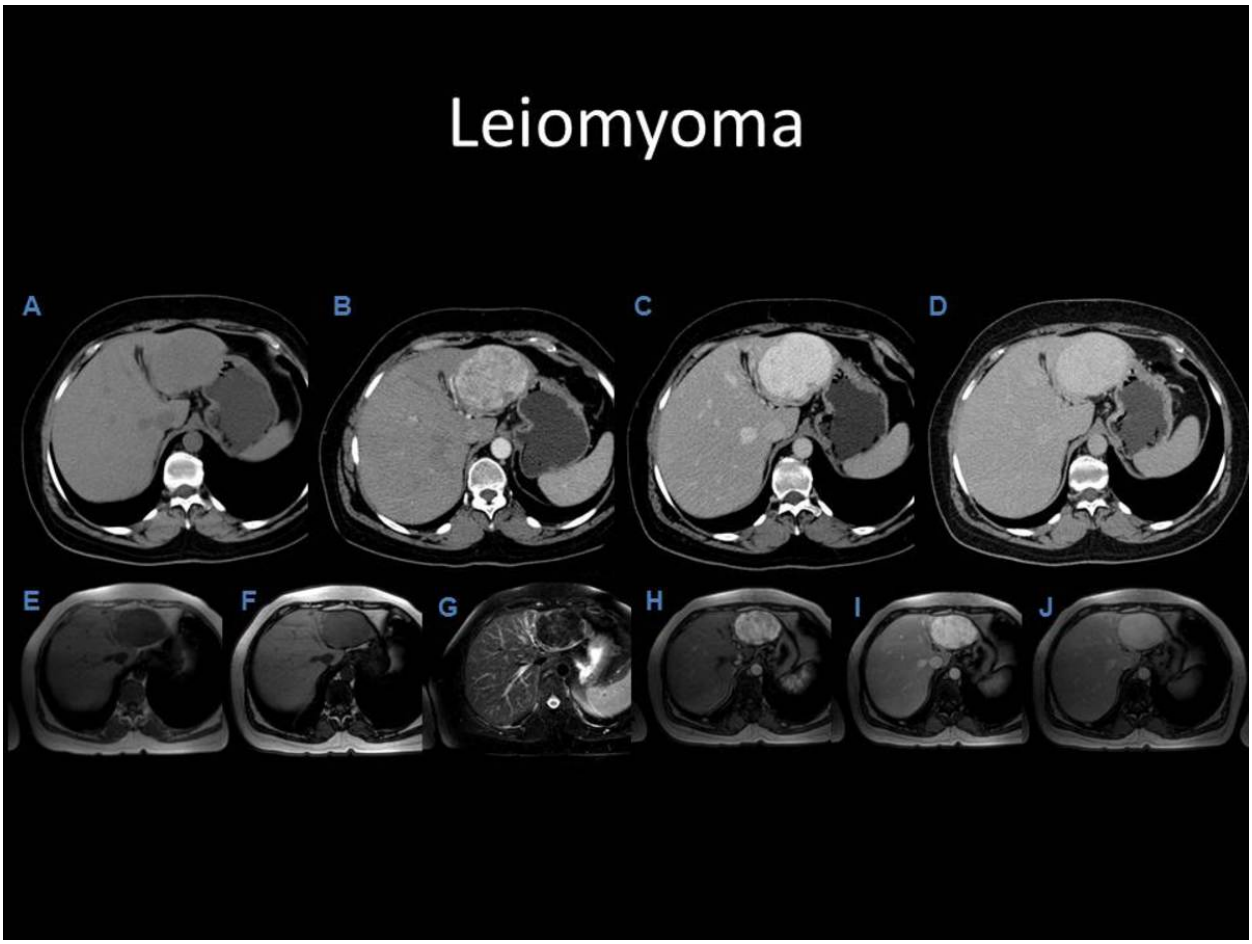

Fig. 29: 61-year old woman with an asymptomatic epigastric mass. A. Unenhanced CT shows an isoattenuating left lobe mass. B-D. In dynamic CT study it shows a marked, progressive and homogeneous enhancement throughout the liver enhancement phases. E,F Axial T1 weighted in-phase and out-of-phase MR images show low signal intensity. G. T2 fat-saturated weighted axial MR image shows also low signal intensity. H-J. In Dynamic MR study the lesion shows identical behaviour as on the CT scan.

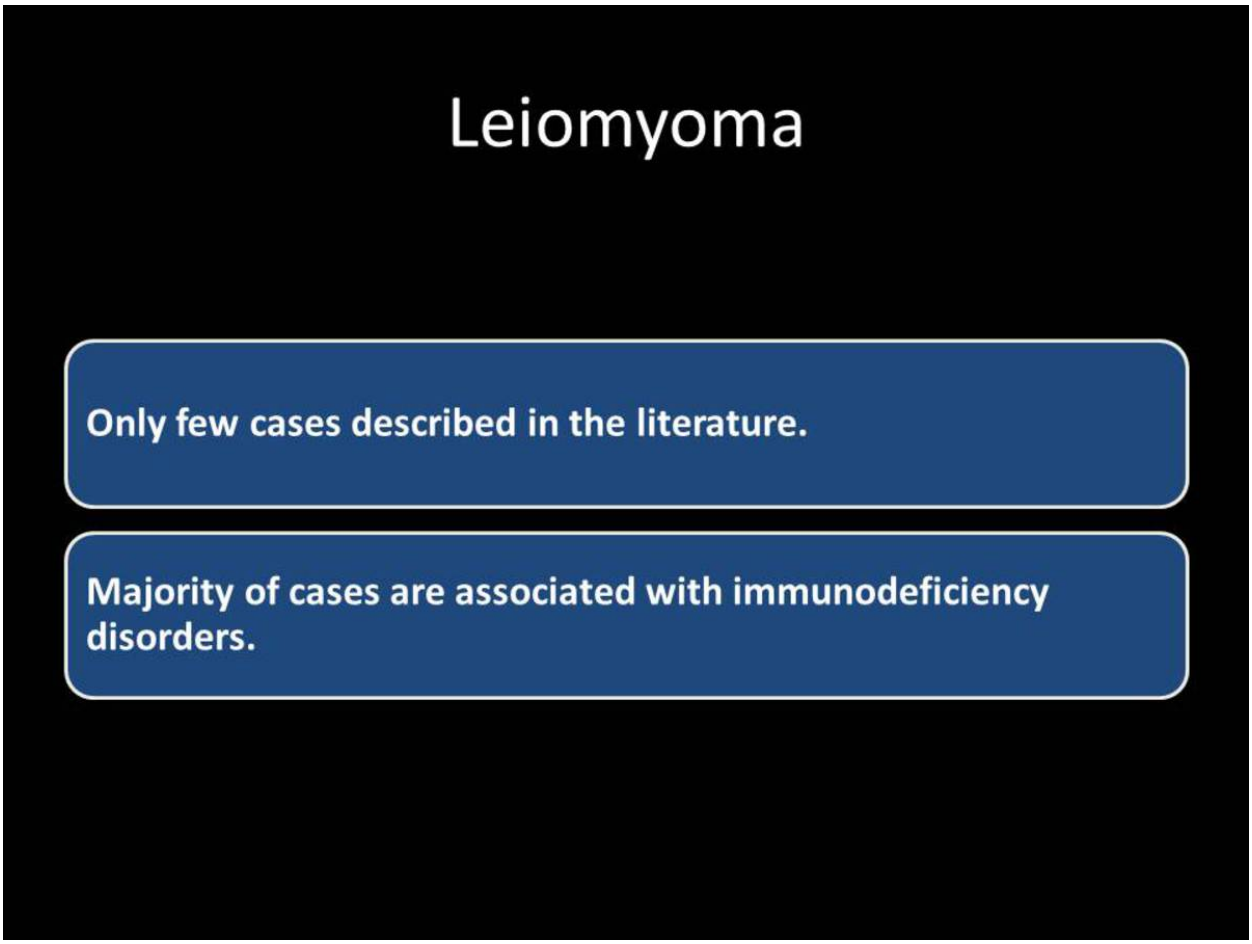
Leiomyoma
Only few cases described in the literature.
Majority of cases are associated with immunodeficiency disorders.

Fig. 28: 28

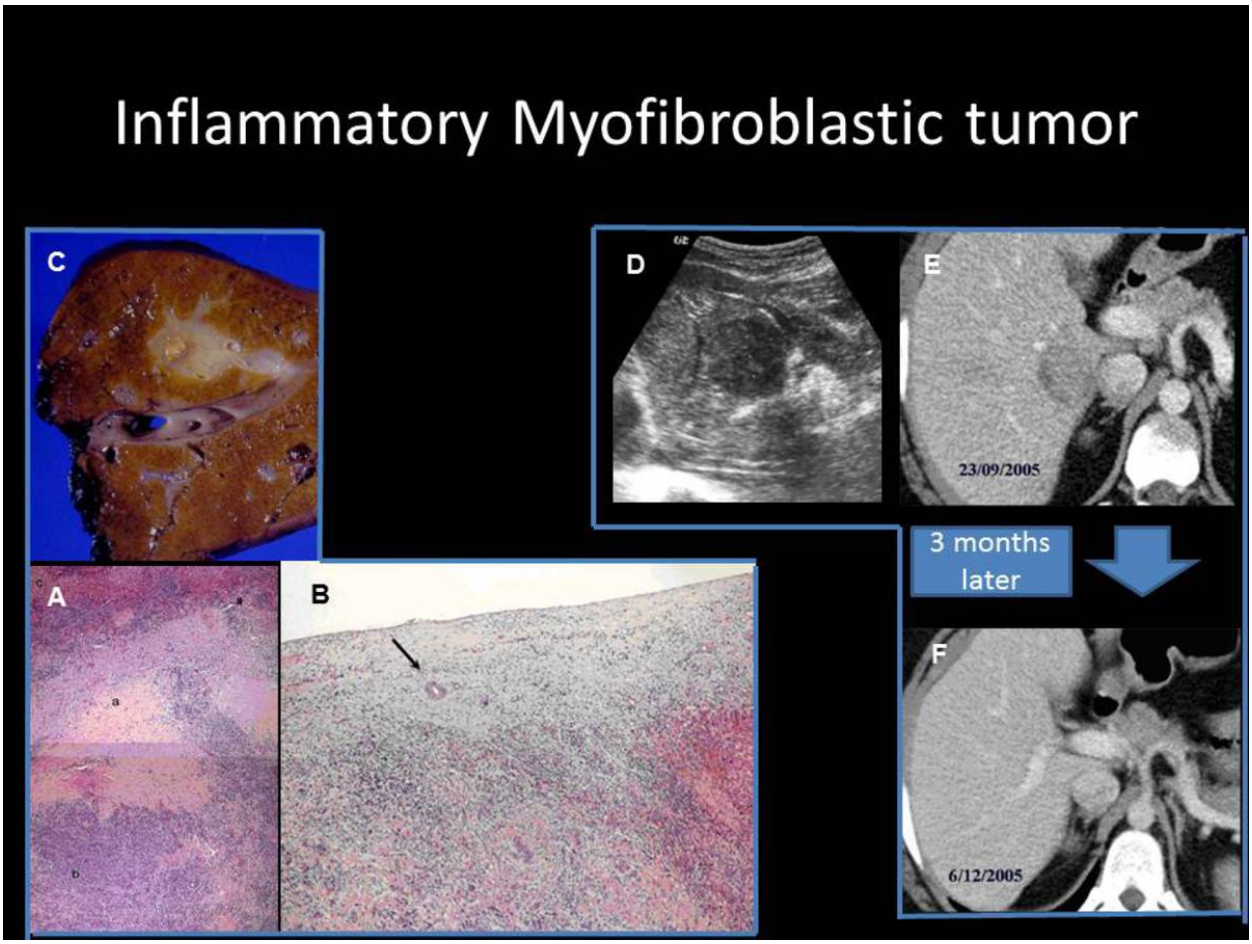

Fig. 27: A. Composed high-power photomicrograph shows prominent fibrosis and proliferating myofibroblasts at the periphery of the mass (a) contrasting with a cellular lymphoplasmocytic infiltrate central core (b). The liver parenchyma away from the disease process has normal arquitecture (c). B. High-power photomicrograph. Portal tracts are expanded by fibrosis and granulation tissue, with occlusive phlebitis (arrow). C. Pathologic specimen showing a tender heterogeneous mass with a yellowish, smooth core surrounded by an ill-defined hyperemic halo. D. US: the mass is relatively well-defined, heterogeneous and hypoechoic. E, F: A follow-up CT scan 2 months later performed after a course of antibiotics and anti-inflammatory drugs, showed complete resolution of the lesions.

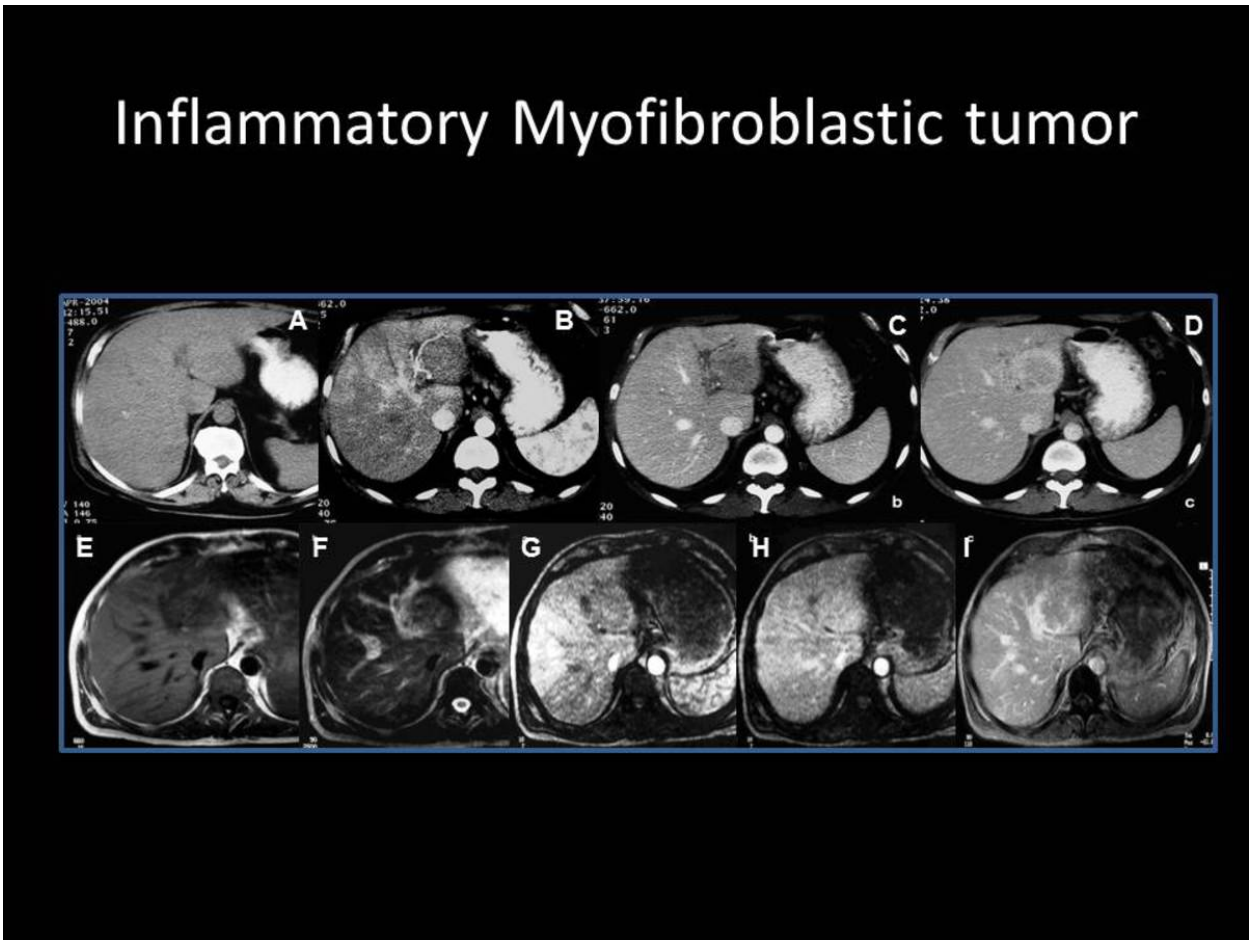

Fig. 26: 53 year-old man presented after 3 months with low grade fever, weight loss, general fatigue and upper abdominal pain. A. Unenhanced CT shows an isoattenuating mass in the left liver lobe. B-D. In dynamic CT study the lesion is heterogeneously hypodense at the arterial and portal venous phases of the dynamic liver study. In the delayed phase, a broad peripheral hyperdense halo was noted. E, F In T1-weighted image the mass appears heterogeneous with slight hyperintensity on the T2-WI. G-I. In Dynamic MR study it shows hypovascularity, with a peripheral ill-defined and irregular rim noted on the late interstitial phase of liver enhancement.

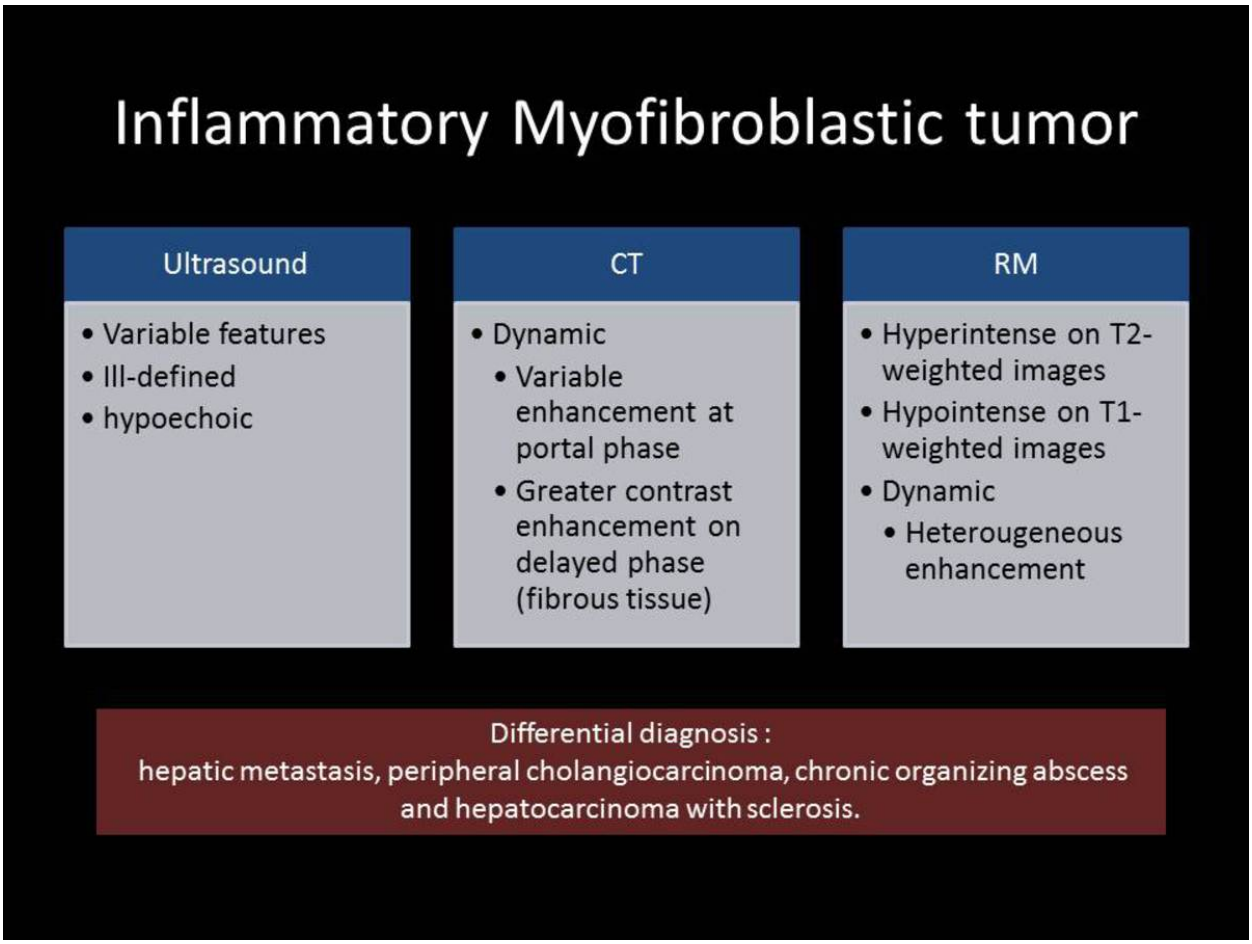
Inflammatory Myofibroblastic tumor
Ultrasound
• Variable features
• Ill-defined
• hypoechoic
CT
• Dynamic
• Variable enhancement at portal phase
• Greater contrast enhancement on delayed phase (fibrous tissue)
RM
• Hyperintense on T2-weighted images
• Hypointense on T1-weighted images
• Dynamic
• Heterougeneous enhancement
Differential diagnosis :
hepatic metastasis, peripheral cholangiocarcinoma, chronic organizing abscess and hepatocarcinoma with sclerosis.

Fig. 25: 25

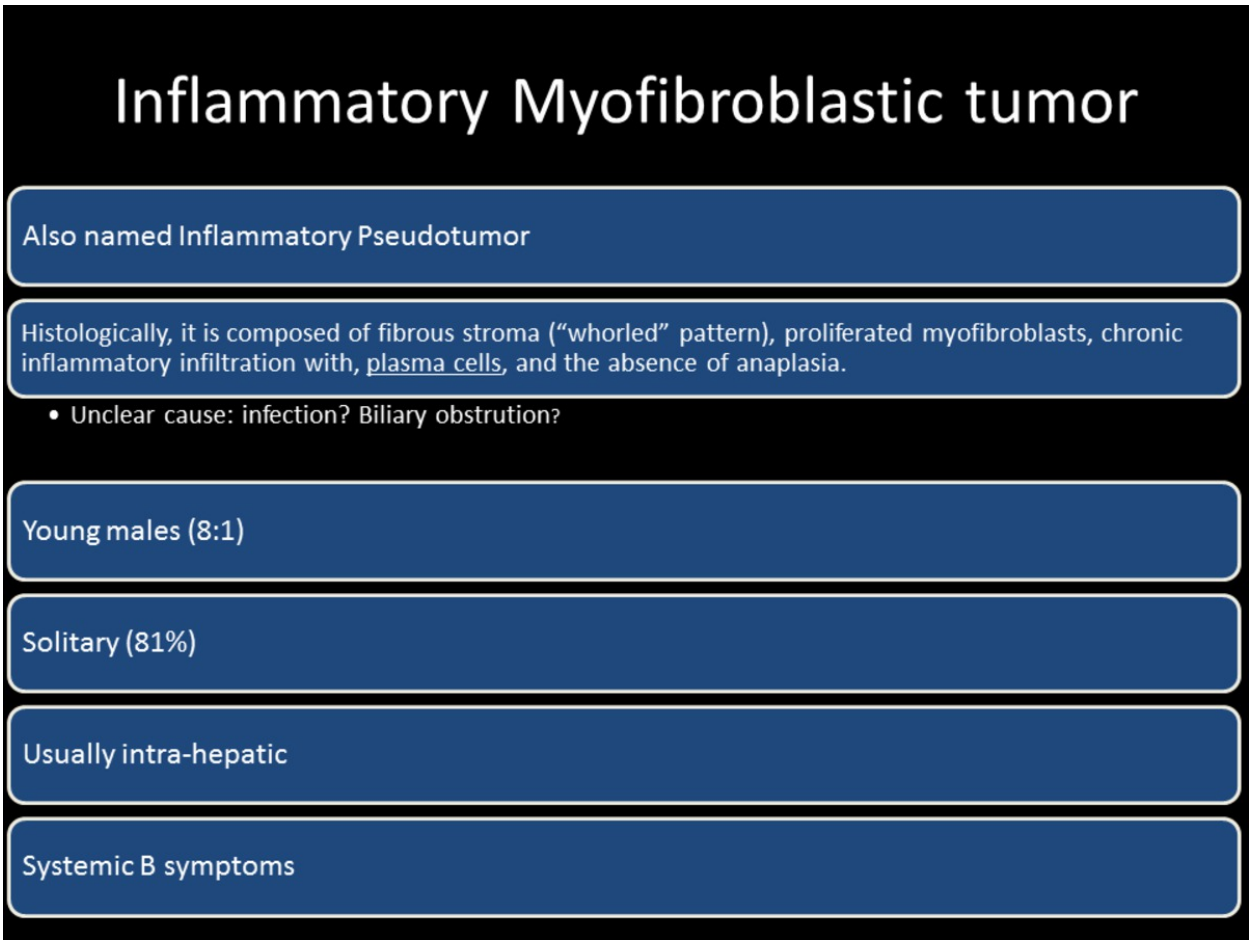
Inflammatory Myofibroblastic tumor
Also named Inflammatory Pseudotumor
Histologically, it is composed of fibrous stroma ("whorled" pattern), proliferated myofibroblasts, chronic inflammatory infiltration with, plasma cells, and the absence of anaplasia.
• Unclear cause: infection? Biliary obstrution?
Young males (8:1)
Solitary (81%)
Usually intra-hepatic
Systemic B symptoms

Fig. 24: 24

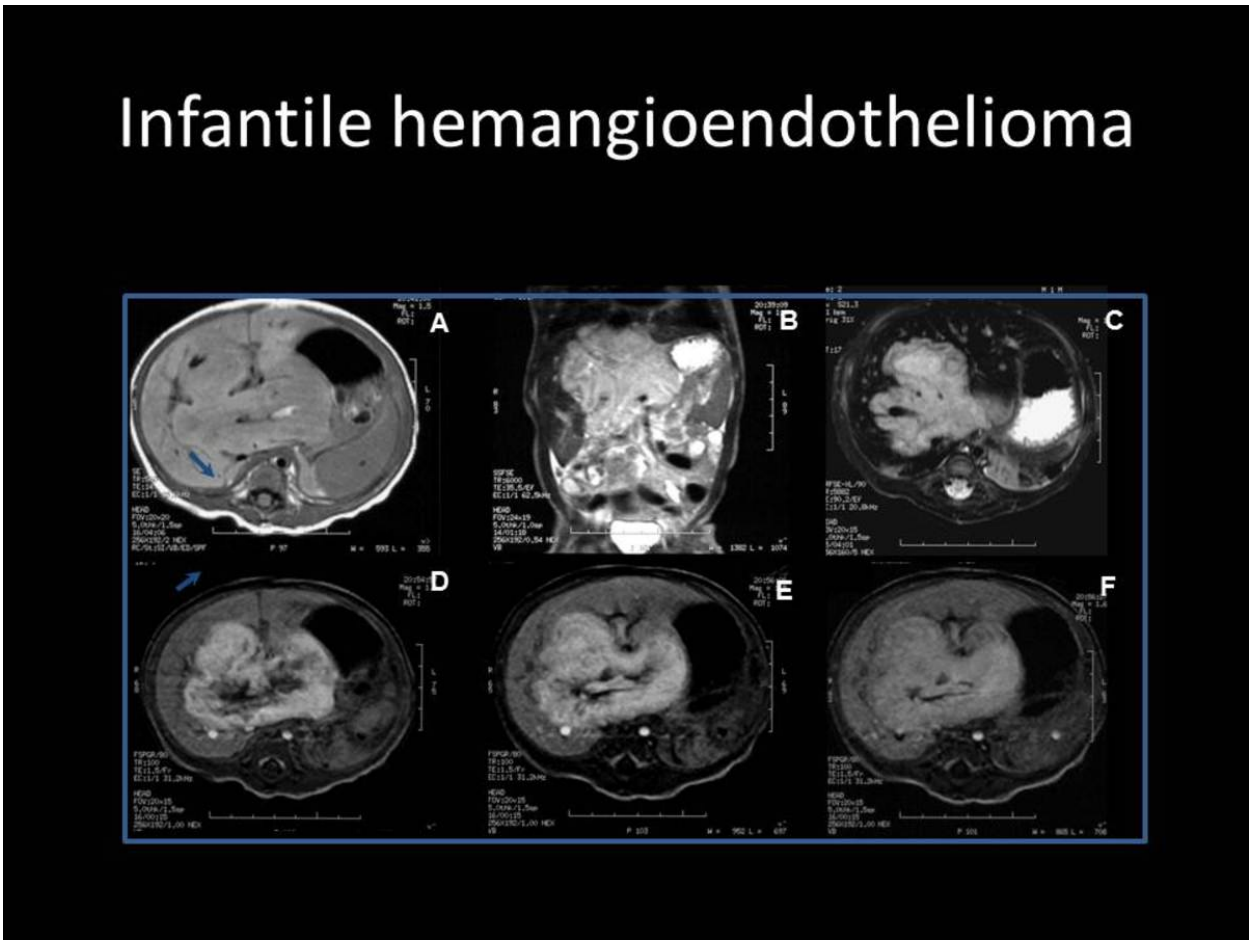

Fig. 23: A. On T1-weighted image the mass shows slight heterogeneous isointense signal and mild hyperintensity on the T2-WI (B,C). In Dynamic MR study (D-F) it shows a peripheral, ill-defined and irregular hyperenhancement. The signal intensity then decreases, until the late interstitial phase of liver enhancement, when the lesion is only slightly hyperintense. After 2 years of treatment with interferon the tumor completely disappeared.

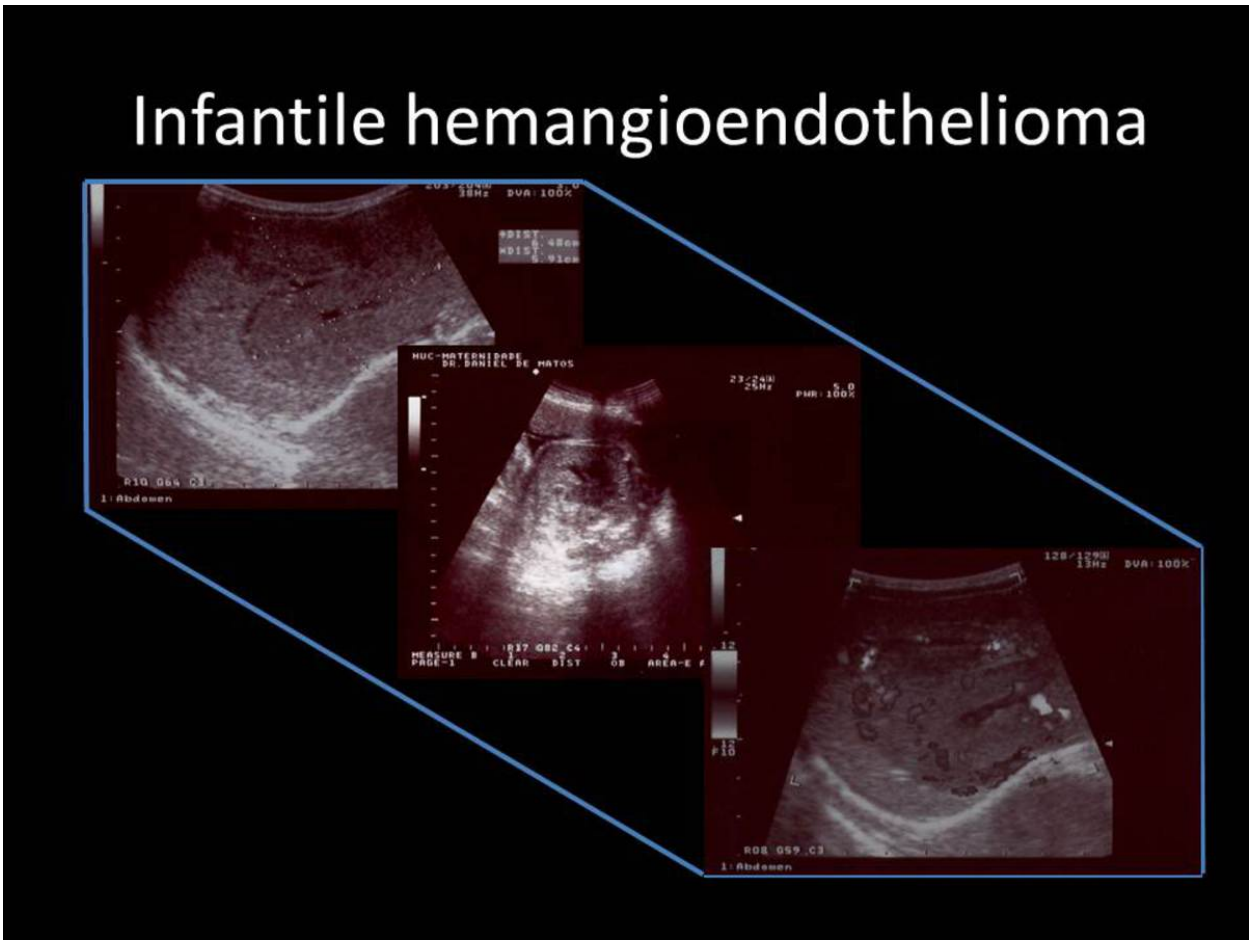

Fig. 22: Obstetric US (26th week-gestation) shows a nodular hypoechoic lesion in the liver. B. After birth US confirms the right liver lobe mass with lobulated borders. C. US-Doppler demonstrates a hypervascular lesion.

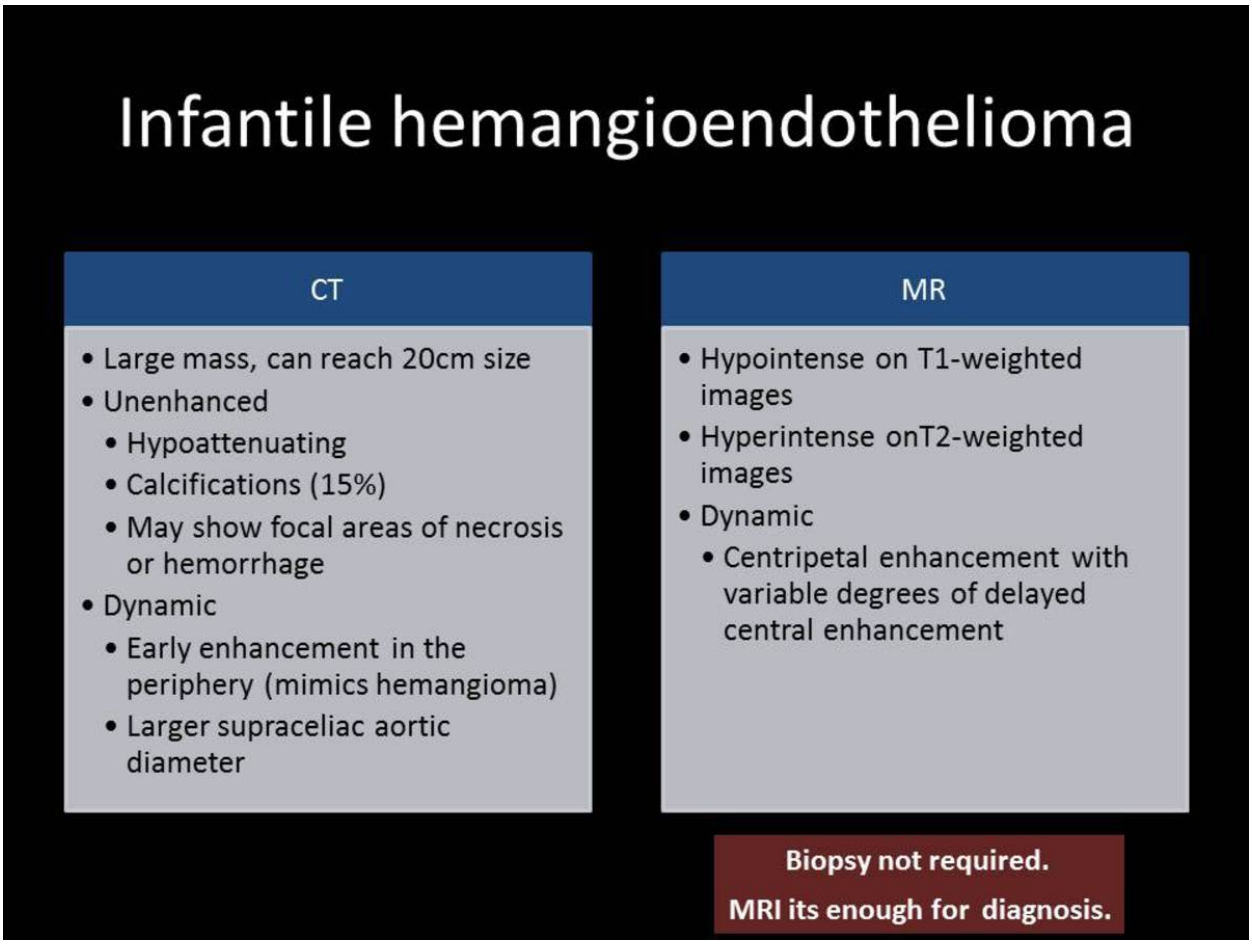
Infantile hemangioendothelioma
CT
• Large mass, can reach 20cm size
• Unenhanced
• Hypoattenuating
• Calcifications (15%)
• May show focal areas of necrosis or hemorrhage
• Dynamic
• Early enhancement in the periphery (mimics hemangioma)
• Larger supraceliac aortic diameter
MR
• Hypointense on T1-weighted images
• Hyperintense onT2-weighted images
• Dynamic
• Centripetal enhancement with variable degrees of delayed central enhancement
Biopsy not required.
MRI its enough for diagnosis.

Fig. 21: 21

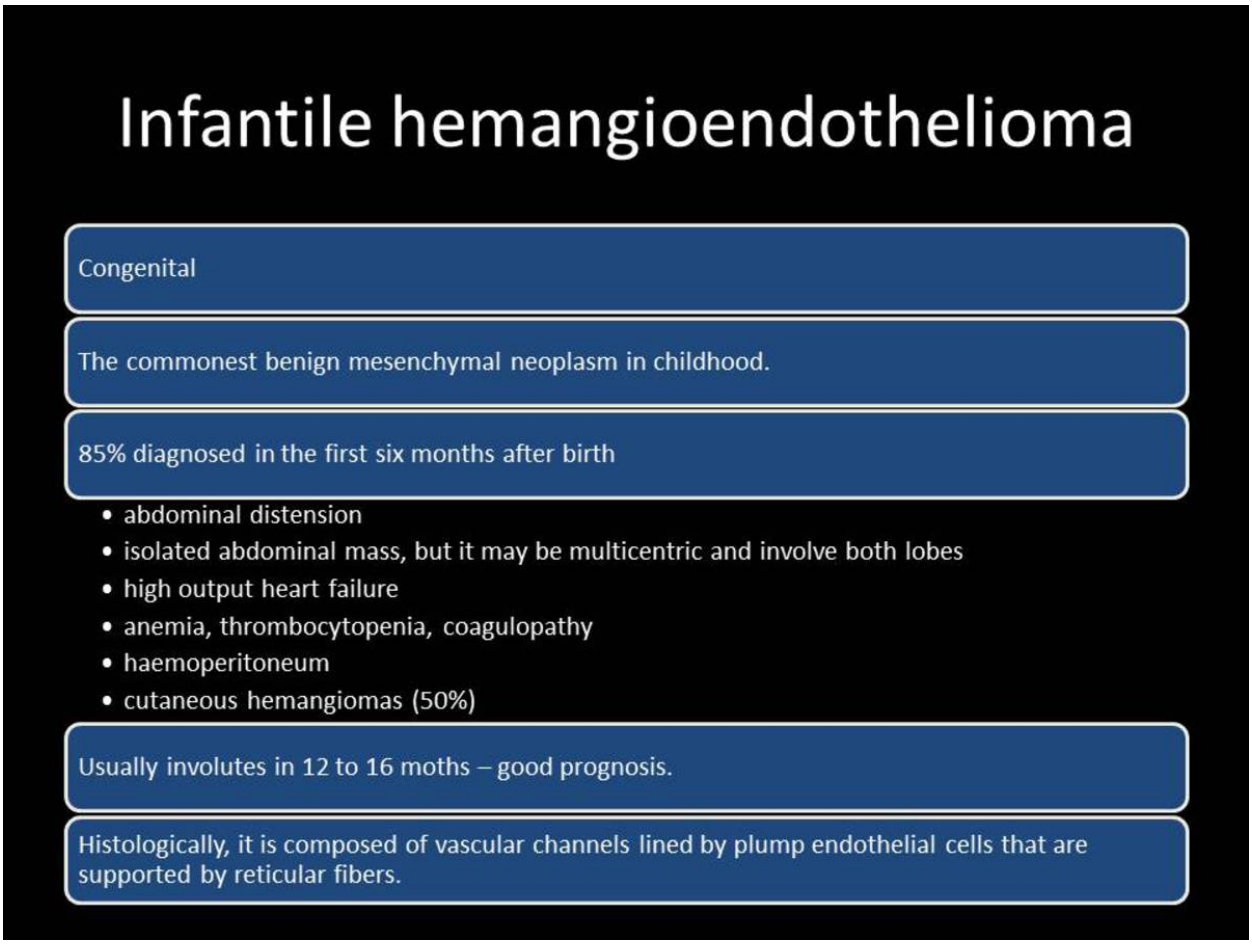
Infantile hemangioendothelioma
Congenital
The commonest benign mesenchymal neoplasm in childhood.
85% diagnosed in the first six months after birth
• abdominal distension
• isolated abdominal mass, but it may be multicentric and involve both lobes
• high output heart failure
• anemia, thrombocytopenia, coagulopathy
• haemoperitoneum
• cutaneous hemangiomas (50%)
Usually involutes in 12 to 16 moths – good prognosis.
Histologically, it is composed of vascular channels lined by plump endothelial cells that are supported by reticular fibers.

Fig. 20: 20

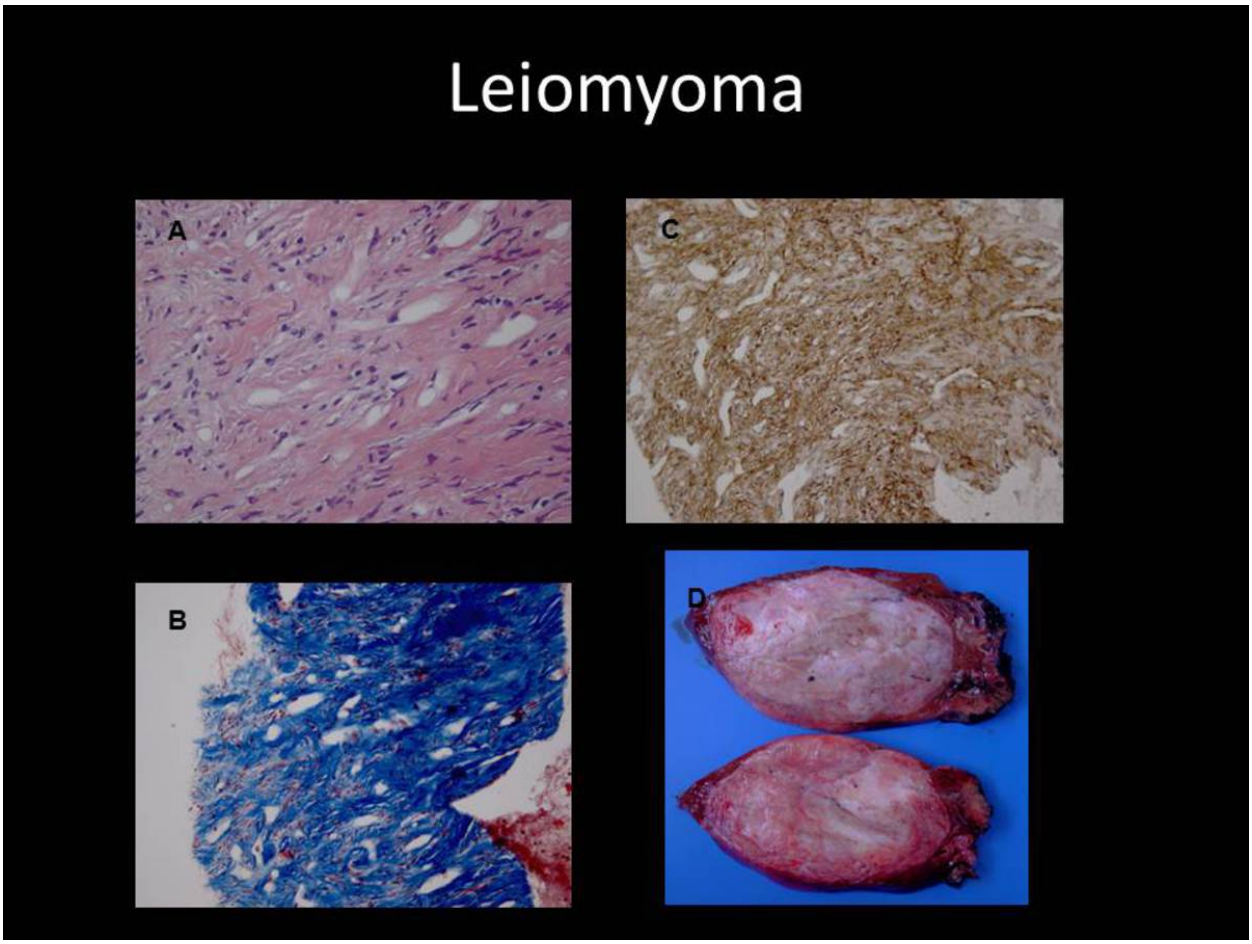

Fig. 30: High-power photomicrographs. A. Smooth muscle fibers without atypia. Histochemical study positive for trichrome (B) and for smooth muscle actin (C). D. Pathologic specimen the left liver lobe mass.

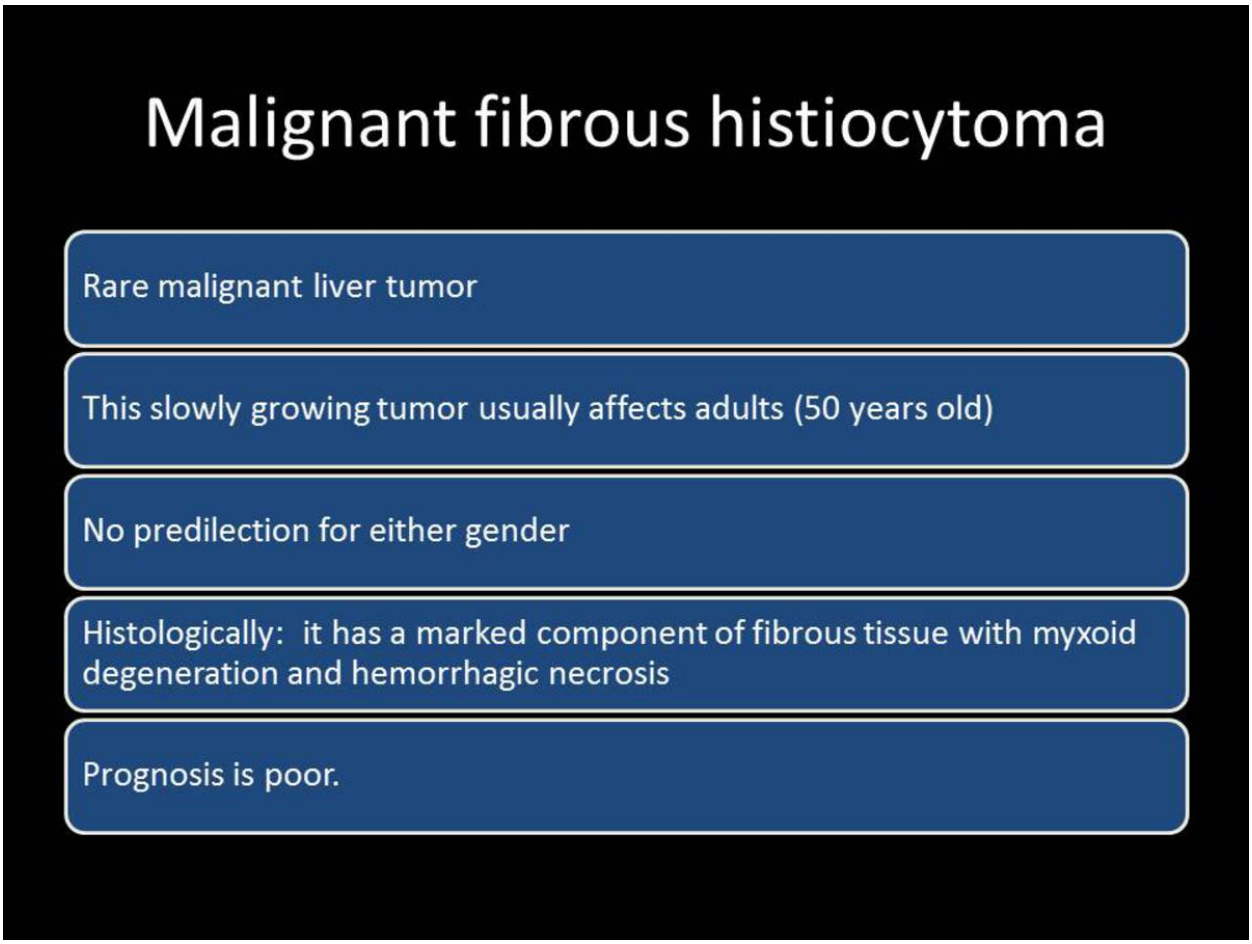
Malignant fibrous histiocytoma
Rare malignant liver tumor
This slowly growing tumor usually affects adults (50 years old)
No predilection for either gender
Histologically: it has a marked component of fibrous tissue with myxoid degeneration and hemorrhagic necrosis
Prognosis is poor.

Fig. 42: 42

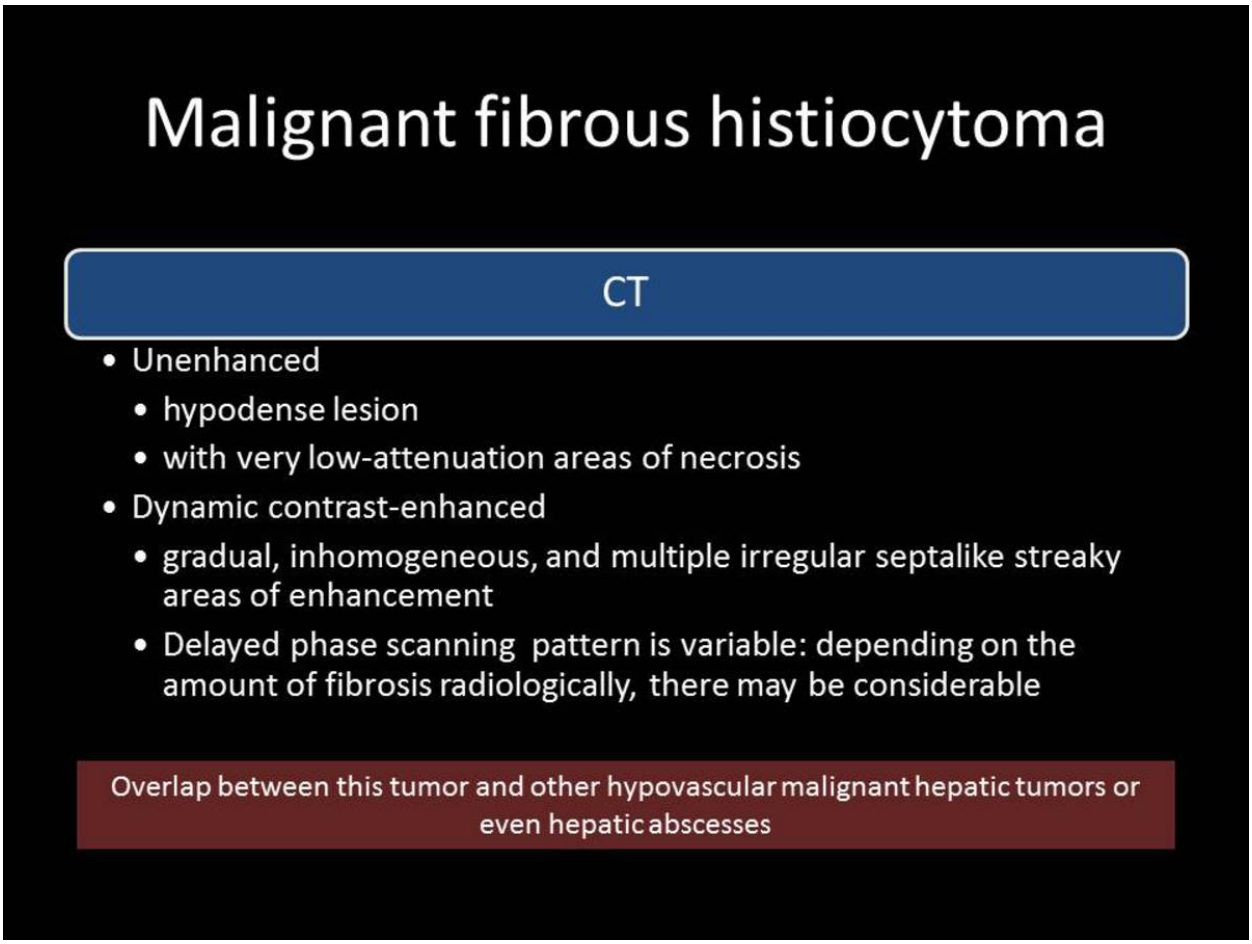
Malignant fibrous histiocytoma
CT
• Unenhanced
• hypodense lesion
• with very low-attenuation areas of necrosis
• Dynamic contrast-enhanced
• gradual, inhomogeneous, and multiple irregular septalike streaky areas of enhancement
• Delayed phase scanning pattern is variable: depending on the amount of fibrosis radiologically, there may be considerable
Overlap between this tumor and other hypovascular malignant hepatic tumors or even hepatic abscesses

Fig. 43: 43

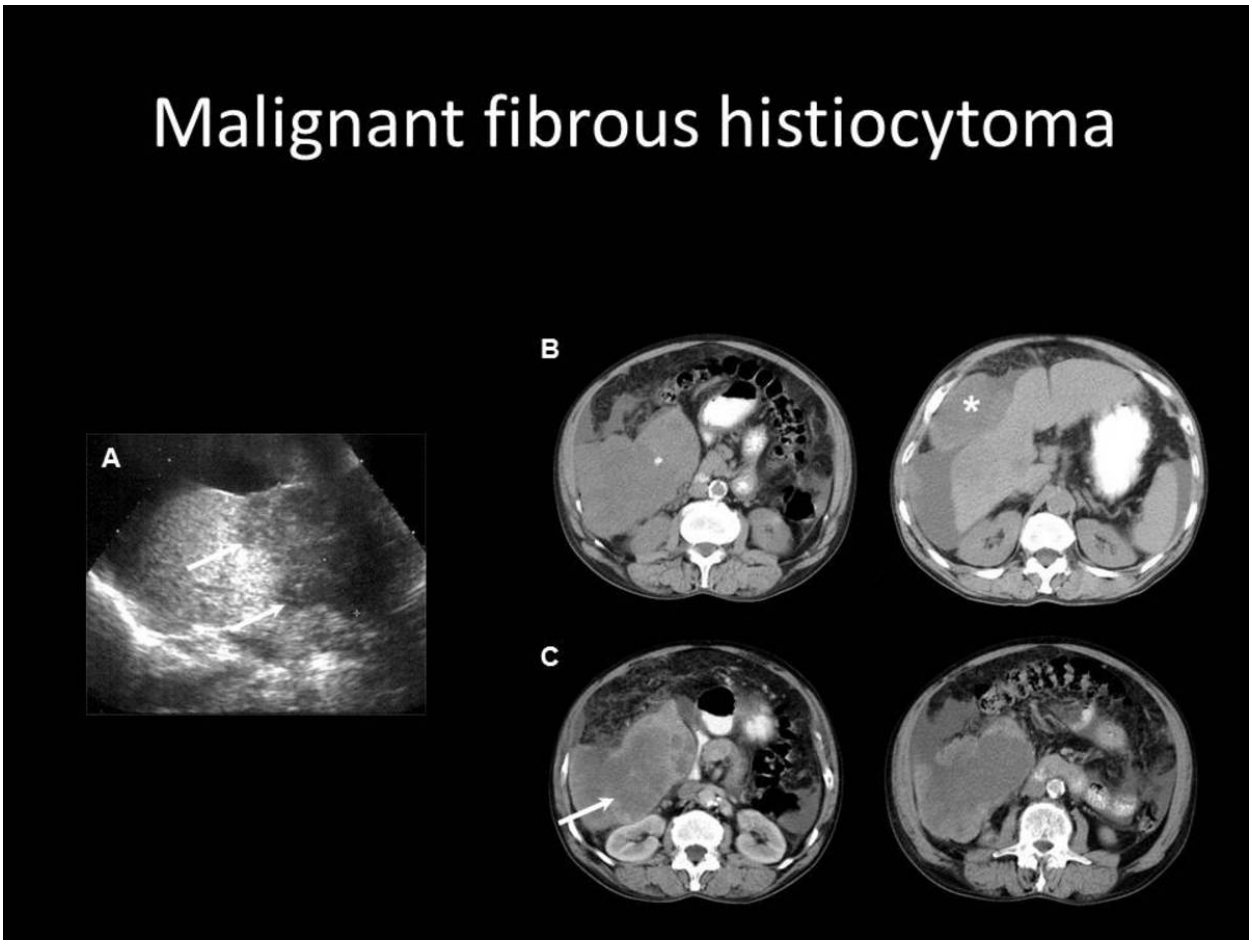

Fig. 44: 63-year-old man with progressive weight loss and distended abdomen. A. Ultrasound shows an heterogeneous hypoechogenic liver mass (arrows). B. Unenhanced CT shows a low- attenuation soft tissue liver mass with a calcification. It is also shown peritoneal tumor metastasis (arrow-head). C. Enhanced CT (portal phase) confirms the heterogeneity and the marked low attenuation of the mass representing necrosis. There is also ascites. Delayed phase (not shown) enhancement depends on the amount of fibrosis.

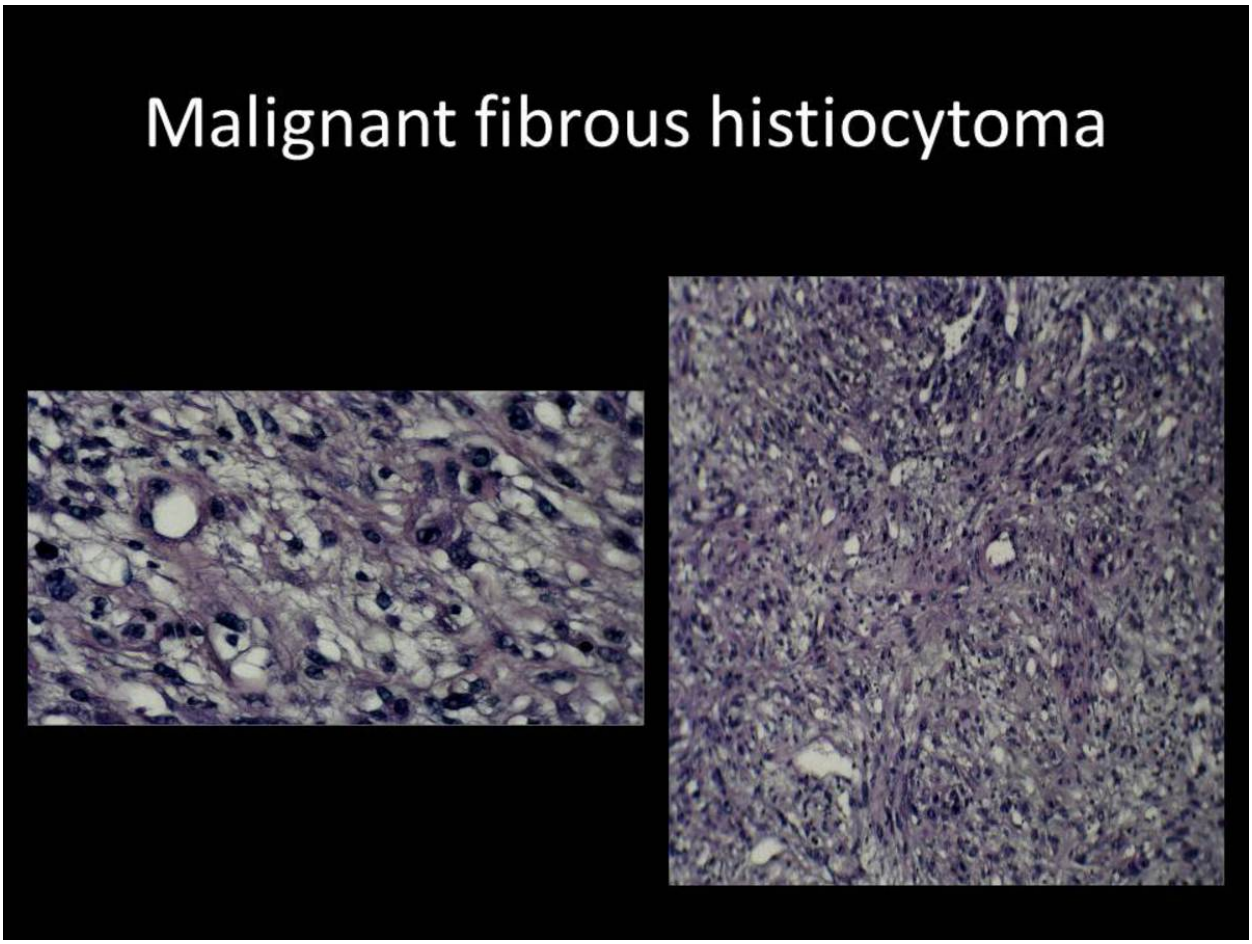

Fig. 45: High-power photomicrographs show a pleomorphic-storiform pattern with giant cells.

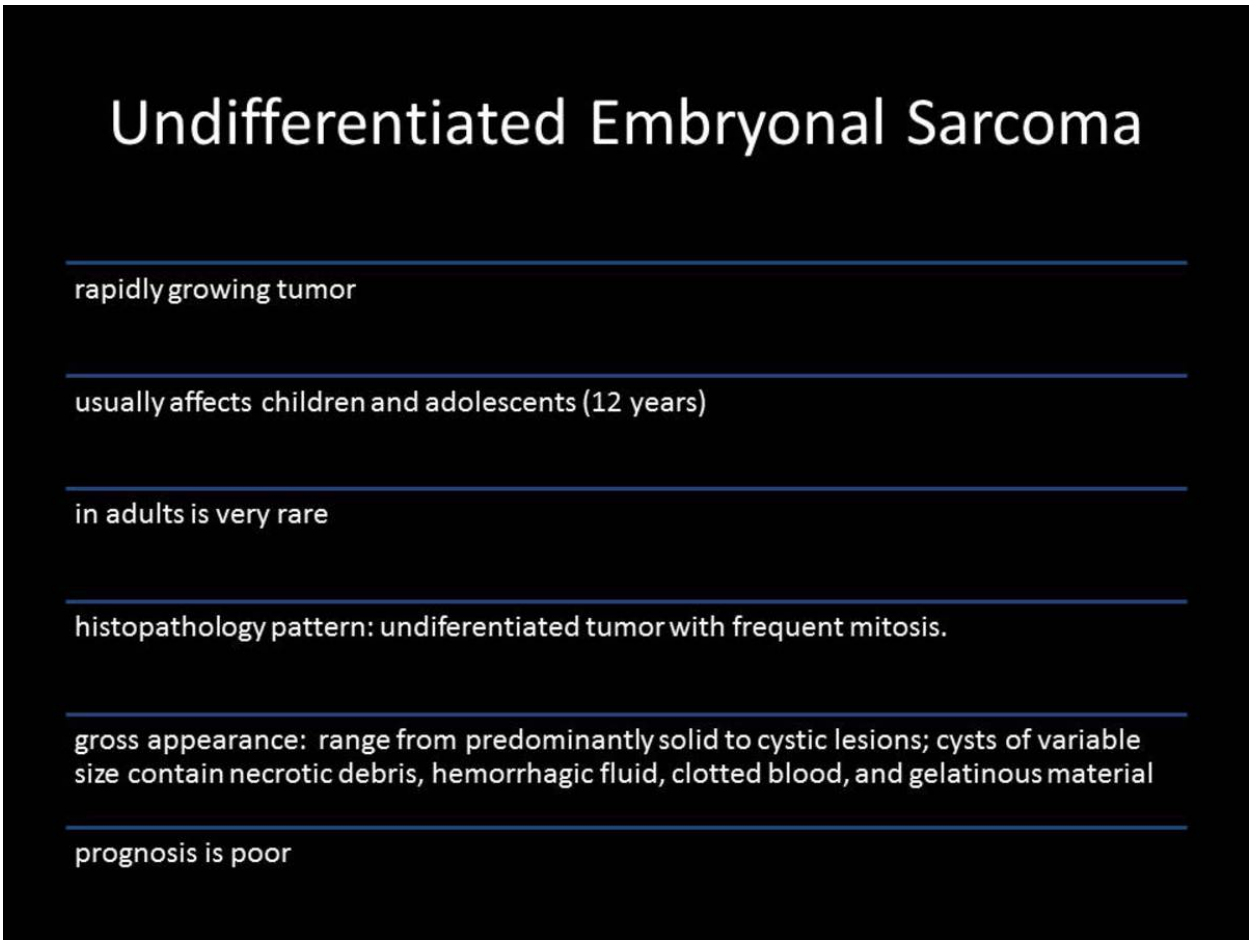
Undifferentiated Embryonal Sarcoma
rapidly growing tumor
usually affects children and adolescents (12 years)
in adults is very rare
histopathology pattern: undiferentiated tumor with frequent mitosis.
gross appearance: range from predominantly solid to cystic lesions; cysts of variable size contain necrotic debris, hemorrhagic fluid, clotted blood, and gelatinous material
prognosis is poor

Fig. 46: 46

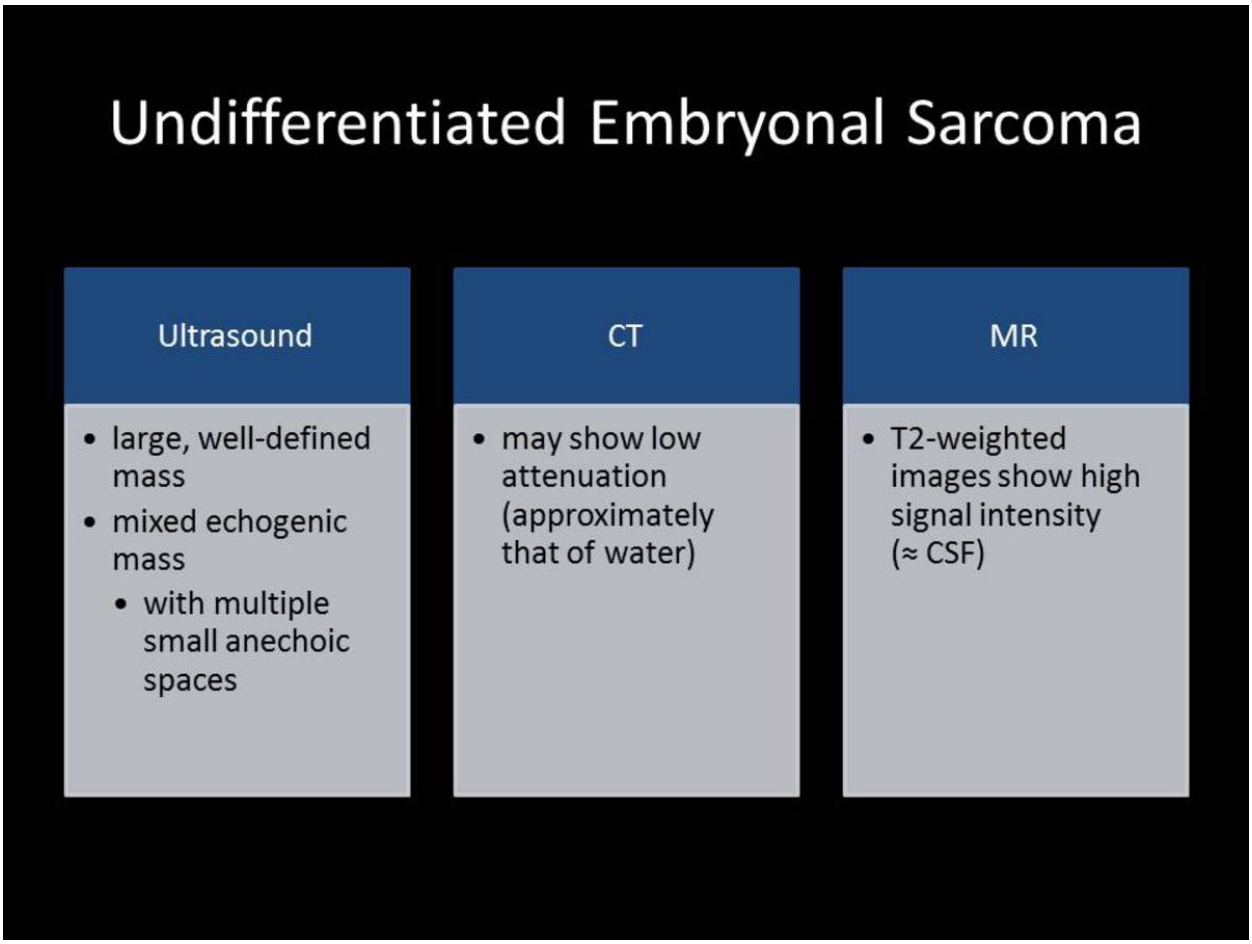
Undifferentiated Embryonal Sarcoma
Ultrasound
• large, well-defined mass
• mixed echogenic mass
• with multiple small anechoic spaces
CT
• may show low attenuation (approximately that of water)
MR
• T2-weighted images show high signal intensity (≈ CSF)

Fig. 47: 47

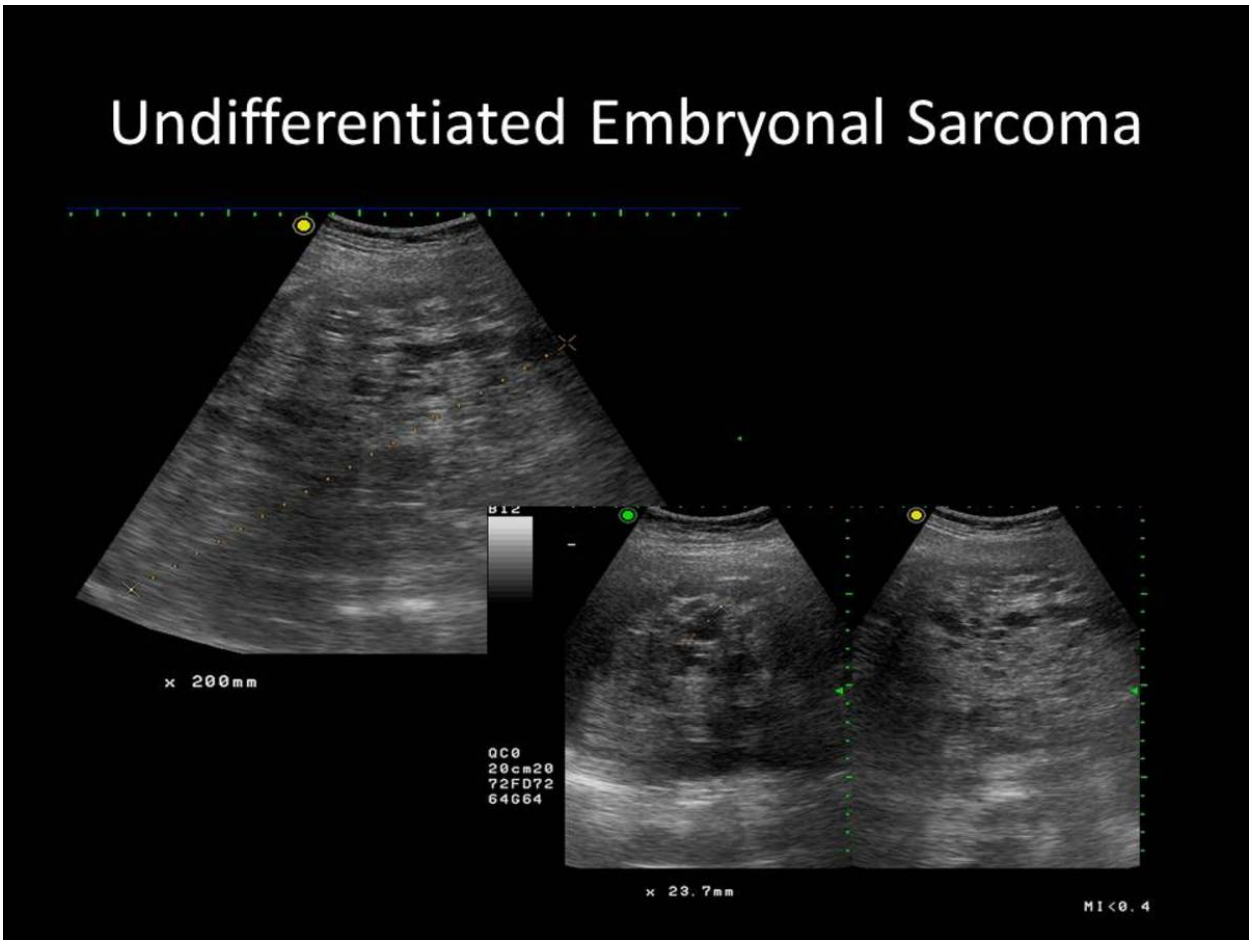

Fig. 48: Ultrasound shows an heterogeneous echogenic liver mass with several anechogenic areas, of different sizes.

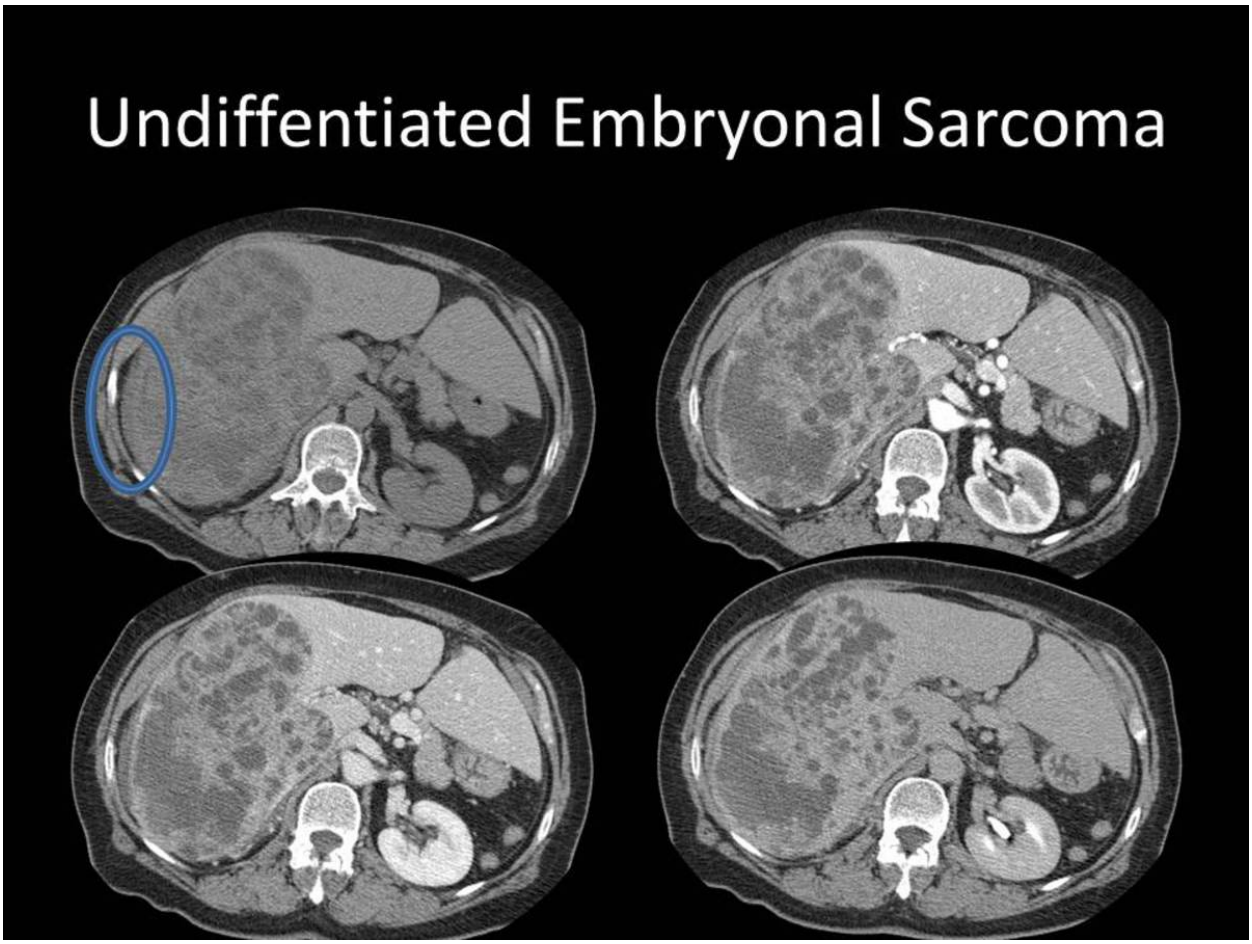

Fig. 49: A. Unenhanced CT shows a soft tissue mass with multiple low attenuation areas. A focal spot of peritoneal hemorrhage is also shown (blue circumference). C-E. Dynamic study demonstrates the multiple cystic components of the mass. Other areas represent necrotic debris, clotted blood and hemorrhagic fluid

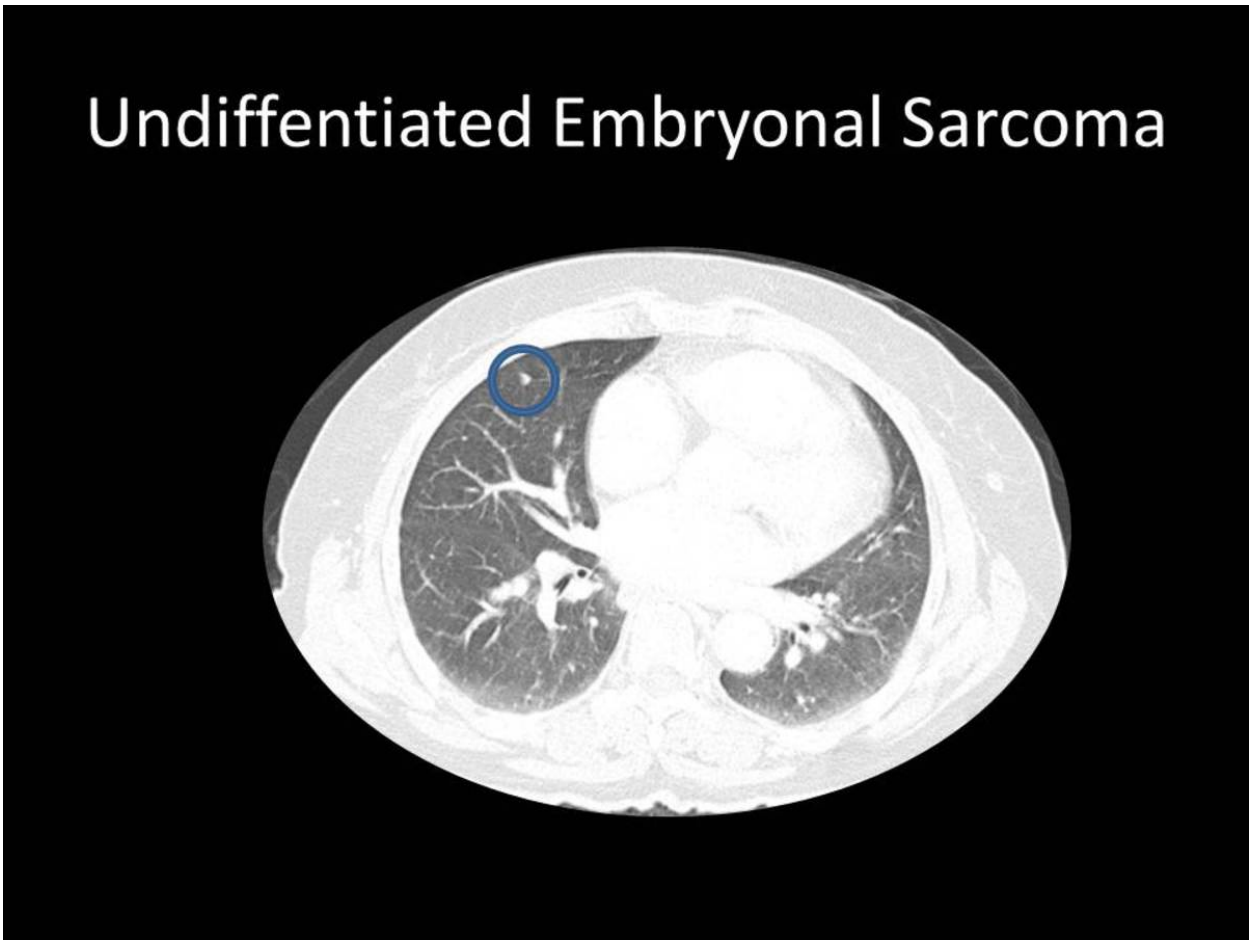

Fig. 50: C - Thoracic axial computed image, lung window: Right superior lobe metastasis (1cm).

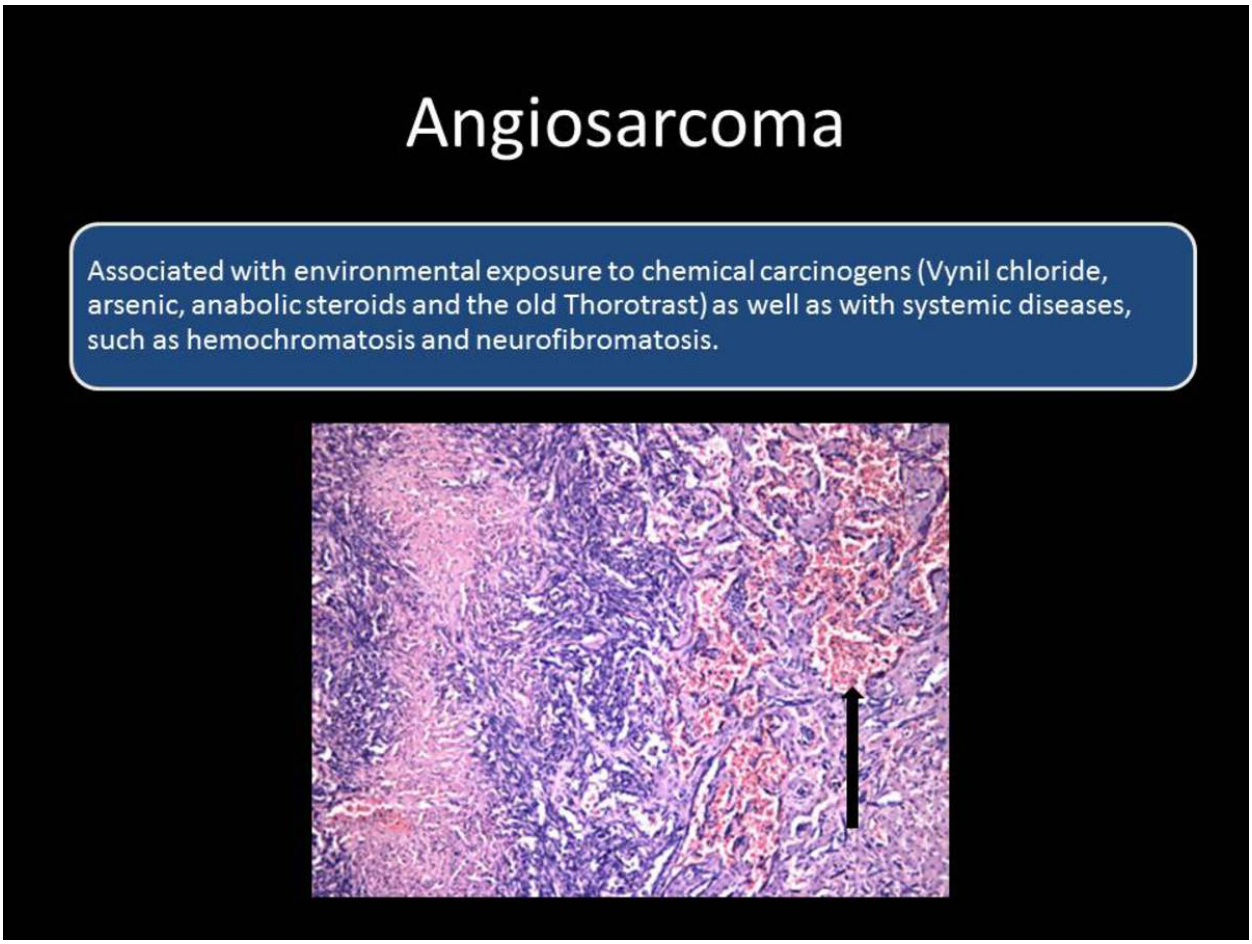

Fig. 41: High-power photomicrograph shows malignant spindle and pleomorphic cells. These cells origin new sinusoidal vessels (arrow).

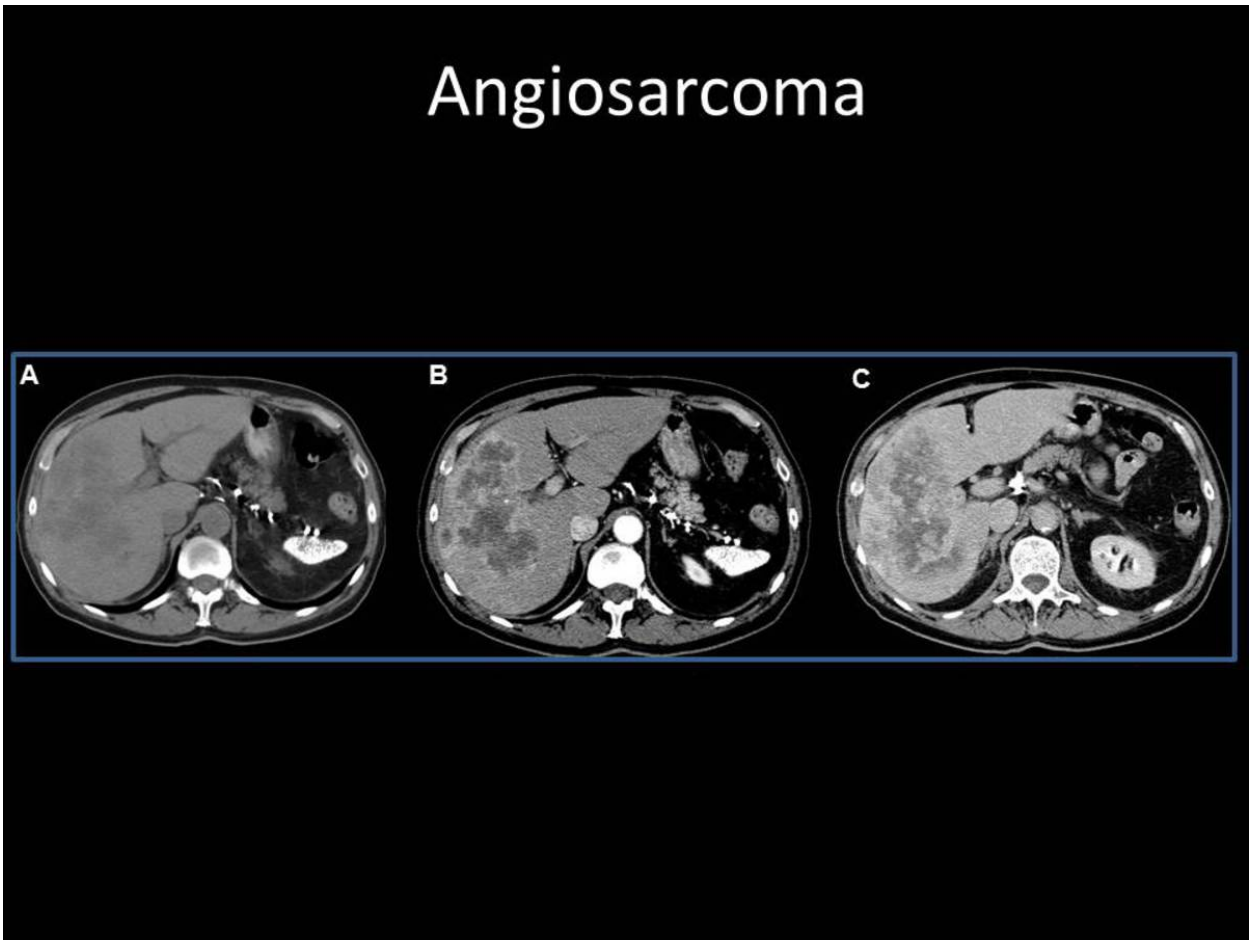

Fig. 40: 72-year old man with history of Thorotrast exposure. A. Unenhanced CT shows an heterogeneous hypoattenuating mass. B. Enhanced-CT (arterial phase) shows a bizarre shaped mass with hypervascular heterogeneous enhancement and central areas of low attenuation representing old hemorrhage. C. Progressive and heterogeneous enhancement is shown in venous phase.

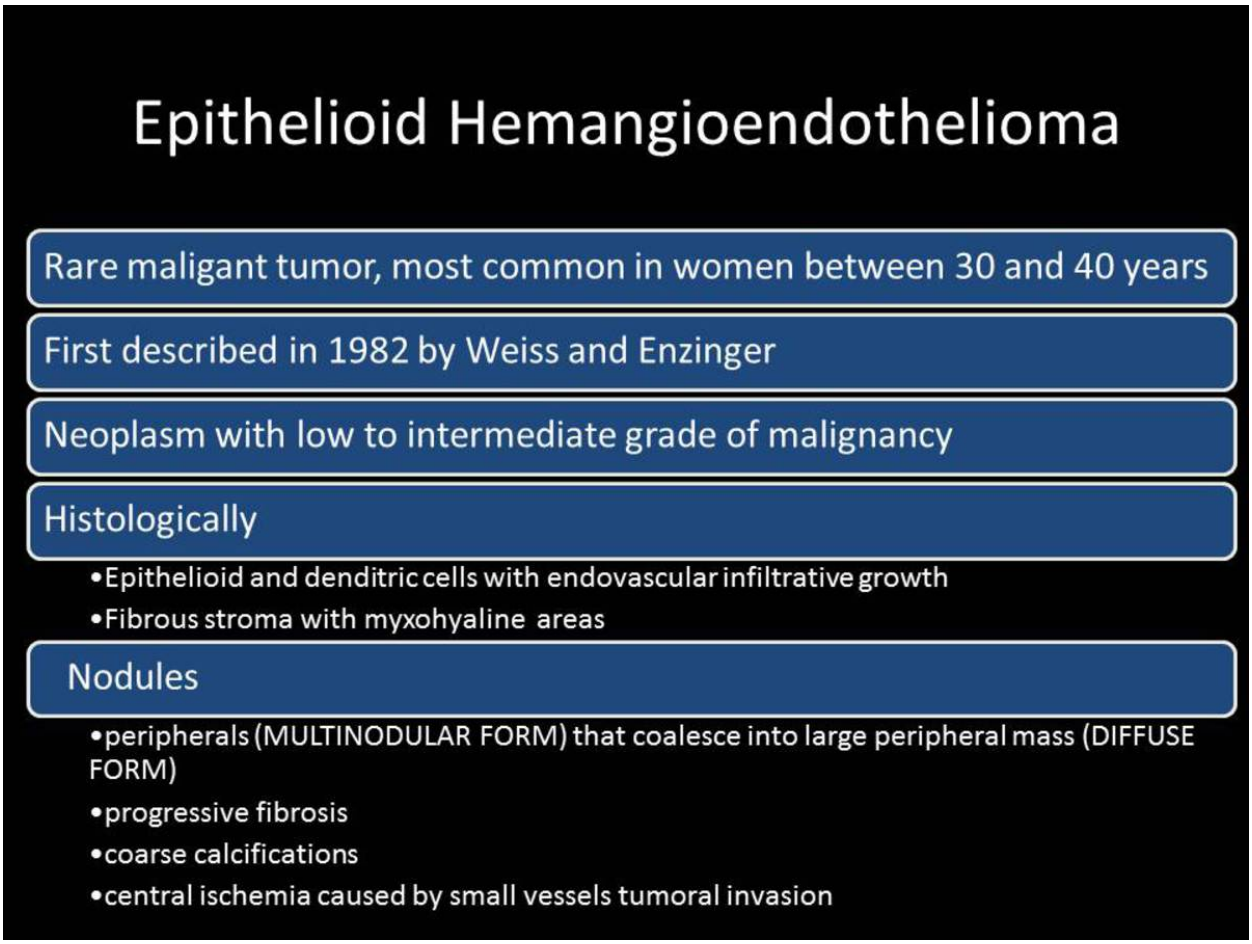
Epithelioid Hemangioendothelioma
Rare maligant tumor, most common in women between 30 and 40 years
First described in 1982 by Weiss and Enzinger
Neoplasm with low to intermediate grade of malignancy
Histologically
•Epithelioid and denditric cells with endovascular infiltrative growth
•Fibrous stroma with myxohyaline areas
Nodules
•peripherals (MULTINODULAR FORM) that coalesce into large peripheral mass (DIFFUSE FORM)
•progressive fibrosis
•coarse calcifications
•central ischemia caused by small vessels tumoral invasion

Fig. 31: 31

Epithelioid Hemangioendothelioma

Ultrasound	CT	MR

• multinodular
  • hypoechoic
  • heterogeneous echo structure
• diffuse
  • extensive heterogeneous involvement
	• multiple nodules
	• confluent peripheral hypodense mass extending to the capsule
	• capsular retraction(<25%)
	• calcifications
	• peripheral uptake in the portal phase (target sign)
	• isodense in the delayed phase
		• T1: low signal intensity
		• T2: heterogenous high signal intensity
		• Peripheral enhancement surrounded by thin non-enhancing rim corresponding to a narrow avascular zone

The multinodular form of endothelial hemangioendothelioma is indistinguishable from metastatic disease.
In favor: temporal evolution into the diffuse form, peripheral subcapsular growth, increased vascularity, hypertrophy of the uninvolved liver.

Fig. 32: 32

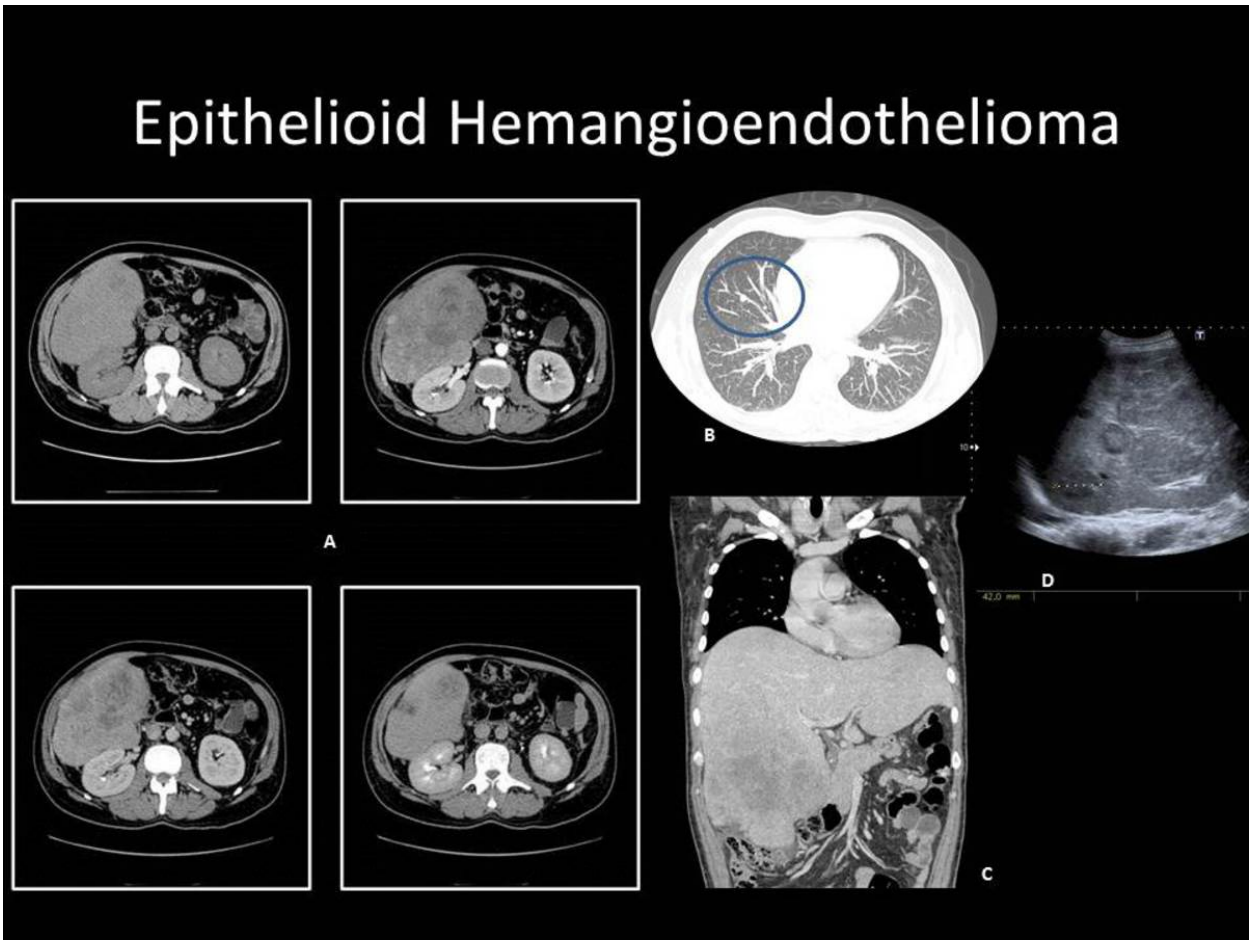

Fig. 33: A - Axial abdominal CT images: lobulated liver contour, with capsular shrinkage and exophytic nodules. There are peripheral areas that suffer moderate enhancement on arterial phase, with centripetal progression in later stages (becoming partly isoattenuating). The larger lesion has 16 x 12cm, and keeps hypodense central areas at all phases. B - Axial Lung CT images (MIP): Lung metastasis. C - Coronal CT image: Heterogeneous hepatomegaly. D - Ultrasonography: multiple small, sometimes confluent, nodules with target appearance.

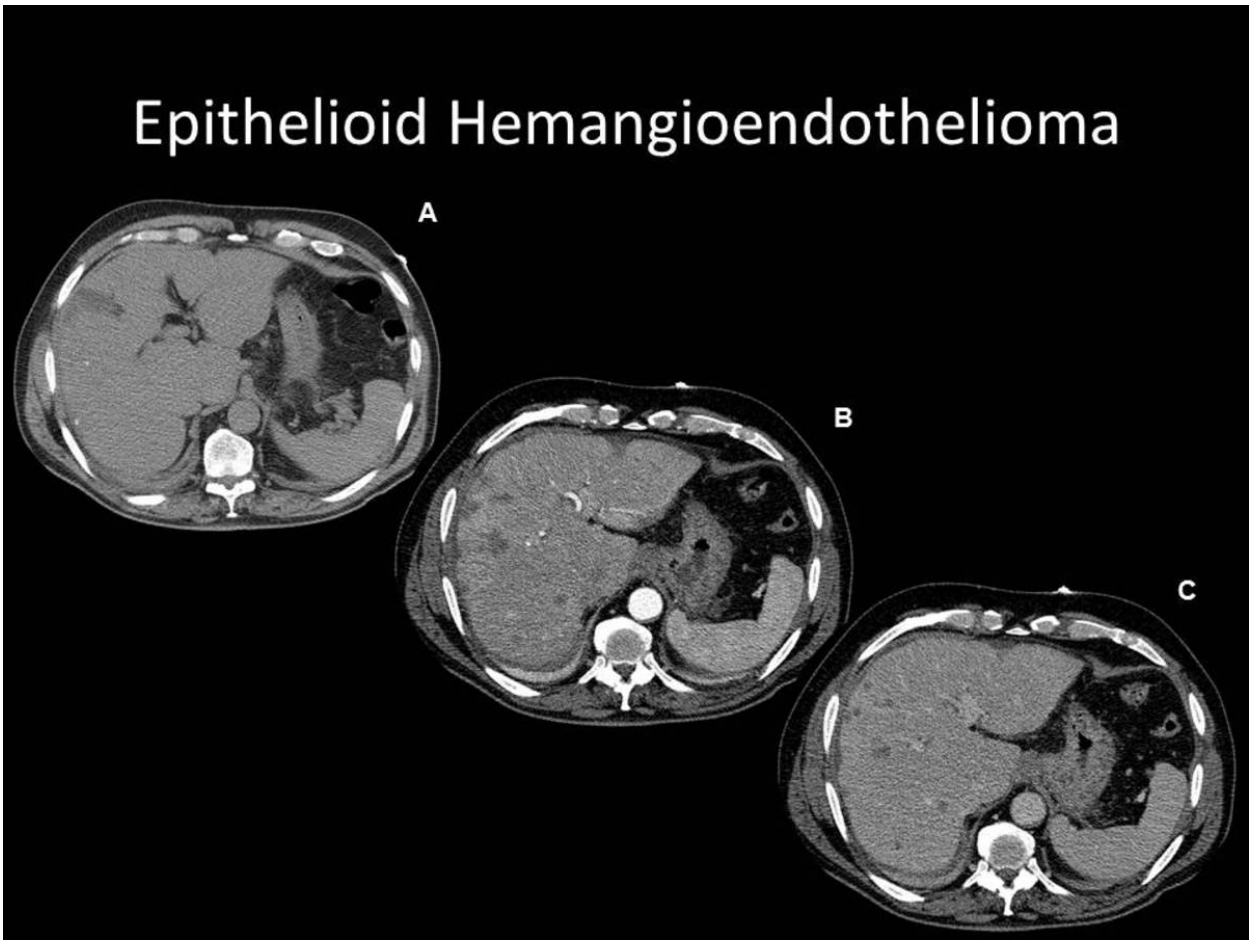

Fig. 35: A. Unenhanced CT image shows hepatomegaly with some calcifications visible in the right lobe. B. Enhanced-CT (arterial phase) shows multiple liver nodules in the right and caudate lobes: most are hipodense, but some show peripheral. B. The portal phase image demonstrate gradual centripetal enhancement progression. Note irregular liver border associated with the nodules suggesting capsular retraction.

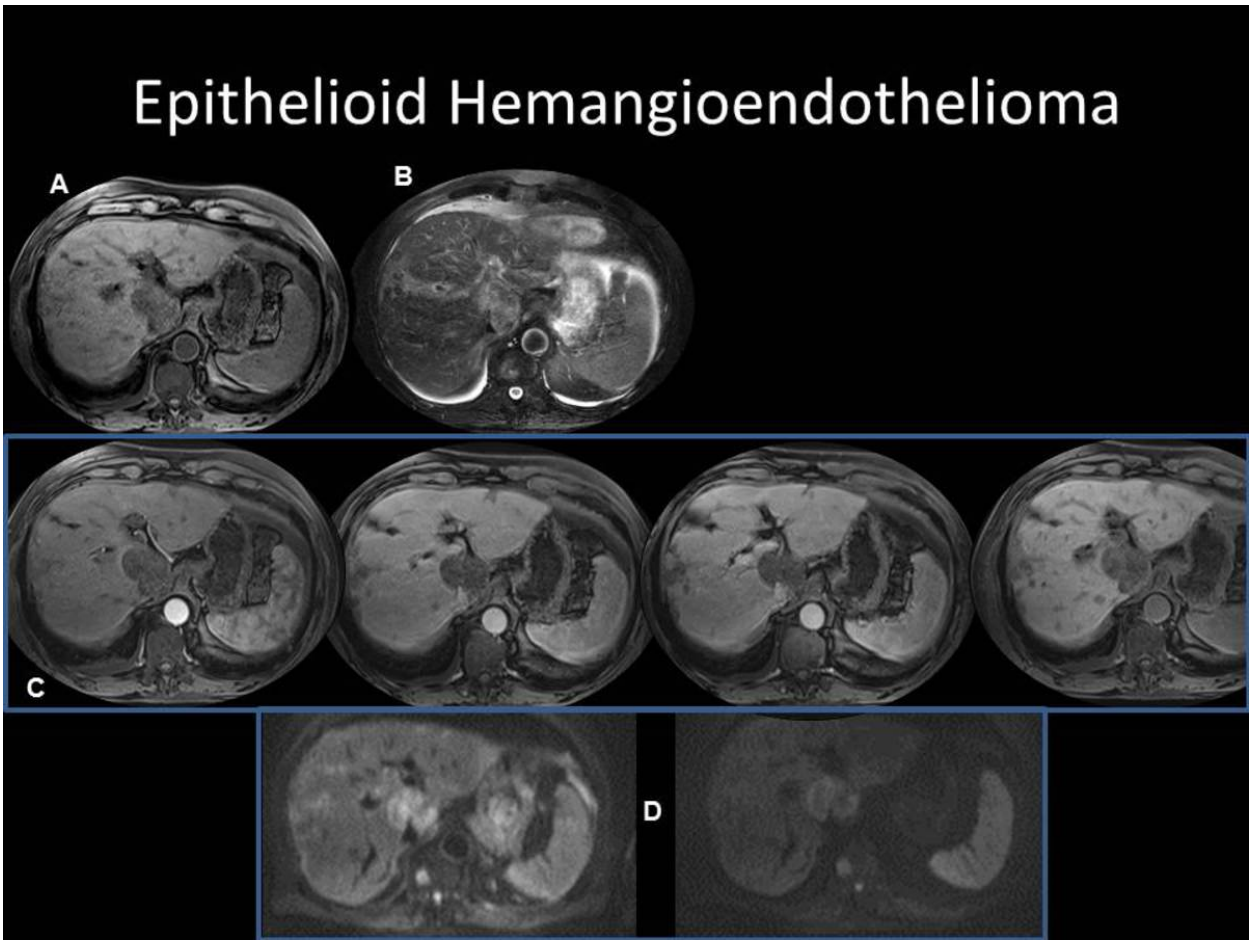

Fig. 36: A. T1-weighted image: hypointense large mass in the caudate lobe and small nodules in the right and left lobes. B. The mass is slightly hyperintense on T2-weighted MR images, but the small nodules show an hypointense rim. C. Gd-EOB-DTPA-enhanced images: only the mass in the caudate lobe slightly enhances in the hepatobiliary phase. D - In the diffusion-weighted study the lesion has no diffusion restriction.

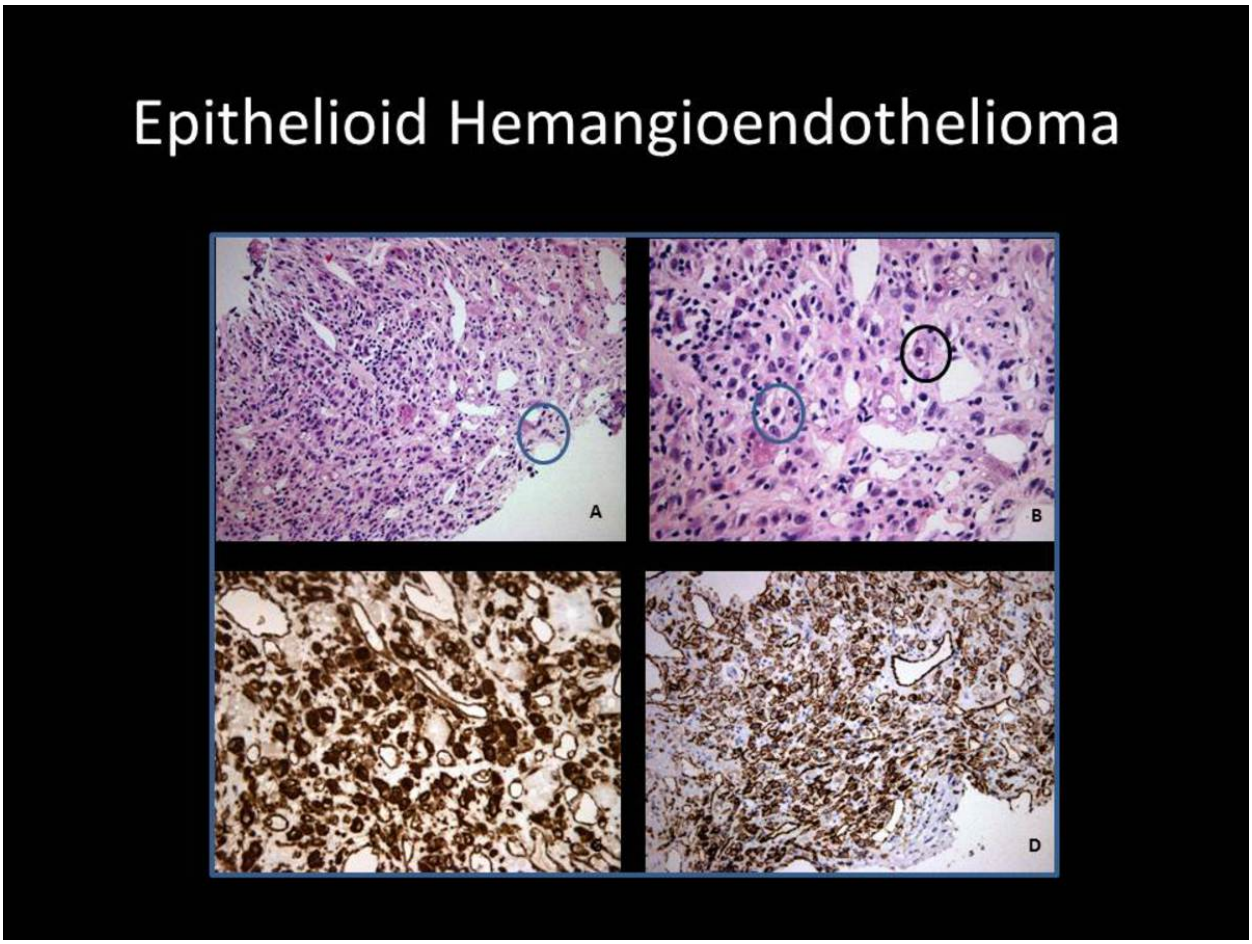

Fig. 34: A - High-power photomicrograph shows epithelioid tumor cells sccattered in fibrohyaline stroma. B - High-power photomicrograph shows epithelioid cells with intracytoplasmatic vacuoles (black circumference). C - Immunohistochemical staining, tumor cells show positivity for vimentin. D - Immunohistochemical staining, tumor cells show positivity for CD31.

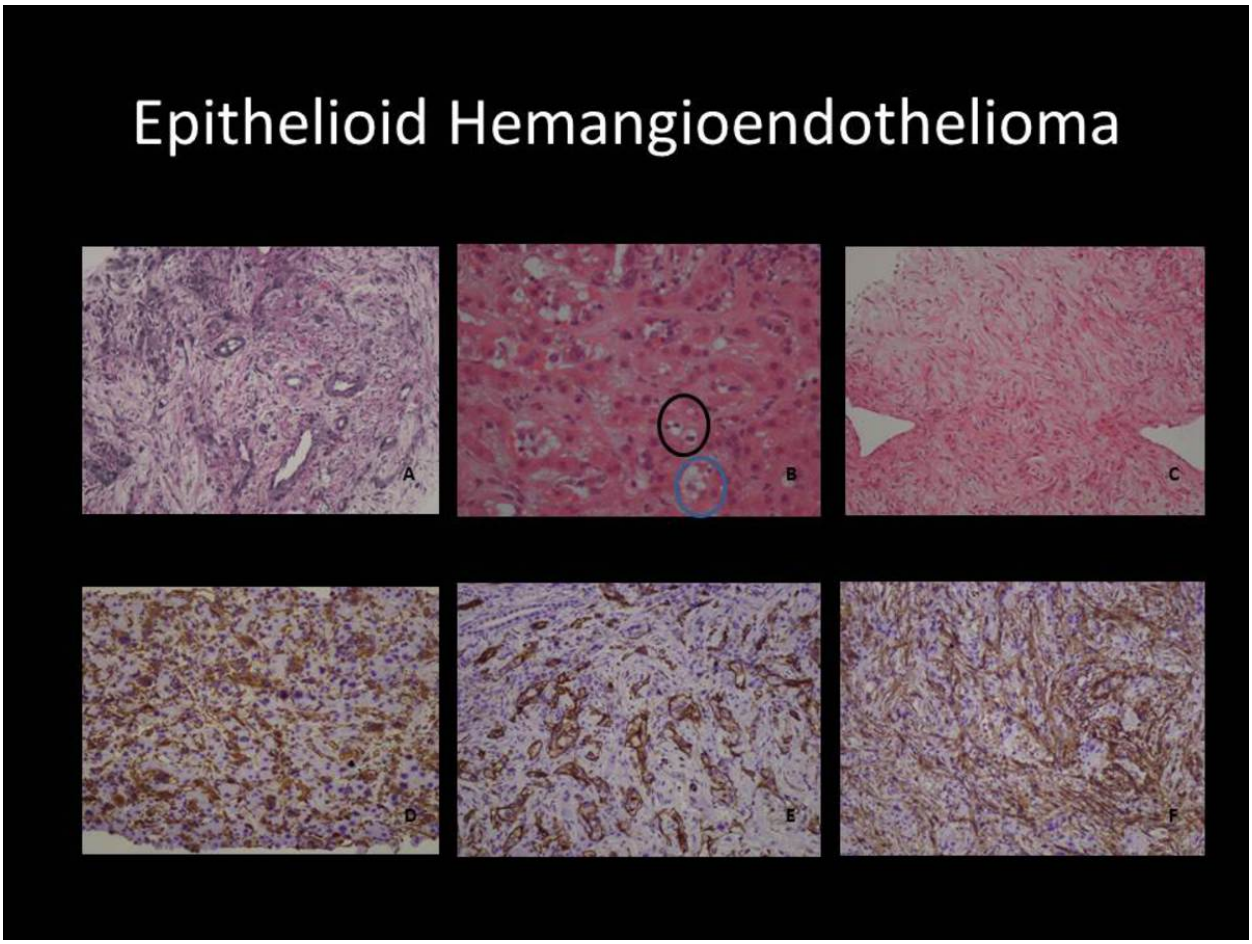

Fig. 37: A - High-power photomicrograph shows epiethelioid cells growing along preformed vessels B - High-power photomicrograph shows some cells with intracytoplasmatic vacuoles (blue circumference: cell with intracytoplasmatic vacuoles containing red blood cells). C - High-power photomicrograph shows spindle tumor cells sccattered in fibromyxoid stroma. D - Immunohistochemical staining, tumor cells show positivity for vimentin. D - Immunohistochemical staining, tumor cells show positivity for CD34. E - Immunohistochemical staining, tumor cells show positivity for CD31.

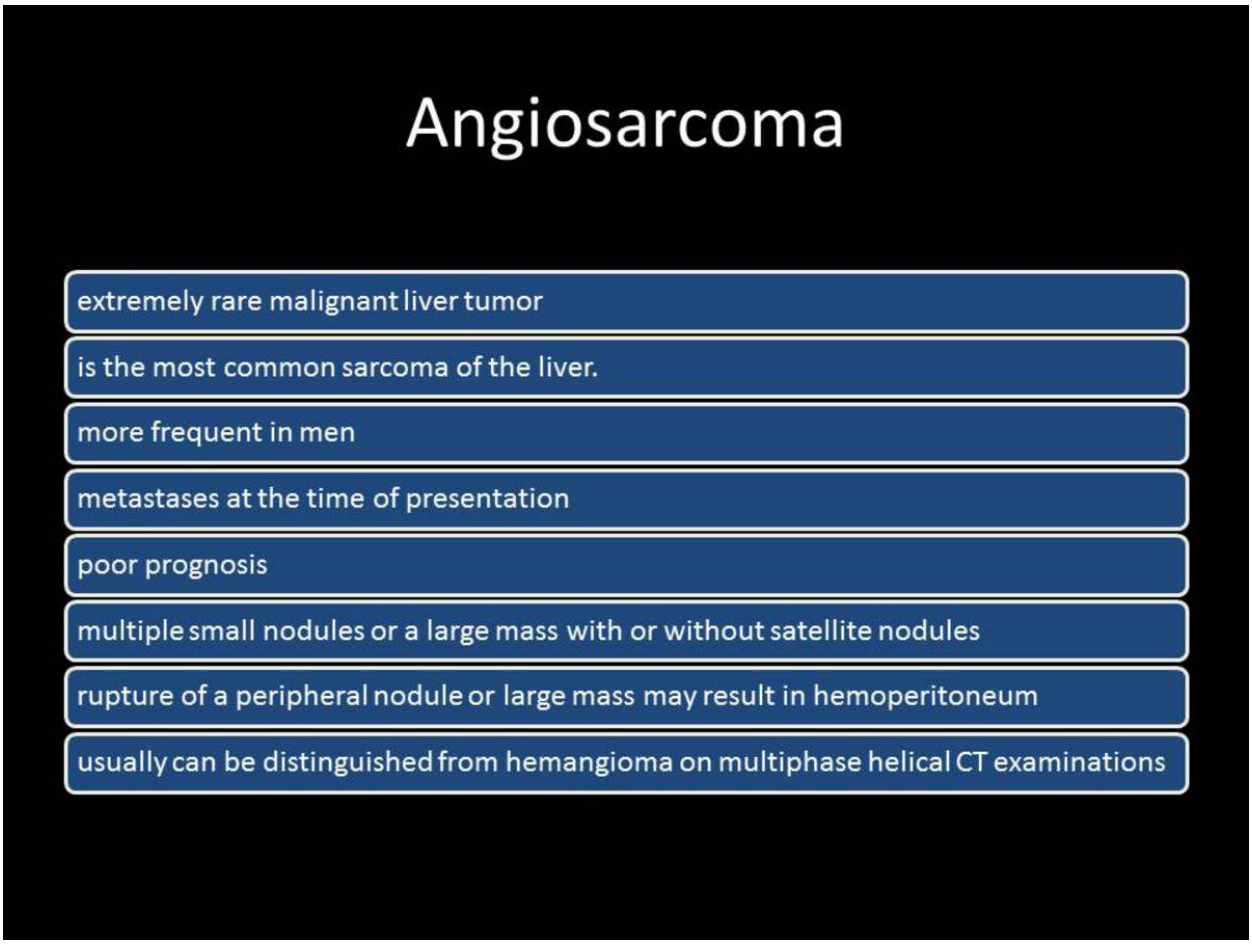
Angiosarcoma
extremely rare malignant liver tumor
is the most common sarcoma of the liver.
more frequent in men
metastases at the time of presentation
poor prognosis
multiple small nodules or a large mass with or without satellite nodules
rupture of a peripheral nodule or large mass may result in hemoperitoneum
usually can be distinguished from hemangioma on multiphase helical CT examinations

Fig. 38: 38

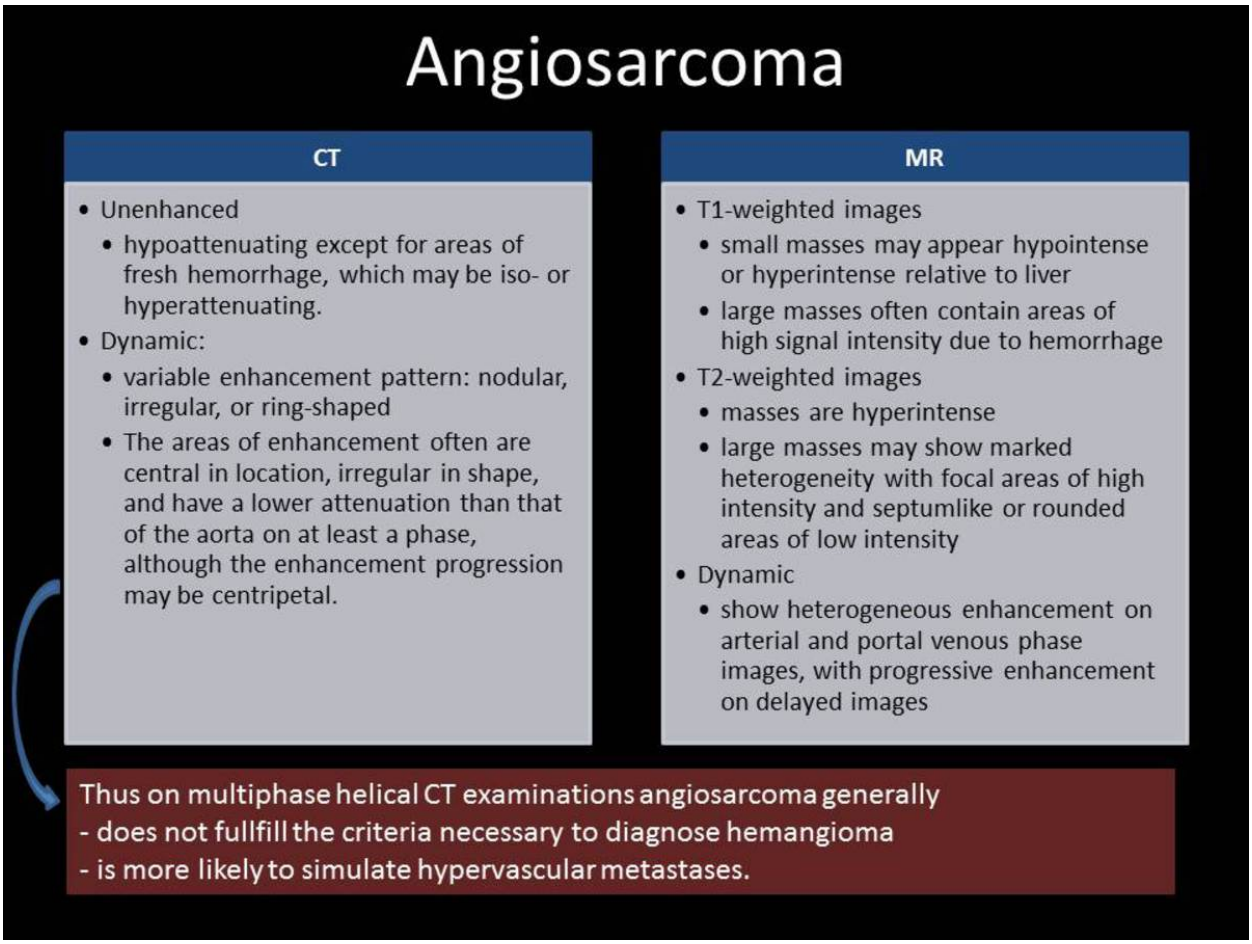
Angiosarcoma
CT
• Unenhanced
• hypoattenuating except for areas of fresh hemorrhage, which may be iso- or hyperattenuating.
• Dynamic:
• variable enhancement pattern: nodular, irregular, or ring-shaped
• The areas of enhancement often are central in location, irregular in shape, and have a lower attenuation than that of the aorta on at least a phase, although the enhancement progression may be centripetal.
MR
• T1-weighted images
• small masses may appear hypointense or hyperintense relative to liver
• large masses often contain areas of high signal intensity due to hemorrhage
• T2-weighted images
• masses are hyperintense
• large masses may show marked heterogeneity with focal areas of high intensity and septumlike or rounded areas of low intensity
• Dynamic
• show heterogeneous enhancement on arterial and portal venous phase images, with progressive enhancement on delayed images
Thus on multiphase helical CT examinations angiosarcoma generally
- does not fullfill the criteria necessary to diagnose hemangioma
- is more likely to simulate hypervascular metastases.

Fig. 39: 39

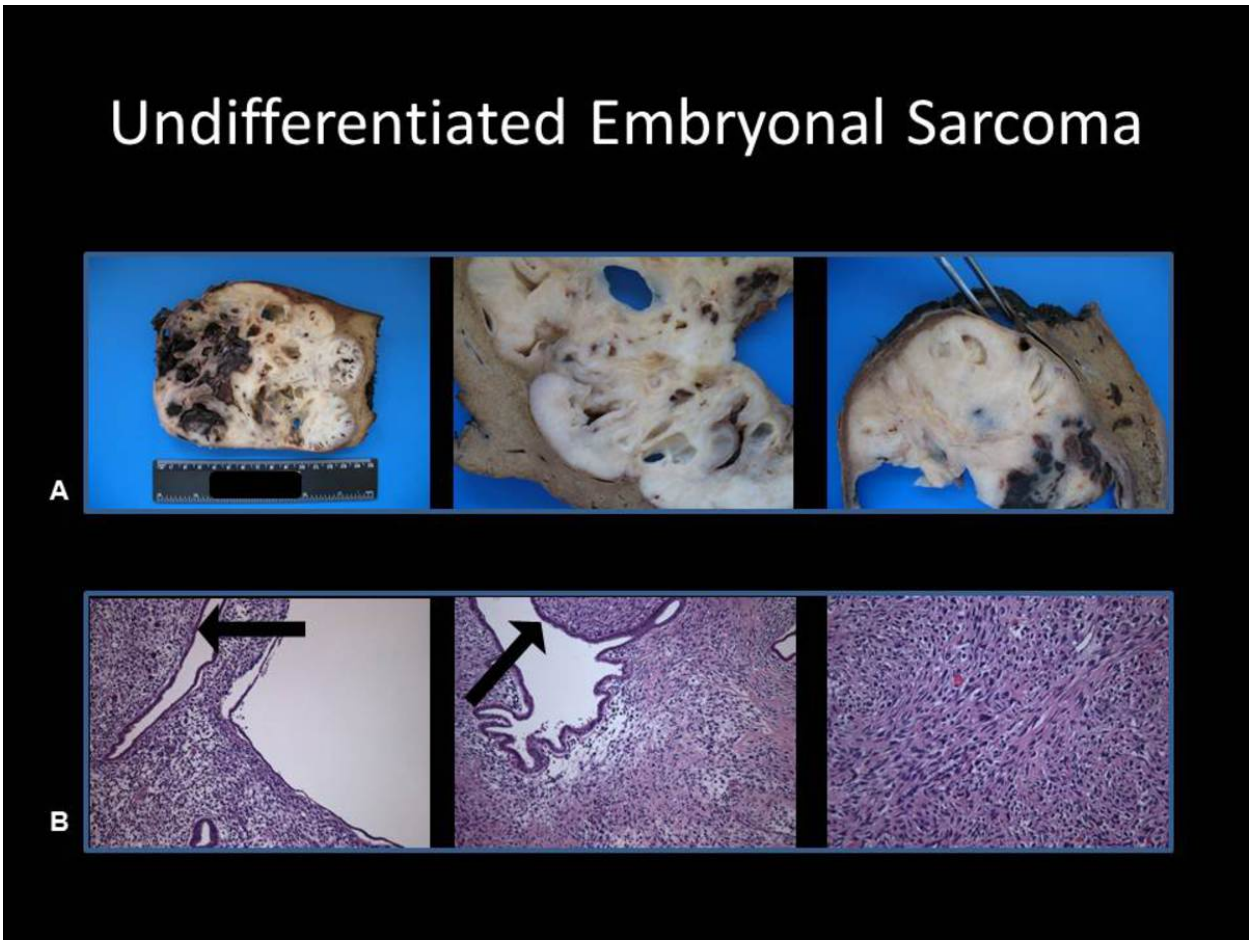

Fig. 51: A. Pathologic specimen shows the tumor huge size and several areas with necrotic debris and clotted blood distending the billiary tree in the hilar region but without infiltration. The third image depicts its pseudocapsule. B. High-power photomicrographs show malignant stellate and spindle shaped cells and benign embrional epithelium lining glandular cystic spaces. The epithelial lining of the cysts (arrow) is spared.

Conclusion

• Mesenchymal liver tumors have a wide spectrum imaging, both in benign and malignant lesions

• Understanding the pathologic features of these neoplasms is of pivotal importance since it may help to understand the imaging findings on ultrasound, computed tomography and magnetic ressonance studies.

• The knowledge of their more frequent and distinctive features, particularly when a multimodality approach is used can:

1. avoid invasive approaches (biopsy or surgical excision), and if not possible…
2. at least restrict the differential diagnosis

Personal Information

References

1. Kyoung Ah Kim, Kyoung Won Kim, Seong Ho Park, Se Jin Jang, Mi-Suk Park, Pyo Nyun Kim, Moon-Gyu Lee, and Hyun Kwon Ha. Unusual Mesenchymal Liver Tumors in Adults: Radiologic - Pathologic Correlation. Am. J. Roentgenol. Nov 2006; 187: W481-W489
2. Prokop M., Galanski M.; Spiral and Multislice Computed Tomography of the Body; Texas; Thieme; 2003; 406-495
3. Lee J.; Sagel S.; Stanley R.; Heiken J.; Computed Body Tomography with MRI Correlation; Philadelphia, 4th Edition; Lippincott Williams & Wilkins; 2006; 829-912
4. Lyburn ID, Torreggiani WC, Harris AC, Zwirewich CV, Buckley AR, Davis JE, Chung SW, Scudamore, Ho SGF; Hepatic Epithelioid Hemangioendotehelioma: Sonographic, CT and MR Imaging Appearances; American Journal of Radiology, 2003; 180: 1359-1364;
5. Caseiro-Alves F, Brito J, Araujo AE, Belo-Soares P, Rodrigues H, Cipriano A, Sousa D, Mathieu D. Liver haemangioma: common and uncommon findings and how to improve the differential diagnosis. European Radiology. 2007 Jun;17(6): 1544-54.
6. Earnest F; Johnson C.; Case 96: Hepatic Epithelioid Hemangioendothelioma; Radiology 2006; 240: 295-298.

7. Ponteferrada A., Salcedo M, matilla A, Nunez O, Banares R, Alvarez E, Clemente G; Heterogeneidad clínica y evolutiva del hemangioendotelioma epietelioide hepático; Gastroenterol hepatol. 2005; 28(6):321-5.
8. Woodward PJ, Sohaey R, Kennedy A, Koeller KK. From the archives of the AFIP: a comprehensive review of fetal tumors with pathologic correlation. Radiographics. 2005 Jan-Feb; 25(1): 215-42.
9. Mani H, Van Thiel DH. Mesenchymal tumors of the liver. Clin Liver Dis. 2001 Feb; 5(1):219-57.
10. Mani H, Van Thiel DH. Mesenchymal tumors of the liver. Clin Liver Dis. 2001 Feb; 5(1):219-57
11. Mark S Peterson, Richard L Baron, and Sheila C Rankin. Hepatic Angiosarcoma: Findings on Multiphasic Contrast-Enhanced Helical CT Do Not Mimic Hepatic Hemangioma. Am J Roentgenol. Jul 2000; 175: 165-170.
12. Vilgrain V, Boulos L, Vullierme MP, Denys A, Terris B, Menu Y, Imaging of Atypical Hemangiomas of the Liver with Pathologic Correlation. RadioGraphics 2000; 20:379-397
13. P Wunderbaldinger, W Schima, M Harisinghani, S Saini. Primary malignant fibrous histiocytoma of the liver: CT and MR findings AJR:180, January 2003. 1999 Jul; 173(1):244.
14. IJ Jang, TK Kim, HK Lim, SJ Park, JS SIm, HY Kim, JH Lee, Hepatic Hemangioma: Atypical Appearances on CT, MR Imaging, and Sonography. American Journal of Radiology: 180, January 2003